PhD degree in Molecular Medicine

European School of Molecular Medicine (SEMM),

University of Milan and University of Naples “Federico II”

Faculty of Medicine

Settore disciplinare: MED\04

Functional dissection of the histone demethylase Jmjd3 in B cell lymphopoiesis

Mahshid Rahmat

IFOM-IEO Campus, Milan

Matricola n. R08907

Supervisor : Dr. Stefano Casola

IFOM-IEO Campus, Milan

Added Supervisor : Dr. Marina Mapelli

IFOM-IEO Campus, Milan

Academic year 2013-2014

Table of contents

List of abbreviations

AID	Activation induced cytidine deaminase
ARF	Alternative reading frame
Bcl2	B cell CLL/lymphoma 2
Bcl6	B cell CLL/lymphoma 6
BCR	B cell receptor
BM	bone marrow
bp	base pair
Casp-GLOW	FITC-conjugated VAD-FMK
Cbx	chromobox homolog
cDNA	complementary DNA
ChIP	chromatin immunoprecipitation
c-KIT	CD117
CLP	common lymphoid progenitor
CSR	Class-switch recombination
DLBCL	Diffuse large B cell lymphoma
DMEM	Dulbecco's Modified Eagle medium
DNA	Deoxyribonucleic acid
dNTP	Deoxynucleoside triphosphate
Eed	Embruonic ectoderm development
ELISA	Enzyme-linked immunosorbent assay
ESC	Embryonic stem cell
Ezh2	Enhancer of zeste homolog 2 (Drosophila)
FACS	Fluorescence activated cell sorting
FDC	Follicular dendritic cell
Flt3	Fms-related tyrosine kinase 3

Fo	Follicular
GC	Germinal center
H	Histone
H2AK119mUb	mono-ubiquitinated Histone H2A at lysine 119
H3K27me3	Tri-methylated Histone H3 at lysine 27
H3K4me3	Tri-methylated Histone H3 at lysine 4
HSC	Hematopoietic stem cell
Ig	Immunoglobulin
IgV	Variable gene
IgH	Immunoglobulin heavy chain
IL	interleukin
Ink4a	Inhibitor of cyclin-dependent kinase 4A
Irf4	Interferon regulatory factor 4
Jmjd3	Jumonji domain-containing protein 3
JAK-STAT	Janus kinase/signal transducers and activators of transcription
kDa	kilodalton
LMPP	Lymphoid-primed multipotent progenitor
LN	Lymph node
loxP	Locus of X-over of P1
LPS	lipopolysachharide
mAB	Monoclonal antibody
MACS	Magnetic-activated cell sorting
Mb-1	CD79a molecule, immunoglobulin-associated alpha
Mcl-1	Myeloid cell leukemia sequence 1
MHC	Major histocompatibility complex
MLN	Mesenteric lymph node
MPP	Multipotent progenitor
mRNA	Messenger RNA

MZ	Marginal zone
NFAT	Nuclear factor of activated T-cell
NF-κB	nuclear factor kappa-light-chain-enhancer of activated B cell
NHEJ	Non-homologous end joining
NP-CGG	Nitrophenyl coupled to chicken gamma globulin
Pax5	Paired box 5
PBS	Phosphate buffered saline
PC	Plasma cell
PcG	Polycomb group
PCR	Polymerase chain reaction
PFA	paraformaldehyde
PRC	Polycomb repressive complex
Prdm-1	PR domain response element
Rag	Recombination activation gene
RNA	Ribonucleic acid
RSS	Recombination signal sequence
RT	Room temperature
qRT-PCR	Quantitative real time-PCR
Sca-1	Stem cell antigen-1; Ly-6A/E
SHM	Somatic hyper mutation
Suz12	Suppressor of zeste 12 homolog (Drosophila)
TF	Transcription factor
TLR	Toll-like receptor
TP53	Tumor protein 53
WT	Wild-type
Xbp-1	X-box binding protein 1

Figures index

Tables index

Abstract

Histone H3 lysine-27 trimethylation (H3K27me3) is an epigenetic mark that exerts a critical role in heritable gene repression. Levels of H3K27me3 at genomic target sites are tightly controlled by the opposing action of H3K27me3-specific methylases and demethylases, respectively. Modulation of H3K27me3 levels influence cell proliferation, survival and differentiation. In mammalian cells, Polycomb group protein Enhancer of Zeste Homologue 2 (Ezh2) catalyzes H3K27 trimethylation as component of the Polycomb Repressive Complex 2. Deposition of H3K27me3 at target genes is reversed by the action of H3K27me3 demethylases. The Jumonji-C containing proteins JMJD3/KDM6B and UTX/KDM6A are the only known enzymes involved in H3K27me3 demethylation. Jmjd3 has been previously shown to play an important role in mediating macrophage driven inflammatory responses and in in regulating somatic cell reprogramming and cellular senescence. In immune cells including B cells expression of Jmjd3 is tightly controlled. Whereas basal Jmjd3 levels are detected throughout B cell development, strong upregulation of demethylase expression is observed after stimulation through respectively the B cell antigen receptor, Toll-like receptors and members of the TNF receptor superfamily.

To study the role of JMJD3 in B lymphocyte development and activation, I generated Jmjd3 conditional knock-out mice (*JMJD3*^{fl}). Analysis of B cell-specific *Jmjd3* KO mice revealed multiple defects linked to the lack of demethyalse activity. Jmjd3 regulated the size of the B cell progenitor pool acting primarily on the pre-B cell compartment that was reduced in mutant mice. *Jmjd3* deficient animals showed also alterations in peripheral B cell development. An increase in the proportion and absolute number of splenic marginal zone B cells was associated to a reduction in peritoneal cavity B-1a B cells. *In vivo* BrdU labeling assays suggested a longer lifespan of Jmjd3 mutant mature B cells, which was not dependent on improved cell survival. Jmjd3 was dispensable for germinal center formation and T-cell dependent immune responses.

Moreover, measurement of basal serum immunoglobulin titers excluded a major role for Jmjd3 in plasma cell homeostasis.

In vitro stimulation assays revealed a selective defect of Jmjd3 mutant B cells to proliferate in response to the TLR4 ligand LPS, which was alleviated by IL-4 co-stimulation. Jmjd3 was critical to drive the first one-to-two cell divisions following LPS stimulation suggesting a critical role in the initial activation of the resting B cells. Upon stimulation with LPS, Jmjd3 mutant B cells showed neither specific defects in cell-cycle progression nor increased apoptosis. Candidate gene expression analyses, supported by RNA sequencing data, revealed a comprehensive control exerted by Jmjd3 on the expression of a substantial number of cell-cycle regulated genes including those cyclins, CDK inhibitors and factors involved in DNA replication and mitosis. Regulation of gene expression mediated by *Jmjd3* was not associated with measurable changes in global H3K27me3 levels.

All together these results identify Jmjd3 as an important regulator of B cell lymphopoiesis and a selective effector of B cell innate immune responses.

1. Introduction

1.1. Chromatin and epigenetics

1.1.1. Chromatin structure

In eukaryotic cells, genomic DNA is highly compacted by positively charged Histone (H) proteins that form a condensed structure known as chromatin. The nucleosome is the fundamental unit of chromatin. It consists of 147 bp of DNA wrapped around a histone core composed of two subunit each of respectively Histones H2A, H2B, H3 and H4. Sequential nucleosomes generate a fiber of 11 nm diameter that further compacts to a 30 nm structure termed chromatosome via incorporation of linker histone protein H1 (Luger 2003). The mechanisms involved in the establishment of the higher order structure of chromatin remain still poorly understood.

Histone core subunits are structured proteins except for their N-terminal region that gets subjected to a number of post-translational modifications. Histone phosphorylation (serine and threonine residues) (Nowak et al., 2004), acetylation (lysine) (Grunstein et al., 1997), methylation (lysine and arginine) (Zhang et al., 2001), ubiquitination (lysine) (Davie et al., 1990), sumoylation (lysine) (Nathan et al., 2003), ADP ribosylation (Adameitz et al., 1984), glycosylation (Leibich et al., 1993), biotinylation (Hymes et al., 1995) and carbonylation (Wondrak et al., 2000) represent the most common modifications affecting N-terminus tails of core histones. Such covalent modifications exert a critical influence on gene expression by modulating the accessibility to DNA of the basic transcriptional machinery and sequence-specific transcription factors.

The consequences of specific histone modifications on gene expression, DNA replication, DNA damage responses and other related chromatin biology processes have been extensively studied over the past decades. The combination of covalent modifications targeting histone core subunits constitute the so-called “Histone code” which is read by chromatin factors that ultimately influence complex processes such as defining the transcriptional status of a gene (Jenuwein and Allis, 2001).

1.1.2. Epigenetics

Multicellular organisms consist of functionally distinct cell types that are determined by an invariant sequence of DNA. During development, the integration of extracellular signals with intrinsic transcriptional programs contributes to cell specialization and maintenance of cell identity. One central mechanism that contributes to the establishment of transcriptional programs that sustain lineage fate and, cellular identity is the epigenetic regulation of gene expression. The term epigenetics was first coined in 1942 by Conrad Waddington to describe casual developmental processes associated to a defined genotype (Waddington, 1942). Over the years, “epigenetics” has become a more specific term that defines those mechanisms leading to changes in gene expression that are inherited across generations, that are not caused by changes in the DNA sequence. Epigenetic modifications are commonly associated with defined states of the chromatin. Whereas euchromatin defines the portion of the genome readily accessible to the transcriptional machinery, heterochromatin defines a compacted state of chromatin that is commonly associated with gene repression. Heterochromatin can be further defined as constitutive (such as that of centrosomes), or facultative to define a reversible state of chromatin compaction.

In mammals, epigenetic regulation of gene expression is mainly mediated by post-translational modifications of histones, DNA methylation, nucleosomal remodeling and small noncoding RNAs (Jaenisch and Bird, 2003). These mechanisms contribute in a critical manner to define the transcriptome of a specialized cell-type that is inherited through multiple cell divisions, propagating thereby cellular identity.

1.1.2.1 Dynamics of Histone lysine methylation

The N-terminus region of histone proteins undergoes a variety of post-translational modifications (PTMs), which influence a broad set of biological processes that include DNA replication, transcriptional regulation and DNA damage responses.

Unlike Histone acetylation, which is generally associated with transcriptional activation, methylation of different lysine residues on core histone tails has different

transcriptional outcomes depending on the type of covalent modification. Moreover, lysine residues of Histone tails can be respectively unmethylated, monomethylated, dimethylated and thrimethylated contributing thereby to further diversify the biological outputs.

In general, methylation of Histone H3 on lysine-4 (K4), -36 (K36) and -79 (K79) is associated with transcription-competent chromatin. Instead, H3K9, H3K27 and H4K20 methylation is linked to regions of chromatin that are transcriptionally silent (Figure 1). In addition, whereas H3K4me3 is primarily found in close proximity to the transcriptional start site (TSS), H3K36me3 marks preferentially gene bodies (Barski et al., 2007). Silenced genes that are subjected to modulation are often associated with H3K27me3 deposition around the TSS, whereas H3K9me3 defines stably repressed genomic regions. Methylated CpG-islands located predominantly in promoter regions also contribute to stable gene repression (Lachner et al., 2003). The net result of histone marks associated respectively to active and inactive chromatin states define ultimately the transcriptional state of any given gene.

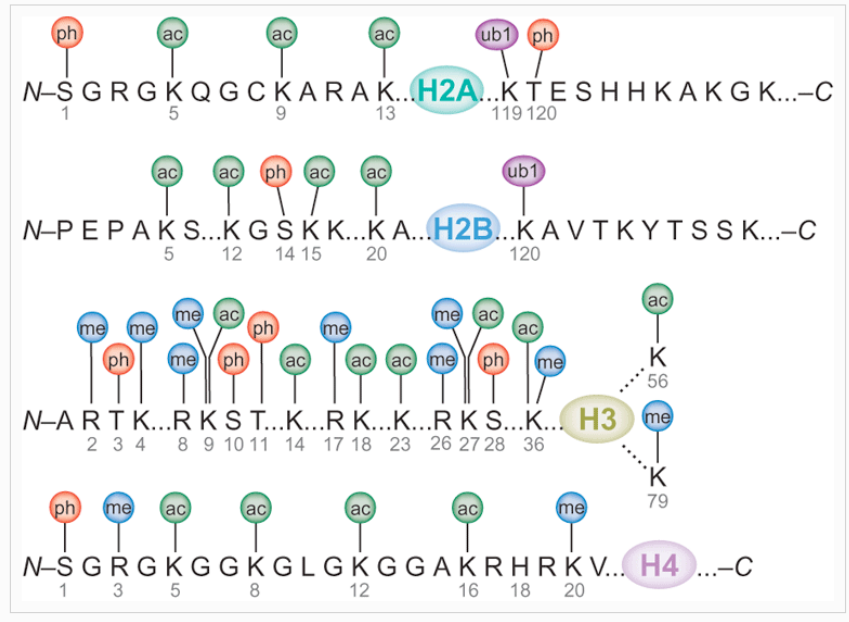

Figure 1. Post-transcriptional modifications of histones. Histone tails undergo a variety of covalent modifications including acetylation (ac), methylation (me), phosphorylation (ph) and ubiquitination (ub), which influence the state of compaction of chromatin (Adapted from Bhaumik et al, 2010).

The degree of histone lysine methylation of any given genomic region is the result of a fine balance between the opposing functions of respectively histone lysine methyltransferases (KMTs) and demethylases (KDMs).

1.1.2.1.1. Histone lysine methyltransferases

SET domain-containing proteins represent a superfamily of histone lysine methyltransferases that catalyze the transfer of a methyl group from a donor substrate (represented by S-adenosyl L-methionine (AdoMat)) to the amino group of specific lysine residues. The SET domain is a highly conserved protein domain that was originally identified in three *Drosophila Melanogaster* Histone methyltransferases identified respectively as Suppressor of variegation 3-9 (Su(var)3-9) (responsible for H3K9 methylation) ; Trithorax (Trx) (that catalyzes H3K4 methylation) and Enhancer of zeste (E(z)) (that promotes H3K27 methylation) (Tschiersch et al., 1994; Jones et al., 1993; Stassen et al., 1995). Among Histone methyltransferases, I will focus my attention in the last part of this section to discuss the contribution of the human orthologues of E(z) represented by Enhancer of Zeste Homologue-1 (EZH1) and- 2 (EZH2).

EZH1 and EZH2 belong to the superfamily of Polycomb group (PcG) proteins. PcG proteins act as transcriptional repressors to regulate a variety of biological processes including cell cycle progression, senescence, apoptosis, tissue homeostasis, X-chromosome inactivation, genomic imprinting and cell fate decision (Gieni and Hendzel, 2009; Bracken et al., 2007; Sparmann and van-Lohuzen, 2006). In mammals, PcG proteins exert their function within two main multi-subunit macromolecular complexes termed Polycomb repressive complex 1 (PRC1) and Polycomb repressive complex 2 (PRC2). The methyltransferase activity of PcG proteins resides within PRC2. It is primarily catalyzed by EZH2 through its SET domain. Other core components of PRC2 include Embryonic Ectoderm Development (EED), Suppressor of zeste 12 (Suz12) and Retinoblastoma suppressor associated protein 46/48 (RbAp46/48) (Kirmizis et al., 2004; Czermin et al., 2002). H3K27 methylation can be also catalyzed by EZH1. However it has a weaker catalytic activity compared to EZH2 (Margueron et al., 2008). PRC2-dependent H3K27 methylation can trigger the recruitment to target sites of PRC1 (Cao et al., 2013). Recent studies

have revealed the existence of multiple independent forms of PRC1. The latter differ in subunit composition acting often in different cell types and/or stages of differentiation on selective sets of target genes. The catalytic subunits of PRC1 consist of the E3 ubiquitin ligases Ring1a and Ring1b/RNF2, which catalyze monoubiquitylation of Histone H2A on lysine-119 (H2AK119Ub). Other components of PRC1 include Bmi1 and members respectively of CBX chromobox and Polyhomeotic homologue (PHC) protein families.

PRC1 and PRC2 complexes are thought to act in concert to promote silenging of target genomic regions. According to a large body of evidences it has been proposed PRc2 is initially recruited to target sites. Here, it catalyzes H3K27 trimethylation, which in turns gets recognized by CBX proteins of PRC1 through their chromobox domain. Ultimately, PRC1 catalyzes H2AK119ub to prevent transcriptional elongation by RNA polymerase II and hence mediate gene repression (Simon et al., 2009; Schuettengruber and Cavalli, 2009) (Figure 2a). Recent studies have, at least in part, put in question this model (Kalb et al., 2014; Cooper and Brockdorff, 2014; Blackledge et al., 2014). Indeed, it was shown that PRC1 could be recruited to target sites independent of PRC2. Once there, ubiquitination of H2AK119 recruited PRC2 in a complex with the H3K4 demethylase Jarid2 and the zinc finger protein Aebp2. Following this event, PRC2 catalyzed H3K27 trimethylation activating thereby a positive feedback loop that facilitated further recruitment of PRC1 (Figure 2b).

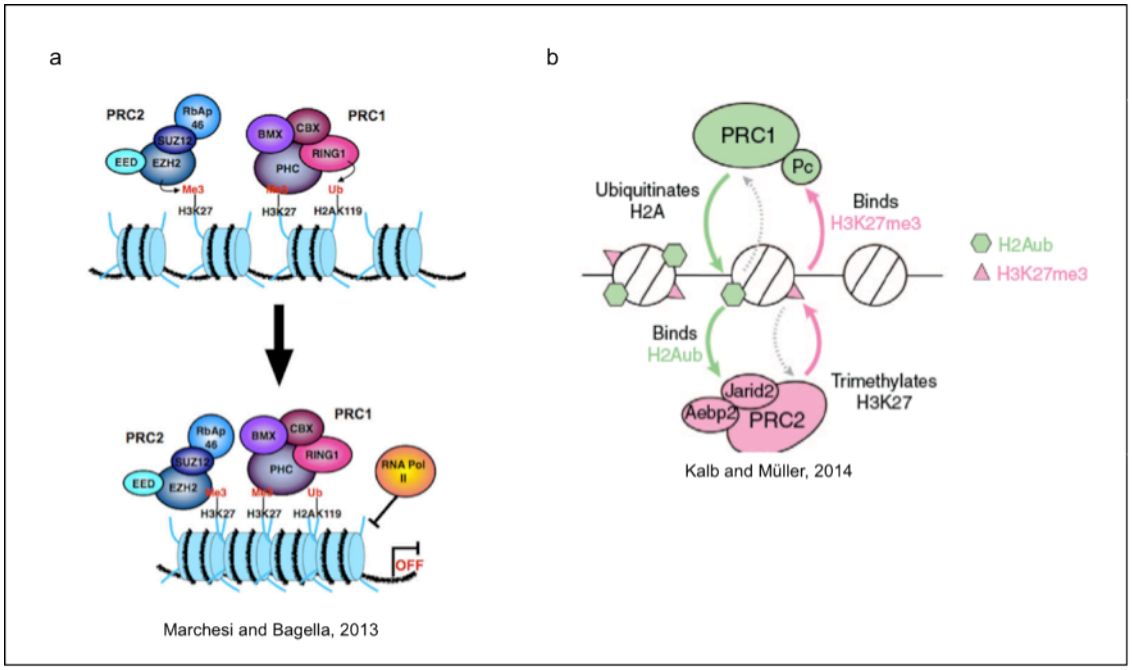

Figure 2.Polycomb-mediated gene silencing. a) Model for PRC2-dependent model for recruitment of PRC1 to target sites, **b)** Alternative model of Polycomb recruitment. Monoubiquitilation of H2AK119 by PRC1 recruits PRC2, which, in turn, facilitates further recuitment of PRC1 to target sites via deposition of H3K27me3.

1.1.2.1.2. Histone lysine demethylases

Studies in the 1970s based on radioactive labeling of histone methyl groups indicated that this epigenenetic modification had approximately the same half-life as that of the histone itself (Byvoet et al., 1972; Borun et al., 1972). Hence, histone methylation was considered as an irreversible modification, explaining thereby how epigenetic information was stored. Later studies revealed however a faster turnover of methylated histones which were constantly exchanged within nucleosomes during the cell-cycle (Annunziato et al., 1995). To explain the turn over of methylated histones, two possible mechanisms were suggested, namely active exchange of methylated histones with their un-methylated counterparts or proteolytic removal of methylated histone tails. The isolation of the first lysine-specific demethylase LSD1/KDM1A confirmed the existence of an active process leading to the enzymatic removal of

methyl-groups from histones (Shi et al., 2004). The mechanism of action of LSD1 is conserved in most eukaryotes. LSD1 acts as an amine oxidase that catalyzes oxidative demethylation of mono- and dimethylated lysine residues using Flavin Adenine Dinucleotide (FAD) as a cofactor (Shi et al., 2004). Following the discovery of LSD1, Tsukada and colleagues described an iron- and α-ketoglutarate-dependent hydroxylation reaction able to promote histone demethylation (Tsukada et al., 2006). This study was confirmed by independent reports (Whetstine et al., 2006; Fodor et al., 2006; Cloos et al., 2006). The idea of iron- and oxygen-dependent demethylation of histones came from the identification in *Escherichia coli* of AlkB, a DNA demethylase enzyme that catalyzes hydroxylation of the methyl group via decarboxylation of α-ketoglutarate. Biochemical approaches using HeLa cells nuclear extracts led to identification of FBXL11/KDM2A that disposes an iron deoxygenase Jumonji-C (JmjC) domain similar to the AlkB catalytic site. The similarities between the catalytic domain of AlkB and the JmjC domain led to the finding of JmjC domain-containing proteins as an another class of histone lysine demethylases. JmjC domain-containing histone demethylases can act on all methylation states through an oxidative demethylation reaction, whereas LSD1 can only demethylate mono- and di-methylated histones because it lacks a protonated nitrogen as hydrogen donor to demethylate the trimethyl mark (Figure 3).

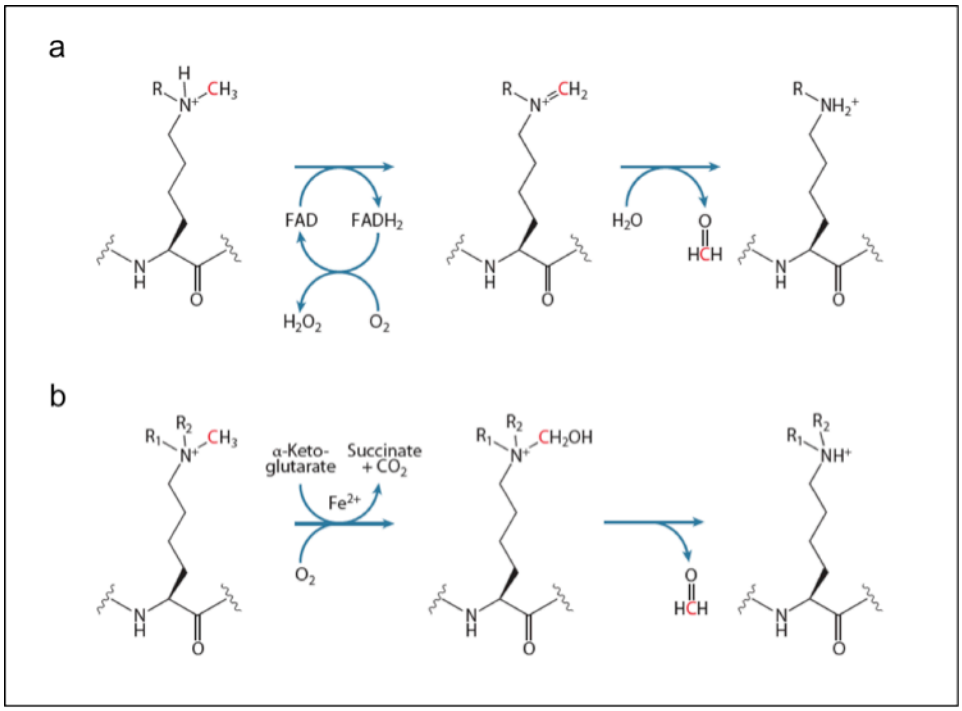

Figure 3. Chemistry of Histone lysine demethylation a) FAD-dependent activity of Histone demethylases such as LSD1. Amine oxidation of protonated nitrogen creates an iminium ion that is spontaneously hydrolyzed and releases formaldehyde thus resulting in a mono-methylated lysine. The mono-methylated residue can undergo the same reaction and be converted to its un-methylated form. **b)** Mechanism of demethylation by JmjC domain-containing proteins. Fe2+, O_2 and α-ketoglutarate coordinately act to hydroxylate the methyl group. JmjC domain-containing proteins are able to remove respectively one, two or three methyl groups form lysine residues. Carbon molecules in red are demethylated in each reaction (Adopted from Mosammaparast and Shi, 2010).

In the past few years, additional JmjC domain-containing families with lysine specific demethylase activity have been identified (Table 1). Among them, only two display histone H3K27-specific demethylase activity, namely Ubiquitously transcribed Tetratricopeptide repeat X (UTX/KDM6A) and Jumonji domain-containing protein 3 (*JMJD3* /KDM6B).

Table 1. Nomenclature of histone demethylases and their substrate specificity

Family name	Family member	Former name	Substrate specificity	References
KDM1	KDM1	LSD1, AOF2,BHC110	H3K4me2/me1 H3K9me2/me1 p53	(Shi et al., 2004)
KDM2	KDM2A KDM2B	JHDM1A,FBXL11 JHDM1A,FBXL10	H3K36me2/me1	Tsukada et al., 2006)
KDM3	KDM3A KDM3B	JHDM2A,JMJD1A JHDM2B,JMJD1B	H3K9me2/me1	(Yamane et al., 2006)
KDM4	KDM4A KDM4B KDM4C	JMJD2A,JHDM3a JMJD2B JMJD2C, GASC1 JMJD2D	H3K9me3/me2 H3K36me3/me2	(Whetstine et al., 2006)
KDM5	KDM5A KDM5B KDM5C KDM5D	RBP2, JARID1A PLU-1, JARID1B SMCX, JARID1C SMCY, JARID1D	H3K4me3/me2	(Christensen et al., 2007; Iwase et al., 2007; Klose et al., 2007; Lee et al., 2007; Liang et al., 2007
KDM6	KDM6A KDM6B	UTX *JMJD3*	H3K27me3/me2	(Agger et al., 2007; Lan et al., 2007)

1.2. Jmj-C domain-containing protein 3 (Jmjd3)

1.2.1. Jmjd3 function in early mammalian development

In mammals, oocyte fertilization gives rise to a totipotent cell called zygote. During pre-implantation development, the parental genomes undergo extensive chromatin remodeling and epigenetic changes. One critical example is represented by extensive, genome-wide redistribution of H3K27me3 that is necessary to support later stages of development (Santenard et al, 2010). In bovine early development, gradual loss of H3K27me3 occurs independent of cell division suggesting an active mechanism for histone demethylation (Canovas et al., 2011). In support of this, inactivation of the H3K27 demethylase *Jmjd3* impairs early bovine embryonic development prior to the blastocyst stage. Notably, the embryo inherits high levels of *Jmjd3* maternal transcripts that are crucial before embryonic genome activation (EGA) that occurs after the first three to four cell divisions (Canovas et al., 2011). Interestingly, reports from gene-targeted mice, have revealed a dispensable role for jmjd3 in early embryonic development. Indeed, in the frame of a collaboration with Dr. G. Testa group (European Institute of Oncology, Milan, Italy) we could show that *Jmjd3* mutant mice developed without major complications up to birth. Lack of Jmjd3 was however incompatible with post-natal life, as no mutant pups survived the first hours following birth, due to respiratory defects (Burgold et al., 2012). Our results have been confirmed by other groups (Satoh et al, 2010;). These findings suggest that, depending on the species, *Jmjd3* contributes at different stages of embryonic development.

1.2.2. Jmjd3 and lineage commitment

Several studies in embryonic and adult stem cells have described the concomitant presence of respectively activating (H3K4me3) and repressive (H3K27me3) histone marks at the promoter of genes encoding for key developmental regulators. This epigenetic configuration has been called bivalent domain (Bernstein et al., 2007; Mikkelsen et al., 2007). Bivalent domains contribute to the silencing of developmental genes in ES cells while keeping them poised for activation at later stages of differentiation. The observation that lineage-specific genes that are marked by H3K27me3 in ES cells, have lost H3K27 methylation in their differentiated progeny pointed to the existence of H3K27me3 demethylases acting on these targets. In support of this hypothesis, it was shown that *Jmjd3* is required for H3K27me3 demethylation of neuronal genes to sustain their expression once ES cells are committed to the neuronal lineage (Burgold et al., 2008). Moreover, through H3K27 demethylation *Jmjd3* facilitates elongation of RNA polymerase II at poised genes (Estaras et al., 2013).

The resolution of bivalent domains causes respectively stable gene activation (if H3K27me3 is erased) or repression (if H3K4me3 is erased). Hence the activity of opposing histone methyltransferases and demethylases targeting the same histone residue (e.g. H3K27) is tightly regulated. Moreover, H3K27me3 demethylases act in tight connection with H3K4me3 methylases to oppose the activity of PcG proteins and induce gene transcription (Cloos et al., 2008). Indeed, biochemical studies have revealed that *Jmjd3* and UTX are commonly found in the same multiprotein complex containing the H3K4 methyltransferases Mixed-lineage leukemia (MLL) -2 and -3 that belong to the Trithorax protein family. It has been proposed that once recruited at bivalent genes, H3K27me3 demethylases erase the H3K27me3 repressive marks while the MLL proteins catalyze H3K4 trimethylation to ultimately facilitate elongation of paused RNA polymerase II (Agger et al., 2007). Through this mechanism, H3K27-specific demethylases play an essential role to activate during development the Hox genes that are essential for axial patterning and antero-posterior embryonic development (Agger et al., 2007; Lan et al., 2007). In a similar fashion, the removal of H3K27me3 from the promoter of mesodermal genes, leads to the recruitment of β-catenin which, in turn, triggers Wnt-induced mesoderm differentiation (Ohtani et al.,

2013). *Jmjd3* has been also shown to associate with the transcription factor Tbx3 to mediate expression of *Eomes* a critical inducer of endoderm differentiation (Kartikasari et al., 2013). Finally, a recent study has shown that *Jmjd3* inhibits somatic cell reprogramming through the induction of cellular senescence by promoting active demethylation of the Cdkn2a locus (Zhao et al., 2013).

1.2.3. *Jmjd3* and cell cycle progression and cellular senescence

A number of recent reports have revealed an essential contribution of the PcG/jmjd3 axis in the regulation of the expression of the tumor suppressor locus *Cdkn2a*. *Cdkn2a* encodes for the cyclin-dependent kinase (CDK) inhibitor $p16^{INK4a}$ and the tumor suppressor $p19^{ARF}$. In young and healthy cells Cdkn2a is repressed by PcG-mediated H3K27 trimethylation : Upon aging or in response to oncogenic stimulation, *Cdkn2a* is strongly upregulated (Kotake et al., 2007; Agger et al., 2009; Barradas et al., 2009). $p16^{INK4A}$, like other members of the INK4 family, prevents G1-to-S transition by inhibiting the binding of CDK4 and CDK6 (CDK4/6) to cyclin D1 and preventing phosphorylation of the Rb protein. In its un-phosphorylated state Rb is complexed to members of the E2F family of transcription activators, preventing their function. Since the induction of target genes is required for the entry into S phase (Serrano et al., 2003; Walkley and Orkin, 2006), the block of E2F activity by *Cdkn2a* blocks G1-to-S transition. Instead, $p19^{ARF}$ exerts its tumor suppressor role by facilitating p53-dependent apopotsis. Specifically, $p19^{ARF}$ binds to the E3 ligase MDM2 preventing thereby its interaction with the p53 tumor suppressor. The net result of this regulation is the elevation of p53 protein levels, which ultimately sensitize cells to undergo programmed cell death (Sherr, 2001).

Cellular stress signals including hypoxia and oncogenic stimulation have been shown to induce *Jmjd3* expression in both mouse and human fibroblasts. This condition, in turn, contributes to the induction of $p16^{INK4A}$ and $p19^{ARF}$ expression and consequently to p53-dependent cell-cycle arrest and/or cell death (Lee et al., 2014; Agger et al., 2009; Barradas et al., 2009). These evidences implicate that *Jmjd3* may act as a tumor suppressor gene.

In addition to its role in the regulation of $p19^{ARF}$ expression, Jmjd3 has been directly involved in the regulation of p53 protein levels. In mouse neural stem cells a direct interaction between p53 and Jmjd3 was described (Sola et al.,2011). It was reported that Jmjd3 regulated the methylation status of p53, facilitating thereby its nuclear localization. Similar results were obtained in glioblastoma stem cells, where Jmjd3 promoted p53-dependent neuronal differentiation (Ene et al., 2012). Williams et al. have recently reported that *Jmjd3* expression is upregulated upon DNA damage and together with p53 gets recruited to p53 target genes to trigger cell apoptosis (Williams et al, 2014). Notably, Jmjd3 binding to p53 target genes did not affect local H3K27me3 levels, pointing to a demethylase-independent tumor suppressor activity exerted by Jmjd3. The modulation of p53 activity through the methylation of lysine residues at the C-terminus of the protein (K370, K372 and K382) has been previously reported for other histone demethylase including LSD1 and for the histone methyltransferases SET8 and SET9 (Huang et al., 2007; Chuikov et al., 2007; Shi et al., 2007).

1.2.4. *Jmjd3* gene regulation and target genes

In macrophage and microglial cells *Jmjd3* expression is induced by NF-kB and the JAK-STAT pathways in response to inflammatory stimuli (De Santa et al., 2007; Przanowski et al., 2014). In mammals, the NF-kB (Nuclear Factor kappa light-chain-enhancer of activated B cells) family of transcription factors consists of five related proteins, p50, p52, p65 (RelA), c-Rel and Rel B. NF-kB family members regulate many biological processes including proliferation, differentiation and survival/apoptosis. In unstimulated cells, NF-kB proteins are found in dimeric complexes in association with cytoplasmic IκB inhibitors that keep them in an inactive form. NF-κB activation, through either the classical or the non-canonical (alternative) pathway, is associated with the phosphorylation of IκB proteins that leads to their proteolytic degradation. Hence, NF-κB dimers are allowed to translocate to the nucleus and activate gene expression. A large set of stimuli can trigger the activation of the canonical NF-κB pathway including pro-inflammatory cytokines, pathogen-associated molecular patterns and antigens binding to T-cell and B-cell antigen

receptors. NF-κB target genes include cell cycle regulators (cyclin D1, cyclin D2, c-myc and c-myb), anti-apoptotic factors (caspase inhibitor of cIAP family of apoptotic proteins, BCl-2 family and Bcl-XL), pro-inflammatory cytokines (TNFα, IL-1, IL-6 and IL-12) and immunoregulatory factors (C3 complement, ICAM, VCAM, TCRα, β and MHC I) (Oeckinghaus and Ghosh, 2009; Jost and Ruland, 2006).

The Janus Associated Kinase (JAK)-Signal Transducer and activator of transcription (STAT) pathway is involved in the transduction of extracellular signals including cytokines and growth factors . STAT transcription factors (from STAT1 to STAT6) are essential regulators of cell proliferation, survival and differentiation in different cell types including lymphocytes. Deregulation of JAK-STAT function is commonly found in several B cell malignancies such as acute lymphocytic leukemia (ALL), chronic lymphocytic leukemia (CLL) and Hodgkin lymphomas (Mitchell and John, 2005; Furqan et al, 2013).

Upon inflammation, monocytes differentiate into functionally distinct M1 (classical macrophages) and M2 (alternatively activated macrophages) macrophages. Several reports have shown that Jmjd3 expression contributes to macrophage polarization facilitating the development of M2 cells. This is achieved through H3K27 demethylation at promoters of M2-specific genes (Ishii et al., 2009; Satoh et al, 2010; Tang et al., 2014). Stimulation of macrophages with IL-4 activates the JAK-STAT6 signaling pathway, which results in translocation of STAT6 into the nucleus where it regulates the expression of specific target genes including *Jmjd3* (Ishii et al., 2009).

Microglia cells are central nervous system monocytes that display functional features of glial cells. Activation of microglia during chronic inflammation is associated with several neurological diseases. A recent work has revealed cooperative activity of NF-κB and STAT transcription factors in the induction of *Jmjd3* gene expression (Przanowski et al. 2014). Specifically, LPS activation of microglia cells triggers NF-kB-dependent *Jmjd3* expression , which, in turn, contributes to the induction of several proinflammatory genes and cytokines including IL-6. The expression of cytokines by LPS-stimulated microglia cells activated in a autocrine/paracrine fashion the JAK-STAT pathway which ultimately through the STAT1/STAT3 heterodimer potentiated *Jmjd3* gene expression. Importantly, Jmjd3-dependent induction of imflammatory genes was independent of H3K27 demethyalse activity.

The genomic distribution of Jmjd3 and its relationship to H3K27me3, H3K4me3 and RNA polymerase II occupancy have been studied in different cell contexts. Genome-wide analysis in macrophages (De Santa et al., 2009) and neural stem cells (Estaras et al., 2013) have shown that Jmjd3 binds to both promoters and gene bodies where it facilitates RNA polymerase II elongation. In a similar fashion, recruitment of UTX to target sites favors first demethylation of the promoter sequence and later RNA polymerase II elongation within the gene body (Seenundun et al., 2010). These results support a model whereby Jmjd3 and UTX facilitate gene transcription at least part in part by altering the chromatin context of targeted loci. In support of this, it was shown that Jmjd3 and UTX can facilitate the recruitment of the chromatin remodeler Brg1 andRNA polymerase II elongation factors SPT6 and SPT16 (Miller et al., 2010).

Genomic distribution of Jmjd3 in activated murine macrophages has revealed a positive correlation between Jmjd3 binding and H3K4 trimethylation. Instead Jmjd3 is not commonly found at genes marked by H3K27me3 and bound by PRC2 (De Santa et al., 2009). This result suggests that H3K27me3 is not required for recruitment of Jmjd3 to its target genes.

Gene expression analyses in Jmjd3 mutant macrophages after LPS activation, revealed a subset of genes deregulated in mutant cells. Importantly, however, H3K27me3 distribution was largely unaffected in Jmjd3 mutant macrophages. (De Santa et al., 2007; Satoh et al., 2010). This results indicates that Jmjd3-dependent gene regulation is not strictly dependent on its demethylase activity.

1.2.5. *Jmjd3* and tumorigenesis

UTX and *Jmjd3* demethylase show a different expression pattern. Whereas UTX is ubiquitously and abundantly expressed in many cell types, Jmjd3 is expressed at low levels and peaks in response to a both cell extrinsic and intrinsic stimuli (De Santa et al, 2007; Burgold et al, 2007).

Somatic inactivating mutations of the *UTX* gene are among the most common genetic alterations identified in several human cancer types including both epithelial and hematopoietic malignancies (van Haaften et al., 2009; Van der Meulen et al, 2014).

Downregulation *of Jmjd3* has been described in various cancers including breast, prostate, lung and liver carcinomas as well as hematopoietic malignancies such as DLBCL, Burkitt‘s lymphoma and multiple myelomas (Agger et al., 2009; Anderton et al., 2011; Pereira et al., 2011; Svotelis et al., 2011;Shen et al., 2012). Importantly, a combination of whole exome and genome sequencing has recently identified Jmjd3 as a commonly mutated gene in Follicular B cell lymphoma (Pasqualucci et al., 2013). In such tumors mutations are predicted to cause inactivation of Jmjd3 function. Human *JMJD3* maps to chromosome 17p in close proximity to *TP53,* which is commonly lost in variety of cancers. Hence it cannot be excluded that cancers showing loss of genomic regions encompassing *TP53* may also lead to Jmjd3 inactivation.

Deregulated expression of the H3K27 methyltransferase Ezh2 is observed in a variety of solid cancers (such as breast, bladder, colon and prostate) and in hematopoietic tumors (Sparmann et al., 2006; Sauvageau and Sauvageau, 2010). Moreover, Ezh2 gain-of-function mutations are observed in over 20% of germinal center derived Diffuse Large B cell Lymphoma (DLBCL) and Follicular B cell Lymphoma (Morin et al., 2010; McCabe et al., 2012; Sneeringer et al., 2010; Beguelin et al., 2013). Instead, inactivating mutations of Ezh2 are commonly found in myeloid malignancies and T cell lymphomas (Ernst et al., 2010).

All together, these results indicate that cell-type and stage specific modulation of H3K27me3 is critical to control cell proliferation, differentiation and survival. Deregulation of such mechanism is commonly associated to malignant transformation.

1.3. B cell development

B-lymphocytes as all other blood lineages are generated from pluripotent hematopoietic stem cells (HSCs) in the fetal liver during embyogenesis and in the bone marrow after birth. Differentiation of early B cell progenitors to mature B cells is a stepwise process that is tightly controlled by extrinsic and intrinsic factors to ensure B cell functionality while avoiding self-reactivity. Extensive research over the past two decades has greatly improved our knowledge on the basic mechanisms underlying B cell lymphopoiesis. This has been possible through the identification of surface markers and molecular events associated with specific stages of B cell development. Since processes that occur during B cell development are often shared with those occurring in other cell lineages, the understanding of the molecular mechanisms underlying regulation of B cell lymphopoiesis has important biological implications especially in the fields of developmental and cancer biology.

1.3.1. Early B cell development

In mammalian, B cell development starts in the fetal liver in prenatal life and continues in the bone marrow after birth as a lifelong process where pluripotent HSCs differentiate through a tightly regulated hierarchical process. The derivation from HSC of multipotent progenitors (MPP) is followed by the generation of the first lymphoid-committed multipotent progenitors (LMPPs). The latter give rise to common lymphoid progenitors (CLPs), which represent a highly committed population of lymphoid precursors. The differentiation of early hematopoietic precursors enriched for pluripotent HSCs defined as lineage negative, stem-cell antigen 1 (Sca1) positive, c-Kit^{hi} cells (LSK subset) into B lineage-committed cells involves the expression of FMS-related tyrosine kinase 3 (FLT3) which is associated with the earliest expression of lymphoid-specific genes (Hardy and Hayakawa, 2001; Welner et al., 2010).

The protective function exerted by B and T cells relies on the ability to recognize a broad repertoire of foreign antigens through respectively the B- and T-cell antigen receptors (BCR and TCR). The BCR consists of two immunoglobulin heavy (H) and

light (L) chains which are linked via disulfide binds. Each Ig chain contains a variable region (V) that is responsible for the binding to the antigen and a constant region. The IgH chain constant region mediates the effector function of membrane-bound BCR, controlling ultimately B cell differentiation, proliferation and survival.

Diversification of the Ig repertoire relies on a recombinatorial mechanism called VDJ recombination that assembles in a stochastic fashion one of multiple copies (in the order of hundreds for the V segments) of V, D and J segments to generate the variable (V) region genes of IgH and IgL chains. VDJ recombination is catalyzed by the Recombination Activating Gene 1 and 2 (RAG1 and RAG2) proteins (McBlane et al., 1995; van Gent et al., 1995; Hoim et al., 1998). RAG proteins cleave DNA in a sequence-specific fashion at so-called Recombination Signal sequences (RSSs) flanking each V, D (for the IgH V gene) and J segment. Once cleaved at RSS sequences, V, (D) and J gene segments are joined together by enzymes involved in the non-homologous end joining repair pathway (NHEJ) (Li and Johnson, 1995).

To assemble the V_H gene, D_H and J_H gene segments are first joined together, followed by a V to DJ recombination step. For the V_L gene, V segments are directly joined to J segments. To further diversify the IgH repertoire non- templated *n* nucleotides are introduced respectively at the joining between V and D, and D and J segments by terminal deoxynucleotidyl transferase (Tdt).

VDJ recombination proceeds in a highly ordered fashion. Specifically, rearrangement of V_H genes precedes always that of V_L genes. IgH V gene rearrangements occur in pro-B cells, which are defined on the basis of surface markers as $B220^+CD43^+c\text{-}Kit^+IgM^-$ cells. Once a functional/productive V_H gene is assembled, expression of an IgH chain leads to the transition of the cells to the pre-B cell stage. In pre-B cells (defined as $B220^+CD43^-CD25^+IgM^-$) the expression of a pre-B cell receptor composed of an IgH chain paired to the surrogate IgL chains V-preB and l5 triggers a proliferative burst that leads to clonal expansion of the cells. This process is driven by Interleukin-7 (IL7) and self-aggregation of the pre-BCR (Martensson and Ceredig, 2000). Following this stage, pre-B cells exit the cell-cycle and reactivate expression of the Rag proteins to ultimately promote IgL chain V gene rearrangements. Once a functional IgL chain is produced, the correct pairing with the IgH chain will lead to the assembly on the surface of the cells of a BCR. The latter will stop further RAG-

mediated recombination events and drive the cells to become $IgM^{hi}IgD^{-/lo}B220^{lo}$ immature B cells. Immature B cells in the bone marrow undergo a stringent selection process that leads to the elimination of cells that express BCRs recognizing self antigens with high affinity. Alternatively, auto-reactive immature B cells may undergo IgL chain receptor editing, a process whereby secondary V_L gene rearrangements are induced to replace the IgL chain as an attempt to eliminate auto/self reactivity of the BCR (Nemazee, 2006; Edry and Melamed, 2004) In some instances, B cells expressing low-affinity self-reactive BCRs may evade clonal deletion and/or receptor editing and leave the bone marrow. As a result of chronic antigen stimulation such cells are usually in an anergic state (Cambier et al., 2007). Finally immature B cells that express functional, non-autoreactive BCRs leave the bone marrow and reach, through the blood stream, peripheral lymphoid organs such as spleen and lymph nodes to eventually complete their maturation (Rajewsky, 1996; Allman et al., 1993) (Figure 3).

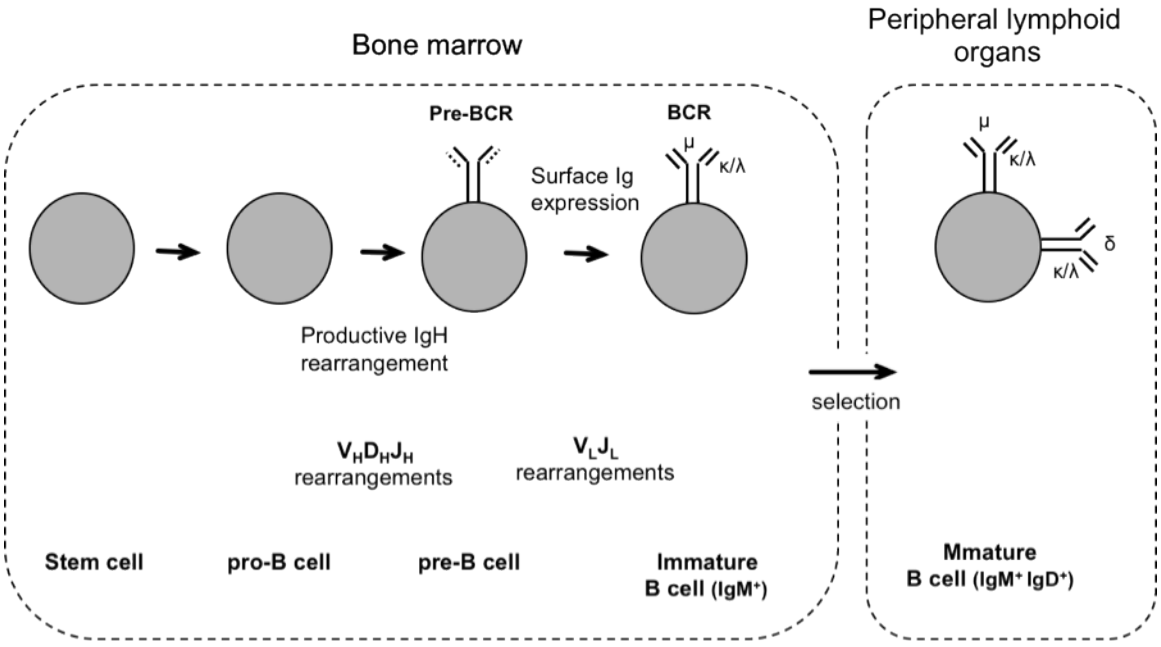

Figure 4. Schematic view of B cell development. Postnatal B cell development starts in the bone marrow, where pro-B cells derived from hematopoietic stem cells undergo initial VDJ recombination at the IgH locus. Upon successful rearrangement of a productive IgH V-gene, the IgH chain pairs to surrogate IgL chains to form the pre-BCR receptor. After pre-BCR driven pre-B cell proliferation, cells undergo IgL chain V gene rearrangements. Once productive IgH and IgL chains are expressed and are able to pair, they form a BCR that is expressed on the B cell surface. The latter cells are defined immature/naïve B cells. The egress of immature B cells from the bone marrow is guaranteed only if cells do not express an autoreactive BCR (Adapted from Rajewsky, 1996).

1.3.2. Peripheral B cell development

1.3.2.1. Transitional B cells

Around 20 million of short-lived $B220^{+}IgM^{hi}IgD^{-}$ immature B cells are generated every day in the bone marrow of wild-type adult mice. Of those only 10% reaches secondary lymphoid organs and the majority of the immigrants die after few days. Therefore only a small fraction of immature B cells completes its development to become long-lived mature B cells (Rajewsky, 1996). Immature B cells, also called transitional B cells, typically express high levels of IgM in combination with the early

differentiation marker AA4.1/CD93 the Heat Stable Antigen (HAS)/CD24 and low levels of B220. Based on the expression of CD23 and IgM, $B220^{lo}AA4.1^{+}$ transitional B cells are divided into different subsets: Transitional T1 cells ($IgM^{hi}CD23^{-}$) represent the earliest immature B cells reaching the spleen. The latter B cells develop into transitional T2 cells ($IgM^{hi}CD23^{+}$) which are the direct precursors of long-lived mature B cells. There exist also a population of so-called transitional T3 cells ($IgM^{lo}CD23^{+}$), but their origin and function is yet to be fully understood (Allman et al., 2001).

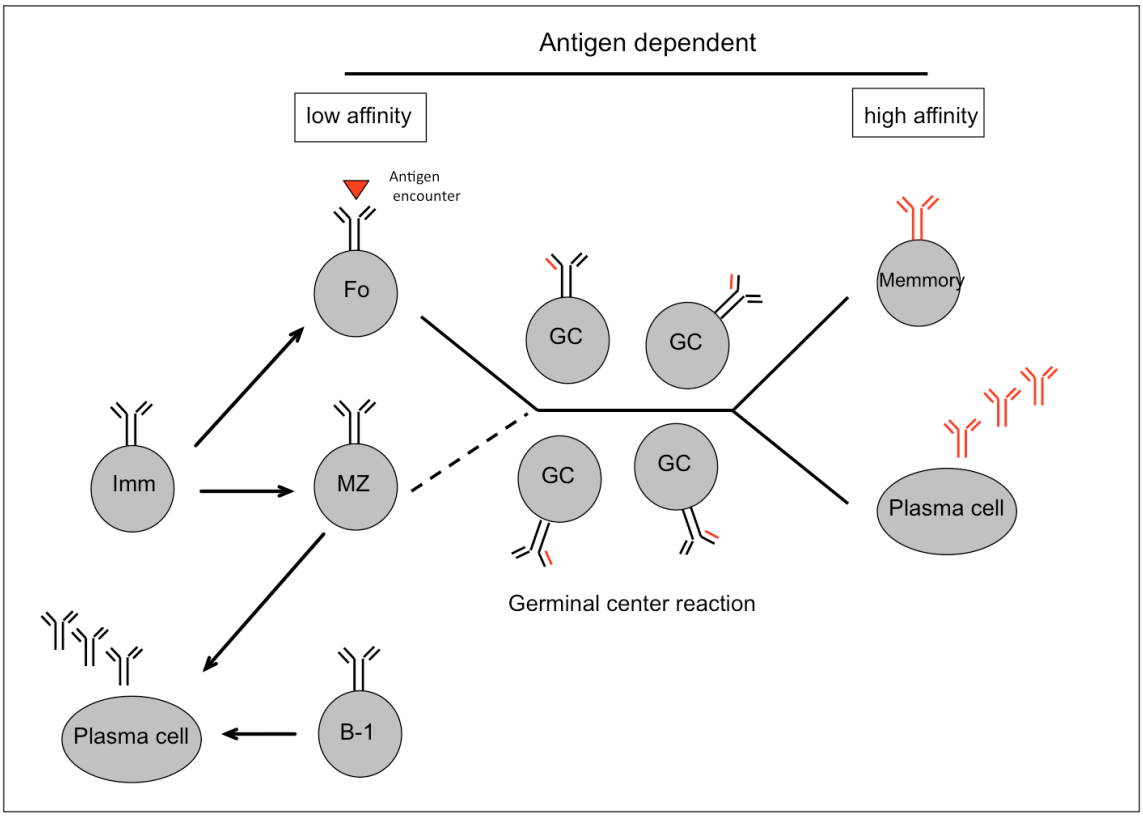

Figure 5. Peripheral B cell development. Newly generated immature B cells expressing functional, non-autoreactive, surface BCR migrate to secondary lymphoid organs where a fraction of them will complete differentiation to become respectively Follicular (Fo), Marginal Zone (MZ) or B-1 B cells. MZ and B-1 B cells are mainly recruited into T-cell independent immune response, giving rise ultimately to short-lived plasma cells. Fo B cells (and in part MZ B cells) are the major subset recruited into T-cell dependent immune responses, Upon antigen recognition and T-cell help, Fo B cells get recruited into germinal centers where they clonally expand and mutate their Ig V genes. Stringent antigen-driven selection leads only few B cells expressing high affinity BCRs to survive and exit the GC reaction as long-lived memory B cells or plasma cells.

1.3.2.2. Mature B cells

Mature B cells in the mouse are divided into three major subsets represented respectively by Follicular, marginal zone (MZ) and B-1 B cells.

1.3.2.2.1. Follicular B cells

Follicular (Fo) B cells also called B-2 B cells, represent the major population of mature B cells. They are identified as $IgM^{lo}IgD^{+}CD21^{+}CD23^{+}$ cells. Fo B cells are located in all secondary lymphoid organs including the spleen, lymph nodes and bone marrow.(Pillai et al., 2004). Fo B cells reside respectively within the white pulp of the spleen and the cortical area of lymph nodes where they home to defined regions called follicles. Fo/B-2 B cells recirculate through the blood stream. They are involved in both T-cell dependent and T-cell independent immune responses. In a T-cell dependent response, recognition of antigen by the BCR promotes the recruitment of Fo B cells into the germinal center (GC) reaction. This process is strictly dependent on $CD4^{+}$ T cells, which recognize through their TCR the processed antigen presented by antigen-specific B cells via MHC-class II molecules. As a result of antibody affinity maturation occurring during the GC reaction, highly selected Fo B cells exit the GC to become long-lived memory B cells or antibody-secreting plasma cells. Fo B cells can also directly differentiate into short-lived low-affinity plasma cells after recognition of T cell-independent antigens (Casola, 2007).

1.3.2.2.2. Marginal zone B cells

MZ B cells ($IgM^{hi}IgD^{lo}CD21^{hi}CD23^{lo}$) are self-replenishing mature B cells (Martin and Kearney, 2002). MZ B cells reside in close proximity to the marginal sinus in the spleen, surrounding B cell follicles. MZ B cells are recruited into both T-cell dependent and –independent immune responses. Given their close vicinity to the bloodstream, MZ B cells represent the first barrier to blood-born pathogens. In this context, MZ B cells get rapidly activated through their BCR, proliferate and ultimately differentiate into low-affinity antibody secreting plasma cells (Cinamon et al., 2008; Martin and Kearney, 2002).

1.3.2.2.3. B-1 B cells

B-1 B cells ($IgM^{hi}IgD^{lo}CD21^{lo}CD23^{lo}$) represent a subset of mature B cells which resides primarily in body cavity serosa including pleural and peritoneal cavities (Casola, 2007). According to CD5 expression, B-1 B cells are divided respectively into B-1a ($CD5^{+}$) and B-1b ($CD5^{-}$) B cells (Stall et al., 1992).

B-1a B cells originate from the para-aortic splanchnopleura in early mouse embryos. At later stages of embryonic development, the fetal liver represents the major source of B-1a B cells. Fetal liver-derived B-1a B cells represent the major subset of B-1a B cells found in post-natal mice (Dorshkind and Montecino-Rodriguez, 2007). Indeed, de novo B-1a B cell generation is highly inefficient in the bone marrow of adult life (Herzenberg, 2000).

B-1b B cells are mainly originated from HSCs residing in the fetal liver. However, differently from their B-1a counterparts, B-1b B cells get also efficiently generated from HSC residing in the bone marrow of adult mice (Dorshkind and Montecino-Rodriguez, 2007). In contrast to continuous *de novo* generation of B-2 B cells from bone marrow precursors, B-1 B cells have self-renewal capacity and undergo limited proliferation to sustain the population size throughout life. B-1 B cells express BCRs that recognize with low affinity self-antigens that cross-react with microbial components. As a result of this, B-1 B cells are the main producers of low-affinity so-called natural IgM antibodies that represent a first barrier against bacterial infections (Hardy, 2006). Upon recognition of T cell independent antigens B-1 B cells are recruited together with MZ B cells into an immune response that leads ultimately to the generation of short-lived antigen-specific IgM- and IgG3-secreting plasma cells (Baumgarth, 2010).

1.3.2.3. Determinants of peripheral B cell development

Differentiation of immature transitional B cells into functionally distinct mature B cell subsets is an essential step in development of B cells and has been intensely investigated for a decade. Maturation of transitional B cells to become respectively

Fo, MZ and B-1 B cells is mediated by a limited number of receptors, signaling pathways and transcription factors that are outlined below.

1.3.2.3.1. The BCR

BCR signaling is an important component controlling the maturation of transitional B cells. Using a number of independent experimental approaches based primarily on the analysis of BCR transgenic and gene targeted mice, it has been proposed that strength of the BCR signal controls the fate of developing immature B cells.

Summarizing a large body of evidences it has been proposed that immature B cells require a stronger signal to develop into B-1 B cells as compared to MZ B and Fo B cells (Casola et al., 2010; Pillai et al., 2004, Casola, 2007) Fo B cells have been suggested to require the lowest BCR signal among all B cell subset, for their development. Whether differences in signal strength reflect quantitative rather than qualitative differences remains to date a highly debated matter. Moreover, it remains to be demonstrated whether antigen plays a role in the selection of immature B cells (Pillai et al., 2004, Casola, 2007). In this regard, recent high throughput antibody repertoire analysis in mouse mature B cell subsets exclude a major contribution of antigen in the selection of short lived immature B cells (Kaplinsky et al 2014).

1.3.2.3.2. BAFF

B-cell activating factor (BAFF) is a member of the tumor necrosis factor family (TNF) that is produced by myeloid lineage cells and plays an important role in the generation and maintenance of mature B cells (Schiemann et al., 2001, Schneider and Tschopp, 2003; Mackay and Browning; 2002; Khan, 2009). BAFF binds to three different receptors: transmembrane activator, calcium modulator, and cyclophilin ligand interactor (TACI); B cell maturation Ag (BCMA); and BAFF-R. BAFF-R is the main receptor that controls maturation and survival of mature B cells. Indeed, BAFF-R mutant mice display a significant reduction in the number of transitional and Fo B cells. An even more dramatic effect was observed for the MZ B cell compartment

which was almost lacking in BAFF-R mutant mice. In sharp contrast, development and persistence of B1-B cells was shown to be independent of BAFF (Crowley et al., 2008: Scholz et al., 2008). BAFF simulation leads to the rapid activation in B cells of the serine/threonine kinase AKT that promotes cell growth, glycolysis and protein synthesis through activation of mammalian target of rapamycin (mTOR) pathway (Matsuzawa et al., 2008; Patke et al., 2006;). Moreover, signaling through BAFF-R induces the expression of anti-apoptotic factors such as B-cell chronic lymphocytic leukemia/lymphoma-2 (Bcl-2) and Bcl-extra long (Bcl-xl) (Woodland et al., 2006). Importantly, recent work has shown a critical intersection between BAFF-R and BCR signaling with the tyrosine kinase Syk being the key signaling molecule connecting the two pathways (Schweighoffer et al., 2013). These studies support a model whereby BAFF-R coopts the BCR to sustain the survival of mature B cells.

1.3.2.3.3. NFAT

Nuclear factor of activated B cells (NFAT) is a family of five transcription factors that regulate the transcription of pro-survival genes in lymphocytes (Rao et al, 1997; Crabtree and Olson, 2002; Muller and Rao, 2010). NFAT family members NFATc1, NFATc2 and NFATc3 are expressed in mature B cells where they get activated in response to BCR cross-linking or CD40 signaling (Verweij et al., 1990; Choi et al., 1994). The latter stimuli induce a transient rise in intracellular Ca^{+} levels, which in turn through the Calmodulin-calcineurin axis promote nuclear relocalization and hence activation of NFAT transcriptional function. NFATc1 is essential for B-1a B cell development and survival(Berland and Wortis, 2003).

1.3.2.3.4. Pax5

The transcription factor Pax5 is a master regulator of B cell development. Pax5 is expressed starting from pro-B cells and remains active throughout B cell development (Fuxa and Busslinger, 2007). Pax-5 gets silenced when B cells differentiate ultimately in antibody-secreting plasma cells. In early B cell precursors Pax-5 is essential to enforce B cell identity by sustaining the activity of other B-lineage transcription factors

(such as Ebf1 and E2A), preventing at the same time expression of determinants (such as Notch-1) driving alternative lineage fates (e.g. T cells) (Nutt et al, 1999; Cobaleda et al., 2007a; Revilla et al., 2012; Souabni et al., 2002). In pro-B cells, Pax5 is critical for VDJ recombination. In particular, it was shown that Pax5 is essential for IgH locus contraction. The latter process is critical to allow RAG proteins to employ distal V_H genes in the recombination process (Fuxa et al., 2004). Elegant experiment in the Busslinger lab have also shown that PAX5 is required to sustain B cell identity in mature B cells. Indeed conditional inactivation of Pax5 in mature B cells caused a major transcriptional reprogramming of mutant cells that could commit to other cell types including T cells and macrophages (Cobaleda et al., 2007b). Pax5 acts both as a transcriptional activator and repressor. Among the genes induced by Pax5 there are critical effectors of the BCR signaling pathway through which it likely controls B cell survival. Conversely, Pax5 represses genes that are expressed in terminally differentiated plasma cells and in other cell lineages to enforce B cell identity (Nera et a;l., 2006).

1.3.2.3.5. Notch2

In mammals, the family of Notch receptors includes 4 members (Notch-1 to -4), which recognize 5 ligands of the Jagged and Delta-like (Dll) families respectively. Notch proteins are membrane-bound receptors that get cleaved in response to ligand interaction. Intracellular cleaved Notch translocates to the nucleus where it regulates gene expression through the transcription factor RBPjk (Kopan and Ilagan, 2009). Notch signaling regulates multiple cell fate decisions in hematopoiesis (Radtke et al., 2004a,b).

Notch2 is the main Notch member involved in the regulation of B cell development. Work performed on Notch2 deficient mice has revealed an essential function for the transcription factor (and its ligand Dll-1) in the development of MZ B cells (Saito et al., 2003). This conclusion was further confirmed analyzing gene-targeted mice lacking critical regulators of the Notch pathway such as RBP-JK and MINT (Tanigaki et al., 2002; Kurado et al., 2003). Recent work has established a critical role for notch2 in MZ B cell maintenance. Indeed, acute inactivation of Notch2 in established MZ B cells

led to the rapid disappearance of B cells residing in the MZ. Interesting such B cells did not undergo apoptosis but rather migrated away from the MZ, indicating that Notch2 is essential for the retention of B cells in the MZ area (Simonetti et al., 2013).

1.3.3. B cell immunity

B cell immune responses are classified respectively as T-cell dependent (TD) and T-cell independent (TI) depending on the nature of the antigens encountered through their BCRs. The end result of a B cell immune response is the production of soluble, antigen-specific, antibodies, which contribute to the establishment of humoral immunity. Soluble antigens are essential for a fully functional immune system as they contribute to the clearance of pathogens in multiple ways including complement fixation, phagocytosis, and prevention of entry into target cells.

1.3.3.1. T-cell independent immune responses

In T-cell independent (TI) immune responses, B cells get activated and differentiate into short-lived plasma cells, without the help of T cells. All major B cell subsets can potentially get recruited into TI immune responses. Given their close proximity to the blood stream, MZ B cells represent the elective subset that is activated in response to blood borne pathogens. During T-cell independent immune responses B cells get activated as a result of the triggering of different types of receptors, depending on the type of antigens they interact with. There are two main types of TI antigens:

Type-1 antigens (TI-1): Trigger a polyclonal B cell response that results from the stimulation of receptors other than the BCR. An example of TI-type 1 antigen is lipopolysaccharide (LPS) a constituent of the cell wall of Gram-negative bacteria. In the presence of high levels of LPS, activation of B cells through Toll-like receptor-4 (TLR) is sufficient to trigger a polyclonal unspecific antibody response. In case LPS levels are in the low range (and hence not sufficient to activate cells only through the TLR4 receptor) only B cells recognizing the antigen through the BCR will get

activated. In this case the antibody response with be antigen (LPS)-specific. Both immature and mature B cells can get recruited in TI-type 1 immune responses.

Type-2 antigens (TI-2): share in common highly repetitive structures. Polysaccharides of encapsulated bacteria including *S. pneumonia, N.meningitidis* and *H. influenza* represent typical examples of TI-2 antigens. Recognition of highly repetitive antigens in a BCR-dependent fashion leads to potent cross-linking of the BCRs, which ultimately triggers terminal differentiation. B-1 B cells and MZ B cells represent the major B cell subsets recruited into TI type-2 immune responses.

1.3.3.2. T-cell dependent immune responses

T-cell dependent immune responses are predominantly triggered by protein antigens that are recognized by the BCR through one of its epitopes. Within the B cells, protein antigens get cleaved in smaller peptides, which are in turn loaded onto MHC-class II molecules and presented to $CD4^+$ T cells. Interaction between antigen-specific B and T cells at the border between T cell and B cell zones leads to full activation of B cells which in turn migrate back to the follicle to nucleate a germinal center (GC). In the GC, clonal expansion of antigen specific B cells is accompanied by substantial genetic rearrangements occurring at the Ig loci. Specifically, Ig somatic hypermutation (SHM) leads to the introduction of non-templated mutations within the V region of Ig genes. At the same time double strand breaks accumulating at IgH constant region genomic loci allow the substitution of Cμ with that of another isotype through a process called Ig class switch recombination (CSR). Both Ig SHM and CSR are catalyzed by Activation induced cytidine Deaminase (AID) (Muramatsu et al., 2000). As a result of Ig SHM, the progeny of the founder antigen-specific B cells that got recruited into the GC undergoes a stringent selection process that allows only very few B cells, namely those expressing high affinity BCRs, to exit the GC after differentiating into long-lived memory B cells of plasma cells (Basso and Dalla-Favera, 2010; Klein and Dalla-Favera, 2008; Rajewsky, 1996).

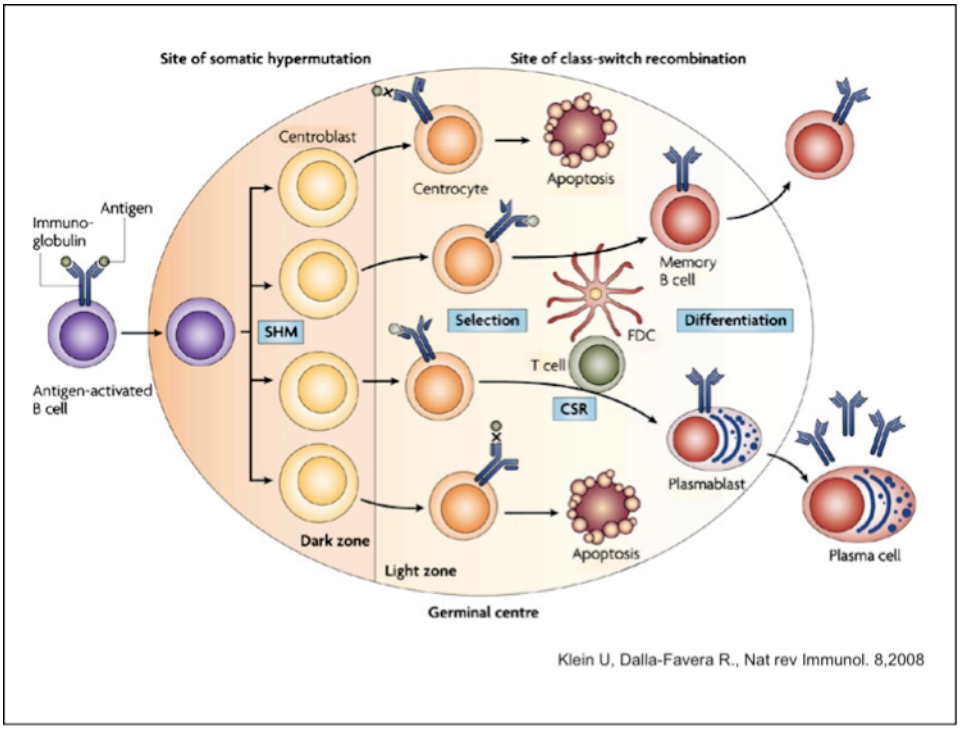

Figure 6. Schematic view of the GC reaction. During a T cell dependent immune response, antigen-specific B cells receive T cell help and initiate a germinal center reaction. In GCs, B cells initially proliferate vigorously within the "dark zone" while they undergo Ig V gene somatic hypermutation (SHM). In the light zone, GC B cells exit cell-cycle and undergo stringent selection based on the recognition through the BCR of antigen presented by Follicular Dendritic Cells (FDC). Capture of antigen and presentation to Follicular helper T cells represents a critical step in positive selection of GC B cells. Iterative cycles of proliferation, Ig SHM and selection allows the generation of B cells expressing high affinity BCrs. Ultimately, the latter cells exit the GC reaction after differentiating respectively into long-lived memory B cells or terminally differentiated plasma cells. The output of the GC reaction includes B cells that have undergone Ig class switch recombination that allows the exchange of the effector function of the immunoglobulins expressed/secreted by post-GC B cells.

1.3.4. Terminal B cell differentiation

Plasma cells represent an essential component of humoral immunity. Depending on their lifespan, antibody-secreting cells can be either short-lived or long-lived. The former are mainly generated during T-cell independent immune response. Short-lived plasma cells accumulate predominantly in extrafollicular regions of secondary lymphoid organs. Instead, long-lived plasma cells are generated as a result of a T-cell dependent immune response. Long-lived plasma cells reside often for a life-long time in the bone marrow where they keep secreting high affinity antibodies. Within the bone marrow, plasma cells occupy specific niches where they receive extrinsic signals that are required to sustain their survival. The Bcma/Mcl1 axis has been recently shown to play a crucial role in the regulation of bone marrow plasma cell survival (Peperzak et al., 2013). The differentiation of B cells into plasma cells is controlled by a complex transcriptional regulatory network which has been heavily investigated in the past decade. Three major transcription factors, namely Blimp1/Prdm1, IRF4 and Xbp1, are required for plasma cell differentiation and maintenance. Terminal differentiation requires also stable repression of the master regulator of B cell identity, Pax5 (Nera et a;l., 2006).

1.3.4.1. Master regulators of PC differentiation

1.3.4.1.1. *B lymphocyte-induced maturation protein-1 (Blimp-1)*

Blimp1 is a transcription factor that is encoded by the *Prdm1* (Positive regulatory domain-containing 1) gene (Sciammas and Davis, 2004). Blimp-1 represses the expression of Bcl6 (Calame et al., 2003), the master regulator of the GC response (Cattoretti et al., 2005) and of Pax5 (Lin et al., 2002). Through this mechanism, Blimp-1 enables the exit of B cells from the GC reaction (BCL6) and the silencing of the B-cell specific program (Pax5). Blimp1 is also critical to induce the expression of Xbp-1, which is strictly required to sustain the unfolded protein response in cells secreting large amounts of antibodies (Calfon et al., 2002). Although Blimp-1 is critical for terminal B cell differentiation (Shapiro-Shelef et al., 2003), its expression is not strictly required to trigger the earliest steps of this process (Kallies et al., 2007).

1.3.4.1.2. *X-box binding protein-1 (Xbp-1)*

Xbp-1 is a basic-leucine zipper transcription factor that is expressed in many cell types. Expression of Xbp-1 is induced upon terminal B cell differentiation (Reimold et al., 2001). Activation of Xbp1 transcriptional activity requires post-transcriptional modification of its mRNA through an unconventional splicing step mediated by the IRE1 endoribonuclease (Calfon et al., 2002). The Xbp1 transcription factor induces the expression of a large set of genes that counteracts proteotoxic stress linked to the high rate of Ig synthesis (Cenci and Sitia, 2007; Cenci, 2012; Shaffer et al., 2004)

1.3.4.1.3. *Interferon regulatory factor 4 (Irf4)*

Interferon Regulatory factor 4 (IRF) is a member of the IRF family, which plays crucial functions at different stages of B cell development (Shaffer et al., 2009). In pre-B cells, Irf4 downregulates pre-BCR signaling through induction of Ikaros and Aiolos transcription factors (Ma et al., 2008). In peripheral B cells, IRF4 plays a critical role in the regulation of the Fo vs MZ B cell fate. Recent work has demonstrated that IRF4 regulates Notch2 protein expression and thereby controls MZ B cell differentiation (Simonetti et al., 2013). Irf4 is required for GC nucleation (Ochiai et al., 2013) and function (Klein et al., 2006; sciammas et al., 2006). Irf-4 deficient mice do not produce antigen-specific antibodies in response to immunization with T-cell dependent antigens. This impairment is in part due to the failure to form GCs and in part to the essential role played by IRF4 in plasma cell differentiation (Sciammas et al., 2006; Klein et al., 2006; Ochiai et al., 2013). IRF4 controls the proliferation and survival of B cells upon BCR cross-linking or LPS treatment *in vitro,* whereas proliferative responses to anti-CD40 stimulation were unaffected by Irf4 inactivation (Mittrucker et al., 1997). IRF4, in cooperation with STAT3, upregulates the expression of *Prdm1*/*Blimp-1* in an IL-21-dependent mechanism (Kwon et al., 2009), linking in this way two central transcription factor required for terminal B cell differentiation. IRF4 plays also a critical role in Ig CSR through regulation of AID expression (Sciammas et al, 2006; Klein et al, 2006). Unlike other IRF family members, IRF4 expression is upregulatd by mitogenic stimuli including BCR engagement, LPS, CD40 ligand and IL-4, through both the NF-κB and JAK-STAT pathways (Mittrucker et al.,1997; Gupta

et al., 1999). In mature B cells (including GC B cells) IRF4 expression levels are tightly controlled (Ochiai et al., 2013) by different mechanism that possibly microRNAs (Gururajan et al., 2010).

1.3.5. Memory B cells

Memory B cells are long-lived, antigen-specific B lymphocytes that are preferentially, but not exclusively (Takemori et al., 2014) generated as a result of the transition of B cells through the GC reaction (Rajewsky, 1996). The molecular mechanisms underlying memory B cell differentiation are yet poorly understood. Scheeren and co-workers have suggested that activation of the STAT5 transcription factor in late GC B cells can drive memory B cell differentiation (Scheeren et al., 2005). Recent work by the McHeyzer-Williams group has revealed the existence of different transcriptional programs sustaining the identity of different types of memory B cells differing for the IgH chain isotype expressed by the cells (Wang et al., 2012). Finally, whether cognate antigen recognition is required for the maintenance of the memory B cell pool remains still highly controversial (Yoshida et al., 2010).

1.4. Role of histone demethylases in hematopoiesis

Functional in vivo studies on histone demethylases have started to unravel the role exerted by these proteins in the control of fundamental biological processes such as stem cell self-renewal, proliferation, differentiation as well as malignant transformation (Kooistra and Helin, 2012). Conditional inactivation of the H3K4/K9me3 demethylase Lsd1 resulted in severe pancytopenia due to the combined defects on early and late hematopoietic differentiation. Deletion of Lsd1 in HSCs caused a severe defects in HSC self-renewal and the loss of myeloid progenitor cells. Bu acting at the level of megakaryocyte-erythroid progenitors, Lsd1 inactivation also interfered with their differentiation into granulocytes and erythrocytes. Finally, Lsd1 inactivation prevented

differentiation of HSC cells by preventing the repression of hematopoietic stem/progenitor-specific genes (Kerenyi et al., 2013).

The H3K27 demethylase UTX has also been implicated in erythroid, megakaryocyte and granulocyte differentiation (Thieme et al., 2013). Utx is expressed in hematopoietic stem and progenitor cells as well as in differentiated blood lineage cells. Utx deficient mice display severe anemia leading to compensatory extramedullary erythropoiesis (Liu et al., 2012; Thieme et al., 2013).

Although several studies have suggested a critical role for Jmjd3 in M2 macrophage polarization (De Santa et al., 2007; Satoh et al., 2010; Ivashkiv, 2013), Jmjd3 function in hematopoietic cells has been yet poorly studied. Using fetal liver transplantation studies, Satoh and colleagues have shown that *Jmjd3*$^{-/-}$ HSCs gavre rise to relatively normal proportions of B- and T-lymphocytes, dendritic cells, natural killer cells, neutrophils and macrophages in the spleen. Moreover, activation of Jmjd3-deficient B with mitogens displayed apparently a normal proliferative response (Satoh et al., 2012). In the present study we have extended this initial findings using a conditional knock-out approach to study the intrinsic role of JMJd3 in B cell development.

2. Materials and Methods

2.1. Mice

Mice strains were housed and bred at IFOM-IEO Campus Animal facility. Animal handling was performed following recommendations of European Community.

2.1.1. Mice strains

JMJD3^{fl} conditional KO mice were bred to Mb1-Cre (Hobeika et al., 2006) and PGK-Cre (Lallemand et al., 1998) strains. These two Cre lines have C57BL/6 genetic background.

2.1.1. Mice immunization

8-10 week old mice were immunized with Alum (Imject ® Alum, aqueous solution of aluminium hydroxide (40 mg/ml) and magnesium hydroxide (40 mg/ml), Pierce) precipitated NP27CGG (100 µg per mouse, 4-Hydroxy-3-nitrophenylacetyl hapten conjugated to chicken gamma globulin, Biosearch Tech.) intraperitoneally.

2.2. DNA methods

2.2.1 Isolation of genomic DNA from mouse-tail biopsies

Tail tips collected by animal facility were incubated in 400 µl of tail lysis buffer containing Proteinase K (100 µg/ml) at 56˚C overnight, shaking at 700 rpm. Tissue lysate was transferred into a new tube and 1 ml of isopropanol was added and mixed

by inverting the tubes several times. After centrifugation at full speed for 10 minutes, DNA pellet was air-dried and resuspended in 200 µl of miliQ water.

Tail lysis buffer

100 mM Tris-HCl

5 mM EDTA

200 mM NaCl

0.2 % SDS

2.2.2. Polymerase chain reaction (PCR)

PCR reactions were performed in three steps: denaturation of DNA template, primer annealing and polymerization (Table 2). Reactions were prepared usually in a total volume of 25 µl with 0.2 mM dNTPs, 0.5 mM primers, DNA template, 0.5 U of GOTaq® DNA polymerase, 25 mM $MgCl_2$ and 1X GoTaq® Felexi buffer.

Table 2. Thermal cycling of PCR amplification

Step	Temperature	Time	Number of cycles
Initial Denaturation	95 ˚C	2 minutes	1 cycle
Deanturation	95˚C	0.5 minute	
Annealing	variable*	0.5 miute	30 cycles
Extension	72˚C	1minute/ kb	
Final extension	72˚C	5 minutes	1cycle
Hold	4˚C		

* The annealing temperature for each pair of primers was optimized based on the sequence of primers.

PCR reactions were run on an agarose gel in presence of 1X Tris-acetate-EDTA buffer (TAE), the percentage of agarose was defined by the size of the DNA fragments:

DNA fragment size	% agarose
< 100 bp	3 %
0.1 to 2.5 kb	2 %
2.5 to 15 kb	1 %
15 to 30 kb	0.4 %

2.2.3. Genotyping sterategy

PCR was performed on genomic DNA extracted from tail biopsies of the mice from different strains using primers listed in Table 3. Reactions were run in automatic thermocycler GeneAmp PCR System9700 (Applied Biosystems).

Table 3. Genotyping primers, annealing temperatures and amplicons

Primers (5'-3')		**Annealing**	**Amplicon**
JMJD3 Frt-βgeo vs. WT			
JBaygd2	AGGATACAGGAGCCACGCG		
GT3 Rev	TCCGGAGCGGATCTCAAAC	60	282 bp
JMJD3 Frt-βgeo vs. Frt-βgeo Cre deleted			
PolyA Fw	TCTTATCATGTCTGGATCCGG		
LoxP R1	GGAAGAGCAGATGAGACTGG	60	132 bp
JMJD3 Frt-βgeo vs. FLP deleted			
JBaygd2	AGGATACAGGAGCCACGCG		
JBaygr2	TGACTCTCCACTCGATCACCC	60	259 bp
JMJD3 fl vs. WT			
Jmjd3 Flox Fw2	GTCTTCTCTGTCCATTGCTGTC		
Jmjd3 Flox Rv	GGCTCTGTTAGGTACTGCCAG	58	169 bp
JMJD3 Cre deleted allele			
JBaygd2	AGGATACAGGAGCCACGCG		

LoxP R1	GGAAGAGCAGATGAGACTGG	60	322 bp
Mb1-Cre			
Mb1-Cre Fw	CCCTGTGGATGCCACCTC		
Mb1-Cre Rv	GTCCTGGCATCTGTCAGAG	58	430 bp
PGK-Cre*			
PGK-CreFw	GCCTGCATTACCGGTCGATGCAACGA		
PGK-Cre Rv	GTGGCAGATGGCGCGGCAACACCAT	58	700 bp

* Mb1-Cre primers can also be used for PGK-Cre genotyping.

2.2.4. Plasmid preparation

Bacteria were grown overnight at 37˚C incubator and plasmids were isolated and purified with the Qiagen Plasmid Mini or Maxi kits (Qiagen). The alkaline lysis based purification procedure was performed according to the manufacturer's protocol.

2.3. RNA methods

2.3.1. RNA extraction and cDNA synthesis

Total RNA was isolated from the cells with the Qiagen RNeasy Micro and Mini kits (Qiagen) according to the instructions of the manufacturer. Finally RNA was resuspended in RNAse-free water and quantified with the NanoDrop ND-1000 spectrophotometer (Thermo Fisher Scientific).

CDNA synthesis was carried out using SuperScript® VILO™ kit (Invitrogen) following the instructions of the supplier. In general, 200 ng of total RNA was reverse transcribed using SuperScript® III Reverse transcriptase and SuperScript® VILO™

Master Mix in 20 µl of reaction volume. Samples were incubated at 25˚C for 10 minutes, 42˚C for 1 hour and 85˚C for 5 minutes.

2.3.2. Quantitative real-time PCR (qRT-PCR)

qRT-PCR was performed on LightCycler® 480 II real-time PCR system (Roche) using SYBR Green I Master Mix. Reaction conditions were 95˚C for 10 minutes, 45 cylces of 95˚C for 1 second, 60˚C for 10 seconds, 72˚C for 1 second. Correct PCR products were confirmed by melting curve analysis. Each sample was analyzed in triplicates and normalized to Ribosomal Protein Large, P0 (RPLP0) housekeeping gene (Laborda 1991; Akamine et al., 2007). Normalization was used to correct sample-to-sample variation in RNA concentration. Relative mRNA amounts were calculated by comparative cycle threshold (Ct) method using formula $2^{-\Delta Ct}$. Primers are listed in Table 4.

To measure the deletion efficiency of *JMJD3*, qPCR analysis was performed on genomic DNA. Primers were used to detect the remaining *JMJD3* exon 4 that is flanked by LoxP sites. Glyceraldehyde-3-Phosphate Dehydrogenase (GAPDH) gene was used as a loading control for genomic DNA qPCRs (Table 4).

Table 4. Primers sequences for quantitative PCR analysis

Rplp0 Fw	TTCATTGTGGGAGCAGAC	RNA
Rplp0 Rv	CAGCAGTTTCTCCAGAGC	RNA
p16/Ink4A Fw	GAACTCTTTCGGTCGTACC	RNA
p16/Ink4A Rv	CCAGCGTGTCCAGGAAG	RNA
p19/Arf Fw	GCTCTGGCTTTCGTGAACATG	RNA
p19/Arf Rv	TCGAATCTGCACCGTAGTTGAG	RNA
Irf4 Fw	CAATGTCCTGTGACGTTTGG	RNA
Irf4 Rv	GGCTTCAGCAGACCTTATGCT	RNA
Tp53 Fw	CAAAAGAAAAACCACTTGAT	RNA
Tp53 Rv	CGGAACATCTCGAAGCGTTTA	RNA
Jmjd3 5F	CAGCTCCTTTACCCCCATCT	RNA
Jmjd3 6R	TTCCTCACTGTCGTGCTCTG	RNA

Jmjd3 7F	CCCAGCTCTGGAACTTTCAT	RNA
Jmjd3 8R	CTAAGGCCCTCCTCTCCTGA	RNA
Jmjd3 9F	GTCTGCCACTCCCTCCAC	RNA
Jmjd3 10R	CCATGGCTCTCTGCTCCT	RNA
Jmjd3 10F	CGTTTCACCAGCAGCATCTA	RNA
Jmjd3 11R	AAAATGGTTTCCGACTGCTG	RNA
Jmjd3 11F	ATG GCAGACCTCACCATCA	RNA
Jmjd3 13R	CCCCTGATGACGGTGATG	RNA
Jmjd3 14F	AGACGAGAACTGGGACCTGA	RNA
Jmjd3 16R	TGCCAAACTTGATGATGTGA	RNA
Jmjd3 ex.16 Fw	AGAGGTGGTTGCCACAGCTA	RNA
Jmjd3 ex.17 Rv	GTTGCCTGTGGATGTTACCC	RNA
Ccnd2 Fw	GGACATCCAACCCTACATGC	RNA
Ccnd2 Rv	CGCACTTCTGTTCCTCACAG	RNA
Cclnd3 Fw	GCTTACTGGATGCTGGAGGTA	RNA
Cclnd3 Rv	AAGACAGGTAGCGATCCAGGT	RNA
c-Myc Fw	TCAAGAGGCGAACACACAAC	RNA
c-Myc Rv	GGCCTTTTCATTGTTTTCCA	RNA
Prdm1 Fw	ACGTGTGGGTACGACCTTG	RNA
Prdm1 Rv	CTGCCAATCCCTGAAACCT	RNA
Jmjd3 Δ Fw	TGCTGACCTGGTAAGGGAAA	DNA
Jmjd3 Δ Rv	CGATGCATCCAGCCTAAATC	DNA
Gapdh4d Fw	AGCGCTGACCTTGAGGTCTCCTTG	DNA
Gapdh4d Rv	GTTGCCTACGCAGGTCTTGCTGAC	DNA

2.4. Protein methods

2.4.1. Immunoblot analysis

Cells were collected by centrifugation at 1200 rpm for 5 minutes and washed with ice-cold PBS. To extract protein, cell pellet was resuspended in 8M Urea lysis buffer (8 M Urea, 0.1 M NaH_2PO_4, 0.01 M Tris pH 8.0) and incubated 30 minutes rotating at 4˚C. Sonication was performed in 3 cylces of 10 seconds each. Cell lyate was then centrifuged at maximum speed for 10 minutes to remove cell debris. Lysates were quantified with a protein assay reagent (BioRad Laboratoris). 20-50 µg of proteins, in Laemmli loading buffer (62.5 mM Tris-Hcl pH 6.8, 2% (w/v) SDS, 5% (v/v) 2-mercaptoethanol and 10% (v/v) glycerol) and 10 µl of NOVEX® Sharp Pre Stained protein standard (Invitrogen) were loaded onto SDS-polyacrilamide gels prepared at different percentage of polyacrilamide based on the size of the protein of interest. In general, to prepare a 6% resolving gel(lower) 30% acrylamide/ bisacrylamide (EuroClone) , 1.5 M Tris pH 8.8, 10% SDS, 10% ammonium persulfate and 1x tetramethylethylenediamine (TEMED, Termo Scientific) were used. For a 5% stacking gel (upper) 30% acrylamide/ bisacrylamide (EuroClone), 1.0 M Tris ph 6.8, 10% SDS, 10% ammunium persulfate and 1X TEMED was made. SDS-polyacrylamide gel was run for 3 hours at 30 v and transferred by iBlot® Dry Blotting Device (invitrogen) onto nitrocellulose membrane (iBlot® Transfer Stack, Invitrogen) in 7 minutes. After blotting, the membranes were stained with Ponceau S staining solution (0.1% ponceau S (w/v) and 5% acetic acid (w/v)) to verify equal loding and transfer. Membranes were rinsed with water and blocked in blocking solution 5% BSA in TBS-T (20 mM Tris-HCl pH 7.4, 500 mM NaCl, 0.1% Tween-20) for 1 hour at room temperature shaking. Filters were then rinsed with water and incubated with primary antibodies (Table 5), diluted in blocking solution for 1-2 hours at room temperature or overnight at 4˚C. After three rounds of 10-minute washes in TBS-T, membranes were incubated with the appropriate horseradish peroxidase conjugated secondary antibody diluted in the proper solution for 1 hour at room temperature rotaiting. After three washes with TBS-T, each for 10 minutes, the bound secondary antibody was revealed using ECL Western Blotting Substrate (Pierce) and detected using

Chemidoc™ XRS+ imaging system (BioRad). Images were then analyzed with Image Lab™ software (BioRad)

Table 5. List of antibodies used for immunoblotting

Primary antibodies	**Clone**	**Company**	**Dilution**
Rabbit anti-Jmjd3 polyclonal	SI0871	Home made	1/300
Rabbit anti-H3K27me3 polyclonal	07-449	Upstate	1/2500
Rabbit anti-H3 total	07-690	Millipore	1/25000
Secondary antibody			
Polyclonal goat anti-mouse	170-6516	BioRad	1/20000
Polyclonal goat anti-rabbit	170-6515	BioRad	1/20000

2.5. Cell culture methods

2.5.1. ES cell techniques

2.5.1.1. Culturing mouse Embryonic Stem (ES) cells

E14-Tg2α ES cells were cultured on 0.1% gelatin in antibiotic-free ES medium containing leukemia Inhibitory Facotr (LIF). ES cells were grown at 37˚C, 5% CO_2 with maximal humidity. Cells were daily fed with fresh medium and passaged every 2-3 days at 70-80% confluency: cells were washed twice with Phosphate Buffered Saline (PBS, without Ca^{2+} and Mg^{2+}) and incubated with trypsin-EDTA at 37˚C for 5 minutes, trypsine-EDTA were neutralized by adding ES medium and cells were dissociated by vigorous pipetting. After 5 minutes centrifugation at 1200 rpm Supernatant was aspirated and cell pellet was resuspended in fresh medium and plated at the proper density (for ES cell maintenance 1-2 × 10^6 cells per 10-cm tissue-culture dish).

To facilitate the ES cell colony pick up, ES cells were plated on Mouse Embryonic Fibroblast cells (MEFs) exposed to Mitomycin C as feeders.

ES cell medium

15% Fetal Calf Serum (FCS)

1 mM sodium pyrovate

200mM 1x L-Glutamine

10 mM 1x non-essential amino acids

100 μM 2-β-mercaptoethanol

1000 U/ml Leukemia Inhibitory Factor (LIF, prepared by Transgenic facility)

Dulbecco's Modified Eagle's Medium (DMEM with high Glucose)

2.5.1.2. Preparing Mouse Embryonic Fibroblast cells as feeder layer

Mouse Embryonic Fibroblasts (MEFs) have been used as feeder cell layers for the culture and maintenance of mouse and human ES cells. MEFs provide an unknown mixture of nutrients and substrates, which allow long-term growth and proliferation of ES cells. To this end MEFs at early passeges (maximum passage three) are mitotically inactivated using mytomicin C which inhibits DNA synthesis and nuclear division.

MEFs at passage zero were provided by the IFOM transgenic facility, cells were expanded and frozen in 90% FBS with 10% dimethylsulfoxide (DMSO) up to passage 3 before MEFs become senesced. When feeder cells were required, MEFs were thawed on 0.1% gelatin coated tissue-culture dishes and incubated at 37˚C, 5% CO_2. Confluent MEFs were then mitotically inactivated in MEF medium containing 10 μg/ml mitomycin C (Sigma) for 3 hours in the incubator. Cells were then washed twice with PBS, trypsinized and seeded at a density of 6×10^4 cells/cm^2 onto the tissue-culture dishes. After inactivation cells can be frozen for later use.

MEF medium

10% fetal calf serum (FCS)

1X sodium pyrovate

200 mM 1X L-glutamine

Dulbecco's modified Eagle's medium (DMEM, high glucose)

2.5.1.3 ES cell transfection

ES cells in low passage number were thawed and cultured for a week in ES cell media. Confluent ES cells were fed with fresh medium a few hours before transfection, then trypsinized and collected to 10^7 cells in 15 ml falcon tube and centrifuged at 1200 rpm for 5 minutes. Cells were then washed with PBS to eliminate the salts and resuspended in 700 µl of PBS. Transfection was done in 4mm Gene Pulser cuvettes using a Bio-Rad electroporator. 25 µg of linearized targeting vector were used for transfection of 10^7 cells. High DNA concentration during transfection results in higher numbers of stable transformants but may also be toxic to ES cells when exceeding 50-100 µg DNA/ml transfection buffer.

100 µl of linearized DNA in water were added to the ES cell suspension in the cuvette and electroporation was performed with the following parameters: exponential waveform, 230 v, 500 µF, ∞ Ω. After electroporation, cells were incubated 5-10 minutes at room temperature, then transferred to 30 ml ES media for each 10^7 cells and plated 3-5 $\times 10^6$ cells per 10-cm dish. To assign the cell viability after electroporation, 10^3 transfected and 10^3 nontransfected cells were plated onto 6 well-plate, cells were grown without selection and colonies were counted after 1 week. Moreover to control the stringency of selection, 5×10^6 nontransfected cells were cultured onto a 10-cm dish and fed everyday with fresh medium containing G418 (Geneticin®; Gibco). The concentration of G418 should be chosen such that no viable cells should remain at day 8-10 of selection when the first transfected colonies may be picked. Selection of targeted ES cells was started 36 hours after transfection.

2.5.1.4. ES cell colony picking

ES colonies were picked starting day 10 post transfection and plated in 96-well plates. ES plates were fed 2 hours before picking with fresh media. Meanwhile, a 96-well plate (U-bottom) was pepared with 20 µl of 2x trypsin-EDTA solution (plus 1% chicken serum). ES 9cm plates were washed twice with 10 ml PBS. After second wash, 10 ml of PBS were added to the plate and colonies were picked under a tissue culture hood equipped with a stereomicroscope using 20 µl micro-pipettor with sterile disposable tips. Each picked colony then transferred into one well of the U-bottom 96-well plate containing 20 µl of 2X trypsin-EDTA. Colony pick up was performed for 30 minutes and picked clones were controlled under the microscope to see whether the cells were dissociated, if not plate was incubated for 5 minutes at 37˚C incubator. 110 µl of ES media were added to each well using multichannel pipettor and cells were pipetted vigorously. Cell suspensions were then transferred to a 96-well plate (flat bottom) containing MEF feeder cells.

To increase the chance of indentifying homologous recombinants, the 9-cm plate with ES colonies was washed twice with PBS and fed with ES media and G418 and placed again at incubator. Colony pick up was repeated every two days.

When cells reached the confluency, each well was washed twice with PBS and 50 µl of 1x trypsine-EDTA were added, plate was incubated 5 minutes at 37˚C and cells were dissociated by pipetting, then trypsin-EDTA were neutralized adding 100 µl of ES medium and cells of each well were divided into three 96-well plates (50 µl of cells per plate) containing MEF feeders in 150 µl of ES media plus G418.

2.5.1.5. Freezing ES cells in 96-well plates

Subconfluent ES cells were washed twice with 100 µl of PBS and trypsinized with 50 µl of 1x trypsine-EDTA, after 5 miniutes incubation at 37˚C, trypsin-EDTA were neutralized with 50 µl of 2x freezing medium (20% dimethylsulfoxide (DMSO) in ES-tested fetal calf serum (FCS)) to each well, cells were dissociated by vigorous

pipetting. 100 µl of sterile mineral oil were added to each well and 96-well plate was sealed with parafilm and store at -80˚C until the end of screening.

2.5.1.6 Isolation of genomic DNA from ES cells in 96-well plate

Confluent ES cells were washed twice with 1X PBS and incubated in ES cell lysis buffer (50µl/ well) overnight at 56˚ C. To precipitate the DNA, 100 µl of 75 m*M* NaCl in absolute ethanol was added to each well and plate was incubated for 3 hours at room temperature, shaking at 350 rpm. After centrifugation at 1300 rpm for < 2 minutes, the DNA pellet was washed three times with 100 µl of ice-cold 70% ethanol. Finally, the dried DNA was resuspended in 25µl of water overnight.

ES cell lysis buffer

10 mM NaCl

10 mM Tris-HCl pH 7.5

10 mM EDTA

0.5 % sarcosyl

1mg/ml Proteinase K (freshly added)

miliQ H2O up to the volume

2.5.1.7. ES cell restriction digest in 96-well plate

To digest the ES genomic DNA, 10 µl of restriction enzyme mixture were added to each well. The plate was wrapped with parafilm and incubated overnight at proper temperature.

Restriction enzyme mixture:

1 mM Dithiotheritol (DTT)

1 mM Spermidine

100 µg/ml Bovine serum albumine (BSA)

50 µg/ml RNase A

1X restriction buffer

20 U restriction enzyme per sample

miliQ H2O up to the volume

2.5.1.8. Southern analysis

2.5.1.8.1. Blotting and prehybridization

Genomic DNA was digested by the relevant restriction enzyme overnight and then the entire digestion reaction was run on 0.9% agarose gel at 40 v overnight. The day after agarose gel was stained with 1 µg/ml ethidium bromide for 20 minutes and DNA digestion checked by exposure to short wavelength UV. To transfer the digested DNA to the nylon membrane, DNA was depurinated in the gel by soaking in 0.25 N HCl for 10 minutes at room temperature, gently shaking. After rinsing the gel with water, gel was equilibrated in alkaline transfer buffer (0.4 N NaOH and 0.6 N NaCl) for one hour. Blot apparatus for upward capillary transfer was assembled and digested DNA was transferred onto an Amersham Hybond™-XL membrane (GE Healthcare) in transfer buffer overnight.

After transfer, the membrane was neutralized by 1 minute incubation with 0.2 M Tris-HCl pH 7.5 in 1X saline sodium citrate (SSC) and baked for 2 hours at 80˚C to crosslink the DNA to the membrane.

Membrane was rinsed with 2x SSC and pre-hybridized in modified Church & Gilbert's buffer at 65˚C in a rotor oven for an overnight.

Modified Church & Gilbert's buffer

32.9 g Sodium phosphate- monobasic (Na_2HPO_4, MW 137.99)

70.1 g Sodium phosphate- dibasic (NaH2PO4, MW 268.07)

7% (w/v) SDS

1.0 g Sodium pyrophosphate

2mM EDTA

miliQ H2O up to 1 liter

2.5.1.8.2. Preparation of radioactive DNA probe

DNA probe was labeled with ladderman™ labling kit (TaKaRa) using [α- ^{32}P]dCTP (3000 Ci/mmol) ; in a safe-lock tube 130 ng (10ng-1µg) of DNA probe were combined with 2µl of random primer and distilled sterilized water up to 14 µl. DNA was denatured at 95˚C for 3 minutes and cooled on ice for 5 minutes. After brief centrifugation, 2.5 µl of 10X buffer , 2.5 µl of dNTP mixture, 5 µl of labeled [α-^{32}P]dCTP (1.85 MBq, 50 µ Ci) and 1µl of *Bca* DNA polymerase were added to the reaction and incubated at 55˚C for one hour. To purify the labeled probes from unincorporated dNTPS, labeling reaction was loaded on illustra ™ ProbeQuant™ G-50 Micro columns (GE Healthcare) and centrifuged at 2800 rpm for 2 minutes. Then labeled probes were denatured by 5 minutes incubation at 95˚C and placed on ice for 2 minutes. After brief spin the labeled probes were added to the modified Church & Gilbert's buffer. The membrane was hybridized overnight in the rotating oven at 65˚C.

After hybridization, membrane was washed with 2X SSC-0.1% SDS for 10 minutes at room temperature to eliminate the probe, then two more washes in 2X SSC- 0.1% SDS at 65˚C for 20 minutes were performed. In case of requirement to stringent washes, the following buffers have been used (indicated according to increased stringency):

1X SSC- 0.1% SDS

1X SSC- 0.5% SDS

0.5X SSC- 1% SDS

Autoradiography was performed by exposing the membrane to BioMax MR film (KODAK) for 7 days at -80˚C.

2.5.1.9. Karyotyping ES cells

ES cells were cultured on 0.1% gelatine to 70% confluency and treated with 0.1 µg/ml KaryoMAX® colcemid (Gibco) in medium for one hour at 37˚C to block the cells in metaphase. Cells were then trypsinized and centrifuged at 1200 rpm for 5 minutes. 10 ml of warm hypotonic solution (0.075 M KCl in water) were added drop by drop to the cell pellet gently shaking and cells were incubated at 37˚C for 25 minutes. For pre-fixation, 10 drops of cold fixative (three parts of methanol and one part of glacial acetic acid) were added to the cell suspension, tube was gently inverted few times and centrifuged at 1200 rpm for 5 minutes. Afterwards, 3ml of cold fixative were added dropwise while gently vortexing to resuspend the cells. after centrifigation at 1200 rpm for 5 minutes, the pellet was resuspended in 1ml cold fixative and 60 µl of the cell suspension were dropped onto the glass slide pre-warmed at 57˚C from about 40 cm height. Drops were then spread all over the slide and air-dried for 15 minutes. Metaphases were stained in 1µg/ml DAPI in saline sodium citrate for 5 minutes in the dark and dried overnight at room temperature light protected. For each slide, 10 metaphases were counted to score the number of chromosomes.

2.5.1.10. Cre-recombination of targeted ES cells

To induce Cre-mediated recombination in targeted ES cells, the cells were treated with TAT-Cre fusion protein (Peitz et al., 2002). the cells were trypsinized and 2 $\times 10^5$ cells were plated on a 6-well tissue culture plate. After 6 hours cells attached and washed three times with PBS. For transduction ES cells were incubated with 5µM of TAT-Cre protein diluted in 1:1 mixture of PBS and DMEM (high glucose with L-glutamine) and incubated 16-18 hours at 37˚C, 5% Co_2. Cells were washed with PBS , trypsinized and cultured for further 1-2 days. Genomic DNA was extracted from treated cells and Cre recombination was confirmed by PCR.

2.5.2. B-cell techniques

2.5.2.1. B cell harvest and purification from different lymphoid organs

For B cell analysis, mice of 8-12 weeks of age were used. BM cell suspension was collected by flushing tibia with 5 ml of B cell medium. Cells of peritoneal cavity lavage ware obtained by injection of 8 ml of B cell medium into the peritoneal cavity followed by collection of 6 ml of medium. SPL, LN and PP were collected and smashed to get single-cell suspension. Erythrocyte lysis was carried out on SPL and BM cell suspensions with incubation of cell pellet in 1 ml of erythrocyte lysis buffer for 3 minutes on ice. Reaction was stopped by adding 10 ml of B cell medium and cells were washed with Fluorescence-activated cell sorting (FACS) buffer. Cells were counted using Erythrosin B dye (sigma) to distinguish live and dead cells. All centrifugation steps were performed at 1200 rpm, 4˚C for 5 minutes.

Erythrocyte lysis buffer

Solution A	0.17 M Tris, pH 7.65
Solution B	0.83 % NH_4Cl
Working solution	9 parts B + 1 part A

B cell medium

10% FBS
200 µM 1X L-glutamine
1mM sodium pyrovate
10 mM non-essential amino acids
50 µM 2-β-mercaptoethanol
DMEM (high glucose)

FACS buffer

1X PBS

1% BSA

0.05 % NaN_3

Spelnic B cells were purified using MACS® Column Technology (Milteny Biotec) following manufacturer's B cell isolation Kit depletion protocol (Milteny Biotec). In general, CD43-expressing B cells (activated B cells, PCs and B-1a B cells), T cells, NK cells, dendritic cells, machrophages, granulocytes and erythrocytes were indirectly magnetically labeled with a cocktail of biotin-conjugated antibodies against CD43(Ly-48), CD4 (L3T4) and Ter-119, followed by Anti-Biotin MicroBeads incubation. This procedure allows the isolation of untouched resting B cells from single-cell suspension of lymphoid tissues.

2.5.2.2. B cell harvest and purification

Purified B cells were cultured in B cell medium and stimulated with 20 µg/ml LPS (Lipopolysachharide, Sigma) with or without 25 ng/ml IL-4 (Recombinant Murine Interleukine 4, GRF-10600, Immunological Science); or 1µg/ml anti-RP105 (Monoclonal rat-anti mouse CD180, functional grade purified RP/14, eBioscience), CpG at final concentration of 10mM, anti-CD40 2µg/ml (eBioscience) with 25 ng/ml IL-4, anti-IgM (Jakson Research, Goat anti-mouse IgM) at concentration of 20 µg/ml. B cells were cultured at a density of 0.5-1 x 10^6 cells/ml at 37˚C, 5% CO_2.

2.6. Imaging methods

2.6.1. Immunoastaining for flow cytometry and cell sorting

Cells were washed with PBS and stained in 10 µl per 1 $\times 10^6$ cells in FACS buffer containing the specific antibodies listed in Table 6. After 20 minutes incubation at 4˚C in dark, cells were washed twice with 200 µl of FACS buffer. Samples were acquired and analyzed using FACSCalibur (Becton Dickinson) and FlowJo software. Cell sorting was performed using FACSAria Cell sorter (Becton Dickinson).

Table 6. List of antibodies used for surface staining

Antibodies and antigen	Company	Dilution
Monoclonal Rat-anti mouse CD5 (PE)	eBiosciences	1/200
Anti mouse CD95 (Fas)	eBiosciences	1/170
Anti mouse IgM clone R331.12 (Alexa 488)	Home made	1/400
Anti Kappa clone R331.18 (Alexa 488)	Home made	1/800
Monoclonal Rat-anti mouse CD138 (PE)	BD Biosciences	1/200
Monoclonal Rat-anti mouse CD19 (Cy7 PE)	eBiosciences	1/400
Monoclonal Rat-anti mouse CD21/CD35 (PE)	eBiosciences	1/1000
Monoclonal Rat-anti mouse CD23 (FITC)	eBiosciences	1/100
Monoclonal Rat-anti mouse CD25 (APC)	eBiosciences	1/200
Monoclonal Rat-anti mouse CD38 (APC)	eBiosciences	1/600
Monoclonal Rat-anti mouse CD43 (PE)	eBiosciences	1/100
Monoclonal Rat-anti mouse IgD (PE)	eBiosciences	1/3000
Monoclonal Rat-anti mouse IgG1 (biotin)	BD Biosciences	35064
Monoclonal Rat-anti mouse/human CD45R (B220) (Cy7 PE)	eBiosciences	1/400
Monoclonal Rat-anti mouse/ Human CD45R (B220) (FITC)	eBiosciences	1/200
NIP (PE)	Home made	1/4000
Antigen Fluorescent Peanut Aglutinin (PNA)	Vector Laboratories	1/800

Streptavidin (APC)	eBiosciences	1/800
Streltavidin (FITC)	eBiosciences	1/400
Streptavidin (Cy7 PE)	eBiosciences	1/400
Streptavidin (PE)	eBiosciences	1/600

2.6.2. Intracellular immunoastaining for flow cytometry

Cells were collected and stained in 10µl/ 1 $\times 10^6$ of FACS buffer with antibodies of choice (Table 4) for 20 minutes at 4˚C in dark and washed twice with 200 µl of FACS buffer. Surface stained cells were fixed in BD Cytofix/Cytoperm™ buffer for 20 minutes on ice in U-bottom 96-well plate, washed by Perm/Wash™ buffer (P/W) and refixed in BD Cytofix/Cytoperm™ buffer for 20 minutes on ice. Cells were then incubated in blocking buffer (10% normal goat serum in P/W buffer) for 30 minutes at room temperature shaking and stained with Alexa 488-labeled Rat-anti mouse IRF4 (IRF 3E4, BioLegend, working dilution 1/400) in staining solution for 60 minutes at room temperature, shaking. Cells were washed twice with P/W buffer and fixed with 1% formaldehyde in PBS. Samples were acquired and analyzed using FACSCalibur (Becton Dickinson) system and FlowJo software. All centrifugation were performed at 1800 rpm for 10 seconds at 4˚C.

2.6.3. Immunostaining for detection of apoptosis

To measure apoptosis in B cells, two methods were used: CaspaGLOW™ Fluorescei Active Caspase and TdT-mediated dUTP-biotin nick end labling (TUNEL). The CaspGLOW assay utilizes a permanent pan caspase inhibitor VAD-FMK (carbobenzoxy-valyl-alanyl aspartyl-[O-methyl]- fluoromethylketone] that irreversibly binds to the catalytic site c caspase protease. TUNEL staining is another method to detect apoptosis *in situ*, it relies o the ability of the enzyme terminal deoxynucleotidyl transferase to identify DNA nicks an incorporate labeled dUTP into free 3'-hydroxyl termini generated by the fragmentation c genomic DNA through apoptotic signaling cascades.

2.6.3.1. CaspaGLOW™ Fluorescein Active Caspase staining

CaspGLOW staining was carried out using CaspaGLOW™ Fluorescein Active Caspase staining Kit with some modifications in supplier's protocol. Cells were incubated in B cell medium containing FITC-VAD-FMK (working dilution 1/100) for 1 hour at 37˚C and 5% CO_2. After centrifugation at 1200 rpm for 5 minutes, cells were washed with wash buffer. If surface staining was required, cells were stained after CaspGLOW as described in the protocol of chapter 2.6.2 (immunostainig for flowcytometry), acquired by FACSCalibur (Becton Dickinson) and analyzed by FlowJo software.

2.6.3.2. TUNEL staining

TUNEL staining was performed using *In situ* cell death detection kit, Fluorscein (Roche Applied Science). Cells were harvested and washed twice with PBS, if required they were surface stained as described above (immunostaining for flow cytometry). Cells were resuspended in PBS at a concentration of 1-2 $\times 10^7$ cells/ml and 100 of suspension were transferred to a U-buttom 96-well plate. Cells were fixed by addition of 100 µl of 1% paraformaldehyde (PFA) and incubated for 30 minutes at room temperature, shaking. After centrifugation at 1200 rpm for 5 minutes, cells were washed twice with 200 µl PBS (staining can be stopped at this step and cells should be kept at 4˚C). Cells were collected by 5 minutes centrifuge at 1200 rpm and resuspended in 100 µl of permeabilization buffer (prepared freshly) containing 0.1% Triton X-100 and 0.1 M sodium citrate in PBS and incubated on ice for 2 minutes. Cells were then washed twice with PBS and resuspended in 50 µl of TdT-reaction buffer: 10µl of Enzyme solution and 40 µl of Lable solution. Cells were then incubated in TdT reaction buffer for 1 hour at 37˚C, 5% CO_2. After two washes with PBS, cells were resuspended in 400 µl of PBS and acquired by FACSCalibur (Becton Dickinson) and analyzed by FlowJo software.

2.6.4. Cell cycle analysis

2.6.4.1. Proliferation assay *In vitro*

To analyze the cell cycle distribution of cells *Ex vivo* or *in vitro*, 5-bromo-2'-deoxyuridine (BrdU) staining was performed. BrdU is a thymidine analog that is incorporated into DNA at the S phase of cell cycle (Givan et al., 1992), the incorporated BrdU (but not the thymidine) is then recognized by a fluorescent-conjugated anti-BrdU which lables the new DNA, while denarured DNA is stained using propidium iodid (PI). To perform the cell cycle analysis, 1×10^6 cells were incubated in 3.3µM BrdU (Sigma, stock 3.3 mM (100X)) in B cell medium for 45 minutes at 37˚C, 5% CO_2; 3×10^5 cells were kept aside as an unpulsed control. After stopping the reaction by addition of PBS, cells were centrifuged at 1300 rpm for 3 minutes at 4˚C. Surface staining was then performed if it was required. Cells were washed in PBS and fixed in 100 µl of BD Cytofix/Cytoperm™ buffer for 20 minutes at room temperature. After wash with Perm/Wash™ buffer (P/W), cells were permeabilized with 70 µl of BD Cytoperm™ Plus buffer (BD Biosciences) for 10 minutes at room temperature (freezing buffer (90% FCS with 10% DMSO) is an alternative for BD Cytoperm™ Plus buffer), cells were then washed with P/W buffer and refixed with 100 µl BD Cytofix/Cytoperm™ buffer for 5 minutes at room temperature. After wash with P/W buffer,cells were treated with 70 µl of deoxyribonuclease I (DNase I; Sigma, 1mg/ml) for 1 hour at 37˚, 5% CO_2 to expose the BrdU-labeled DNA in cell suspension. Cells were then washe with P/W buffer and stained with FITC-conjugated anti-BrdU antibody (BD Biosciences) at working solution 1/5 for 20 minutes at room temperature in dark. After wash with P/W buffer, cells were resuspended in 1ml of 2.5 µg/ml PI (Sigma) and 250 µg/ml of Ribonuclease A solution (RNase A, Sigma) in PBS and incubated overnight at 4˚C. The next day, cells were acquired with FACSCalibur (Becton Dickinson) and analyzed using FlowJo software.

2.6.4.2. Proliferation assay *In vivo*

To assess the proliferation and survival of B cells *in vivo*, mice were fed with 0.8 mg/ml of BrdU (Sigma) with 2% sucrose (light protected) for 7 days in their drinking

water (mice were provided with fresh water containing BrDU every second day). At day 7 mice were sacrificed and B cells were collected from different lymphoid organs. BrdU staining and acquisition were performed as described in 2.6.4.1.

2.7. Biochemical methods

2.7.1. Enzyme-Linked Immunosorbent Assay (ELISA)

ELISA methods are immunoassay techniques that combine the specificity of immunological reactions with the sensitivity of enzyme assays and allow quantification of immunoglobulins or antigens. One of the most common ELISA applications is to measure the amount of immunoglobulins in blood serum. Coating was performed with 50µl of capture antibodies (Table 7) or antigens (Table 6) diluted to the working concentration in coating buffer (0.5 M carbonate-bicarbonate buffer pH 9.6) overnight at 4˚C in NUNC Maxisorp white 96-well plate. Coating solution was removed the next day and plate washed three times with 450 µl of washing buffer (0.05% Tween-20 in PBS). Plate was blocked in blocking uffer (3% BSA in PBS) for 1 hour at 37˚C. then 50 µl of serum or standard (Table 7, Table 8) in Reagent Diluent (1% BSA in PBS) was added to the plate and incubated 1 hour at room temperature. Plate was washed four times with 450 µl of washing buffer and 50 µl of the Detection Antibody (Table 7, Table 8) was added to each well and plate was incubated for 1 hour at room temperature. After five times washing with 450 µl of washing buffer, 50 µl of the Streptavidin-Eu^{3+} (Perkin Elmer, 1/15000 dilution in reagent diluent) were added and plate was incubated for 30 minutes at room temperature in dark. Plate was then washed with 450 µl of washing buffer and incubated with 50 µl of room temperature DELFIA Enhancement Solution (4001-0010 Perkin Elmer) for 15 minutes at room temperature, gently shaking. Absorbance measurement was performed using Victor^3™ 1420 Multilabeled Counter and Wallac 1420 Workstation Software (Perkin Elmer™). ELISA based quantification of antibody titers in blood serum of resting/immunized mice was performed according to the Bethyl ELISA protocol supplied with Mouse ELISA Quantification Set.

Table 7. ELISA reagents for total antibody titers detection of resting mice

Capture Antibodies	**Clone**	**Company**	**Working Conc.**
Monoclonal rat anti-mouse IgM	L-OMM-3	AbD Serotec	1 µg/ml
Monoclonal rat anti-mouse IgG1	LO-MG-13	AbD Serotec	1 µg/ml
Monoclonal goat anti-mouse IgG3	LO-MG3-13	AbD Serotec	1 µg/ml
Monoclonal goat anti-mouse IgG2a	LO-MG2a-9	AbD Serotec	0.5 µg/ml
Monoclonal goat anti-mouse IgG2b	LO-MG2b-1	AbD Serotec	1 µg/ml
Monoclonal goat anti-mouse IgA	A90-130-A	Bethyl	1 µg/ml
Standards			
Mouse IgM	11E10	Southern Biotech	10 ng/ml
Mouse IgG1	15H6	Southern Biotech	10 ng/ml
Mouse IgG3	B10	Southern biotech	100 ng/ml
Mouse IgG2a	HOPC-1	Southern Biotech	100 ng/ml
Mouse IgG2b	A-1	Southern Biotech	100 ng/ml
Mouse IgA	S-107	Southern Biotech	400 ng/ml
Detection antibodies			
Anti-mouse IgM (biotin)	R33.24.12	Home made	125 ng/ml
Anti-mouse IgG1 (biotin)	A85-1	BD Pharmingen	125 ng/ml
Anti-mouse IgG3 (biotin)	R40.81	BD Pharmingen	500 ng/ml
Anti-mouse IgG2a (biotin)	LO-MG2a-7	AbD Serotec	500 ng/ml
Anti-mouse kappa chain (biotin)	R331.18	Home made	500 ng/ml
Anti-mouse IgA (biotin)	11-44-2	Southern Biotech	500 ng/ml

Table 8. ELISA reagent for antigen specific antibody titer detection of immunized mice

Antigens	Clone	Compny	Working Conc.
NP (4)-BSA	N505010	Biosearch technologies	2 µg/ml
NP(23)-BSA	N505010	Biosearch technologies	2 µg/ml
BSA			2 µg/ml
Capture antibodies			
Monoclonal rat anti-mouse IgM	L-OMM-3	AbD Serotec	1 µg/ml
Monoclonal rat anti-mouse IgG1	LO-MG-13	AbD Serotec	1 µg/ml
Standards			
Mouse IgM	11E10	Southern Biotech	10 ng/ml
Mouse IgG1	15H6	Southern Biotech	10 ng/ml
Detection antibody			
Anti-mouse IgM (biotin)	R33.24.12	Home made	125 ng/ml
Anti-mouse IgG1 (biotin)	A85-1	BD Pharmingen	125 ng/ml

2.8. Statistical analysis

2.8.1. Student's t-test

Statistical analysis of normally distributed values (Gausian) was performed by two-tailed unpaired Student's t-test. Differences were considered significant at $p<0.05$.

2.8.2. Wilcoxon signed-rank test

The Wilcoxon signed-rank test is a non-parametric statistical test that compares two paired groups by calculating the difference between each set of pairs. Wilcoxon test can be used as an alternative to the t-test when the population data does not follow a normal distribution.

3. Results

3.1. Establishment of conditional *JMJD3* knock-out mice

To investigate the function of *Jmjd3* in a cell-type and stage-specific manner, a conditional *Jmjd3* knockout (KO) mouse strain based on Cre/loxP recombination technology was generated. To this end, a *Jmjd3* conditional targeting vector was designed and generated in Dr. Giuseppe Testa's lab (European Institute of Oncology, Milan). Although I was not directly involved in the cloning of the targeting vector, I will briefly describe the strategy we employed to inactivate the *Jmjd3* gene.

3.1.1. Generation of a conditional Jmjd3 targeting vector

3.1.1.1. Design to generate mice carrying a multipurpose allele

The *Jmjd3* mutant allele was created using the "Knockout-first" targeting strategy (Testa et al., 2004). This approach is based on the insertion of a gene-trap STOP cassette into the 5' end of the target gene. The STOP cassette consists of a splice acceptor (sA) sequence, the LacZ reporter gene and a polyadenylation signal sequence. Premature transcriptional termination by the STOP cassette leads to functional inactivation of the target gene. The trap cassette provides also the possibility to monitor transcriptional activity of the target gene at the single cell level through measurement of LacZ enzymatic activity. The "knock-out first allele" carries two *frt* recombination sequences flanking the STOP cassette to allow its removal by FLP-mediated recombination. Finally, downstream of the STOP cassette, two loxP sites flank critical exons allowing Cre-mediated inactivation of the target gene in a cell-type and stage-specific fashion. Mice inheriting "knock-out first allele" allow the investigation of the effects of a generalized inactivation of the gene of interest.

Crossing of the latter animals to the FLP recombinase general deleter strain generates offspring that looses the STOP cassette while carrying at the same time a conditional (floxed) allele for the gene of interest (Figure 7).

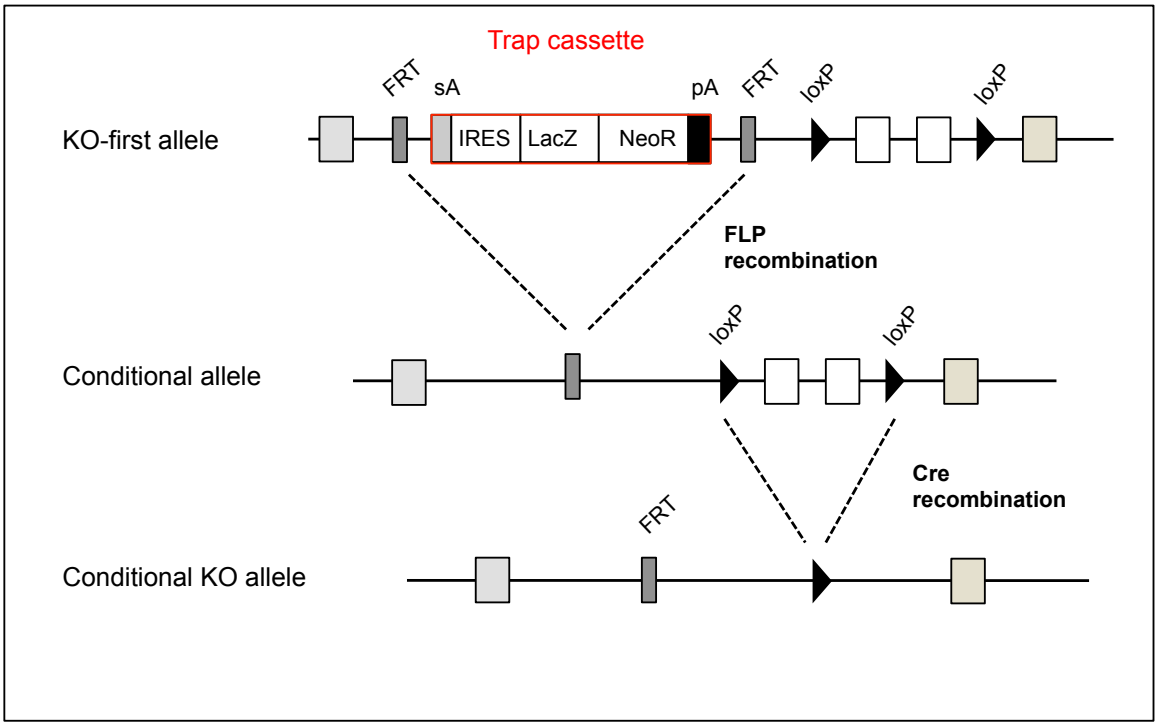

Figure 7. Schematic view of the knockout-first gene targeting strategy. The Knock-out-first allele consists of an frt-flanked gene trap cassette carrying respectively a splice acceptor (sA), an internal ribosome entry site (IRES) sequence, the LacZ reporter gene, a promoter-driven neomycin resistance gene and a poly adenylation (pA) site inserted into one of the first introns of the gene of interest. Downstream of the gene trap two loxP sites flank critical exons. Generation of a conditional KO allele is obtained after removal of the gene trap cassette via FLP-mediated recombination.

3.1.1.1. Strategy to generate mice with a Jmjd3 multipurpose mutrant allele

The mouse *Jmjd3* (*Kdm6b*) gene is located on chromosome 11 and consists of 23 exons with the fourth exon containing the ATG starting codon. Transcriptional analyses and chromatin immunoprecipitation assay indicated two main transcriptional start sites (TSS) mapping upstream respectively of exon 1 and 2 of the *Jmjd3* gene

(De Santa et al., 2007; Lin et al., 2012). Successful inactivation of *Jmjd3* in a recently published mouse knockout line (XB814) carrying a gene trap cassette within intron-1, led to the decision to target the frt-flanked STOP cassette in a similar genomic location.

We employed a targeting vector developed in Dr. G. Testa group (European institute of Oncology) to insert an frt-flanked STOP cassette (including a neomycin (Neo) resistance gene) into intron 1 of *Jmjd3*. Moreover, two loxP sites were placed respectively upstream of exon 2 and downstream of exon 4 to allow conditional *Jmjd3* inactivation. In order to allow homologous recombination in mouse ES cells, the targeting vector was completed by two homology arms consisting respectively of 4.1 and 5.1 Kb (Figure 8).

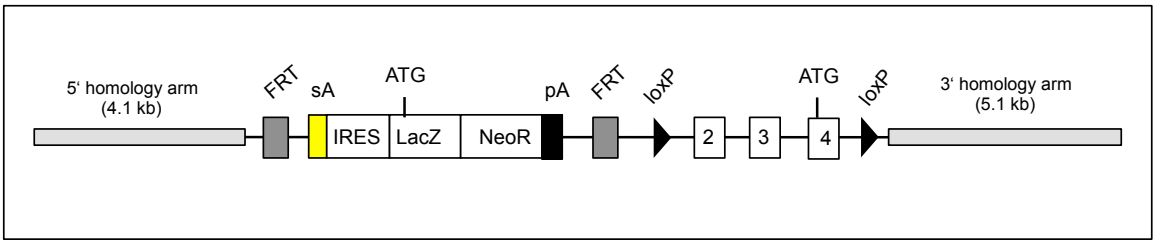

Figure 8. Scheme of the *Jmjd3* multipurpose targeting vector. Schematic view of the targeting vector used to to generate *Jmjd3* mutant ES cells. The plasmid includes respectively two homology arms to promote homologous recombination and the gene trap cassette depicted in Figure 7.

3.1.2. Generation of *Jmjd3* targeted ES cells

The conditional Jmjd3 targeting vector depicted in Figure 2 was linearized and electroporated into the 129SV-derived E14Tg2a mouse ES cell line. 36 hours after electroporation, drug selection was started adding the neomycine analog G418 to the culture medium of transfected and untransfected (control) ES cells. 8 days following G418 treatment, the majority of untransfected ES cells succumbed to the selection procedure. In sharp contrast a substantial number of G418-resistant ES colonies were

observed in the plates that received electroporated cells. Individual G418 resistant ES clones (n=*288*) were picked and expanded for molecular analysis and freezing.

Genomic DNA was extracted from 217 ES clones and subjected to Southern blotting screening to identify homologous recombinants. Specifically, a 5' external probe depicted in Figure 3 was labeled and hybridized to membranes carrying genomic DNA from ES clones digested with EcoR1. The presence of an EcoR1 restriction site in the STOP cassette allowed for the discrimination between the wild-type and the targeted *Jmjd3* allele, with the latter one giving rise to a shorter EcoR1 genomic fragment (Figure 9a). This analysis identified one single homologous recombinant clone (Figure 9b) where the band corresponding to the wild-type Jmjd3 allele was coupled to the one representing the targeted locus (*Jmjd3*$^{frt_{\beta}geo}$).

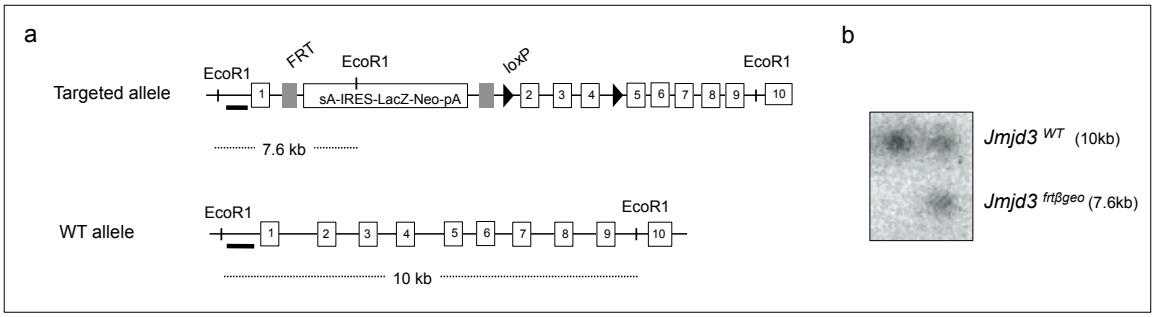

Figure 9. Identification of *Jmjd3* targeted ES cells. a) Schematic view of the *Jmjd3* locus before and after targeting the 5' region of the gene. **b)** Southern blotting analysis of the ES clone carrying the gene trap cassette correctly targeted into the jmjd3 locus. A Jmjd3 wild-type ES-clone was included in the analysis. Neomycin resistant ES clones were screened with the 5' external probe shown in **a.**

To check whether the two loxP sites had both integrated into the *Jmjd3* targeted locus, I transduced the targeted ES clone with recombinant TAT-cre. Genomic DNA was isolated from ES cells before and after Tat-cre transduction and subjected to PCR analysis. Specifically, I used a pair of oligonucleotides annealing to Jmjd3 genomic regions mapping respectively 5' and 3' to the two loxP sites (Figure 10a). This primer combination is predicted to amplify a 1.45 Kb PCR fragment from the Jmjd3 wildype/floxed allele and a 129 bp PCR product from the targeted allele undergoing

successful Cre-mediated recombination. As shown in Figure 4b, PCR amplification of genomic DNA (Table 9) from ES cells exposed to TAT-cre gave rise to a PCR product of 129 bp, thus confirming successful targeting of two functional loxP sites flanking exons 2-4 of the *Jmjd3* gene.

Table 9. Primer combination to verify by PCR successful Cre-mediated recombination of the *Jmjd3*^{fl} allele

Primer	Sequence (5'-3')
Poly A-Fw	TCTTATCATGTCTGGATCCGG
LoxP-R1	GGAAGAGCAGATGAGACTGG

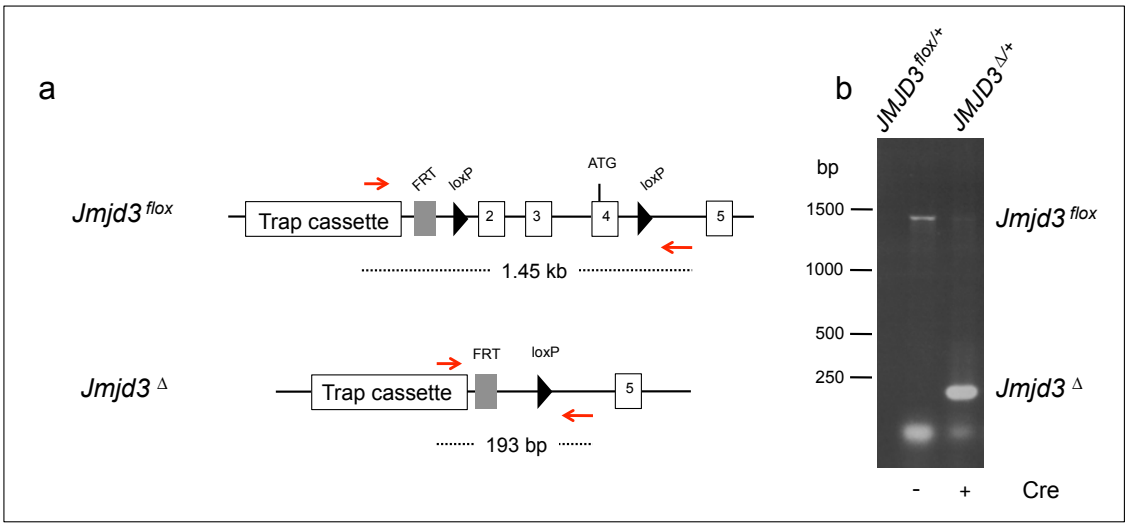

Figure 10. TAT-Cre transduction of *Jmjd3* targeted ES cells. (a) PCR strategy to confirm co-integration of loxP sites in Jmjd3 targeted ES cells.Red arrows indicate primers used for genomic PCR analysis. Numbers indicate expected length of PCR products before (*Jmjd3*^{flox}) and after (*Jmjd3*$^{\Delta}$) Cre-mediated recombination **(b)** Representative gel electrophoresis of PCR reactions obtained using as template genomic DNA extracted respectively from *Jmjd3*^{flox} ES cells before (-) and after (+) Tat-Cre transduction. The faint 1.5 kb band observed in *Jmjd3*^{flox} ES cells exposed to Tat-Cre corresponds to the wild-type *Jmjd3* allele.

Before injection into mouse blastocyst, *Jmjd3* conditional ES cells were subjected to karyotype analysis to exclude aneuploidy (Figure 11) that may affect pluripotency (Lui

et al., 1997; Longo et al., 1997). As shown in Figure 11, analysis of 43 metaphases confirmed that the majority of cells carried a normal chromosome count of 40.

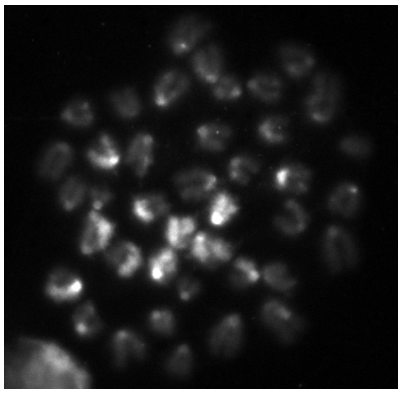

Figure 11. Karyotype of JMJD3$^{Frt\beta geo\text{-}flox}$ targeted ES cells. Representative metaphase spread of chromosomes obtained from *Jmjd3*$^{Frt\beta geo\text{-}flox/+}$ ES cells.

Finally, *Jmjd3* targeted ES cells were injected into C57BL/6 mouse blastocysts. Four male chimeras were obtained and bred to C57BL/6 females. One chimeric animal transmitted the targeted *Jmjd3* allele through the germline. The latter chimera was used to establish the *Jmjd3*$^{Frt\beta geo\text{-}flox}$ mouse line.

3.1.3. Germline transmission of the *Jmjd3* targeted allele

Transmission through the germline of the *Jmjd3* KO-first allele was confirmed by Southern blot analysis. Genomic DNA from offspring mice was digested with EcoRI and hybridized to the probe used for ES cell screening. The presence of 7.6 kb fragment as well as a 10 kb wild-type band proved the successful transmission of *Jmjd3*$^{Frt\beta geo\text{-}flox}$ allele through the germline (Figure 12).

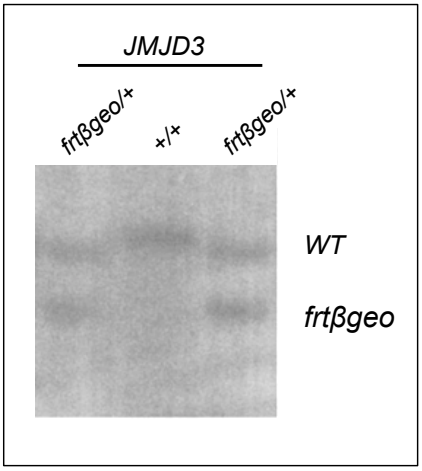

Figure 12. Germline transmission of the *Jmjd3*$^{Frt\beta geo\text{-}flox}$ allele. Southern blot analysis on EcoR1-digested tail genomic DNA from mice displaying germline transmission by coat color. The probe used for screening was described in Figure 9. Two mice (first and third lane) inherited the *Jmjd3*$^{Frt\beta geo\text{-}flox}$ targeted allele.

3.1.4. *JMJD3*$^{Frt\beta geo\text{-}fl}$ homozygous mice are embryonic lethal

Previous work has shown that *JMJD3* mutant mice die around birth (Satohh et al., 2010; Burgold et al., 2012). Since the *JMJD3*$^{Frt\beta geo\text{-}flox}$ knock-out first allele *is* predicted to interfere with JMJD3 expression, we verified this hypothesis by breeding *JMJD3*$^{Frt\beta geo\text{-}flox}$ animals to homozygosity. Out of 37 pups born from crosses of two heterozygous animals, typed 21 days post-birth, none resulted homozygous for the *JMJD3*$^{Frt\beta geo\text{-}flox}$ allele. This result indicates that the frt-flanked βgeo cassette inserted into intron-1 of the *Jmjd3* locus prevents transcription of a full-length mRNA. To test whether *JMJD3*$^{Frt\beta geo\text{-}flox}$ homozygous mutants showed suffered from a late embryonic/early post-natal lethality we isolated embryos at day E18.5 coming from a cross between two *JMJD3*$^{Frt\beta geo\text{-}flox}$ heterozygous mice. Genomic PCR revealed that two out of eight embryos were homozygous for the *JMJD3*$^{Frt\beta geo\text{-}flox}$ allele, in agreement with the predicted Mendelian ratio of allelic inheritance (Figure 13).

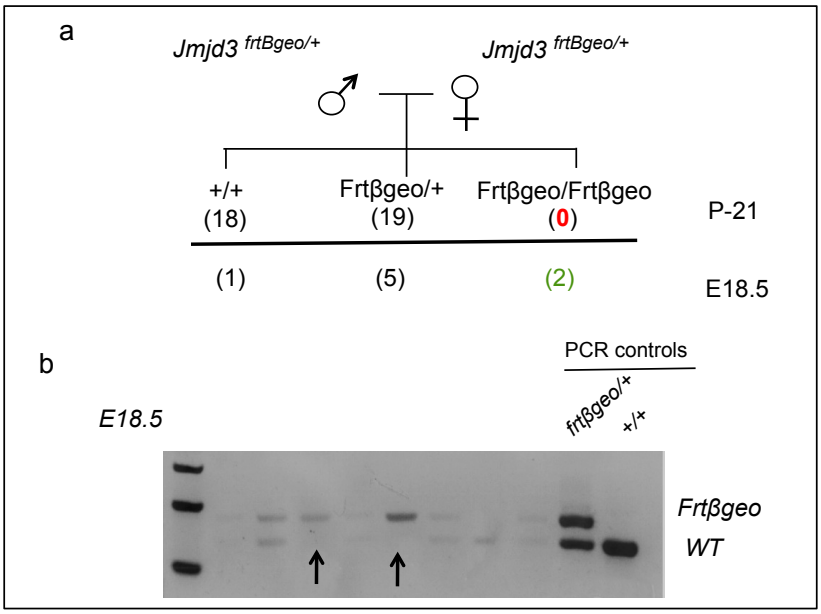

Figure 13. *JMJD3*$^{Frtβgeo\text{-}flox}$ homozygous mice are perinathal lethal. (a) Intercross between heterozygous *JMJD3*$^{Frtβgeo\text{-}flox}$ mice failed to give birth to homozygous mutant mice still alive at 21 days of postnatal life. Instead mutant animals were identified by genomic PCR genotyping performed on E18.5 embryos. **(b)** Representative genomic PCR analysis revealing the presence of homozygous *JMJD3*$^{Frtβgeo\text{-}flox}$ mice at day E18.5. The upper band corresponds to the Jmjd3 targeted locus. Arrows identify two *Jmjd3* homozygous mutants.

Jmjd3$^{Frtβgeo\text{-}flox}$ mice were bred to the FLPe-deleter strain (Rodriguez et al., 2000) to eliminate the frt-flanked βgeo trap cassette and hence generate *Jmjd3*^{fl} conditional KO mice. Functionality of frt recombination sequences and successful removal of the trap cassette was confirmed by PCR using genomic DNA extracted from the tail of F1 mice born from the cross between *Jmjd3*$^{Frtβgeo\text{-}flox}$ and FLPe deleter mice, respectively (data not shown).

Finally, to test the consequences of homozygous inactivation of the *Jmjd3* allele we bred *JMJD3*^{fl} mice to the general pgk-Cre Cre deleter strain (Lallemand et al., 1998). The intercross between F1 mice were analyzed. Similarly to what we had previously observed with *JMJD3*$^{Frtβgeo\text{-}flox}$ mice, we failed to identify mice that inherited both copies of mutant Jmjd3 allele that was this time inactivated through Cre-dependent

removal of exons 2-to-4. All together these result indicate that we successfully generated a *Jmjd3* conditional knock-out mouse strain.

3.2. *Jmjd3* expression during B cell development

3.2.1. *Jmjd3* is expressed throughout B cell lymphopoiesis

To investigate the expression pattern of *Jmjd3* during B cell lymphopoiesis, B cell subsets representing different stages of maturation were purified by cell sorting from bone marrow and spleen (Table 10) and subjected to quantitative RT-PCR analysis (Figure 14).

Table 10. B cell surface markers used for sorting

B cell subset	Surface markers
pro B	IgM^- $B220^+$ $CD43^+$ $CD25^-$
pre B	IgM^- $B220^+$ $CD43^-$ $CD25^+$
Marginal zone	$CD19^+$ $CD21^{hi}$ $CD23^{lo}$ $CD38^{hi}$
Follicular/B2	$CD19^+$ $CD21^+$ $CD23^{hi}$ $CD38^+$
Germinal center B	FAS^{hi} $CD38^{lo}$ $CD19^+$
B-1a	$CD5^+$ $CD23^-$ CD19+ B220+
B-1b	$CD5^-$ $CD23^-$ CD19+ B220+
B-2	$CD5^-$ $CD23^+$ $CD19^{lo}$ $B220^{hi}$
Plasma cells	$CD19^{lo}$ $B220^{lo}$ $CD138^+$

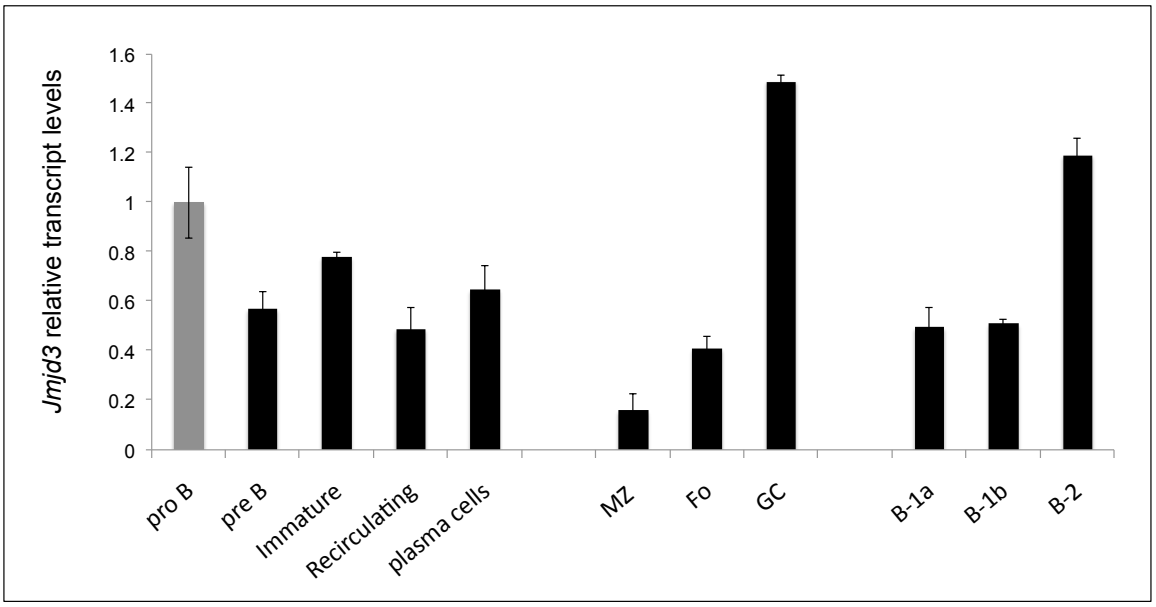

Figure 14. *Jmjd3* is expressed throughout B cell development. Transcript levels of *Jmjd3* in the indicated B cell subsets as assessed by qRT-PCR analysis. Jmjd3 mRNA levels were normalized to the housekeeping *Rplp0* and represented as relative to those detected in pro-B cells. Columns represent mean transcript levels in two mice ± SD.

Jmjd3 transcripts were detected starting from pro-B cells and remained fairly constant throughout the later stages of B cell development.

3.2.2. *Jmjd3* is strongly upregulated upon B cell activation

Jmjd3 expression is induced in response to development and environmental stimuli (De Santa et al., 2007; Burgold et al., 2008; Agger et al., 2009). To test whether the expression of Jmjd3 is induced upon activation of B cells, mature B cells were purified from the spleen and stimulated with LPS, LPS+IL-4, anti-RP105, anti-IgM, anti-CD40+IL-4 and CpG. Quantification of *Jmjd3* transcript levels revealed that *Jmjd3* is strongly induced in B cells in response to both T-cell dependent and -independent mitogens (Figure 15).

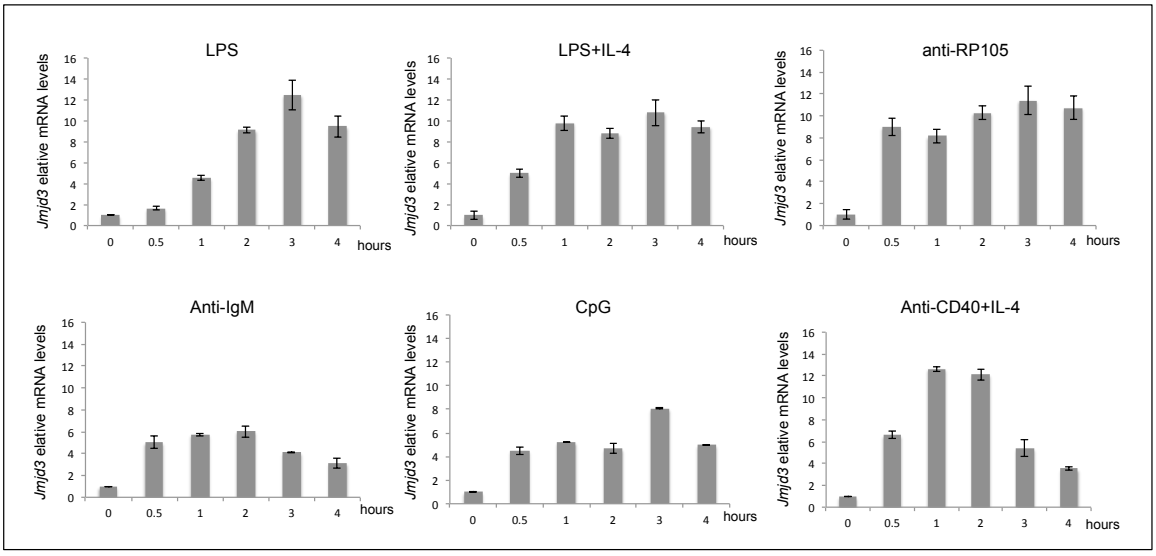

Figure 15. *Jmjd3* expression is rapidly induced upon B cell activation. Quantification by PCR of *Jmjd3* transcripts in primary B cells purified from the spleen of 57BL/6J mice stimulated for the indicated hours with different B cell mitogens. Stimulated B cells with different mitogens were collected at indicated time points and subjected for qPCR analysis. Jmjd3 mRNA levels were normalized to the housekeeping *Rplp0* and represented as relative to those detected in resting (0 hr) B cells. Bars represent the mean values of two mice± SD.

3.2.3. B-cell specific inactivation of *JMJD3* in vivo

Given the constitutive expression of Jmjd3 throughout B cell lymphopoiesis, we decided to inactivate its function starting from the earliest stages of B cell development. To this aim, conditional *JMJD3*^{fl} knock-out mice were crossed to the Mb1-Cre knock-in mice (Hobeika et al., 2006). In Mb1-Cre mice, Cre expression is under the control of the CD79a (mb1/Igα) promoter, which gets activated at the pro-B cell stage (Figure 16). To test the efficiency of Cre-mediated recombination, B cell subsets were sorted from *JMJD3*$^{fl/fl}$*; Mb1Cre* experimental mice and from Mb1-cre controls (Table 10) and subjected to genomic qPCR using primers annealing to the genomic region flanked by loxP sites. Results of the qPCR analysis revealed that Cre-mediated recombination of the JMJd3^{fl} allele started at the pro-B cell stage and reached 98% efficiency in pre-B cells. High efficiency (>90%) of Cre-mediated recombination was also observed in mature B cells of *JMJD3*$^{fl/fl}$*; Mb1Cre* mice, including follicular (Fo), marginal zone (MZ) and B-1B cells (Figure 16).

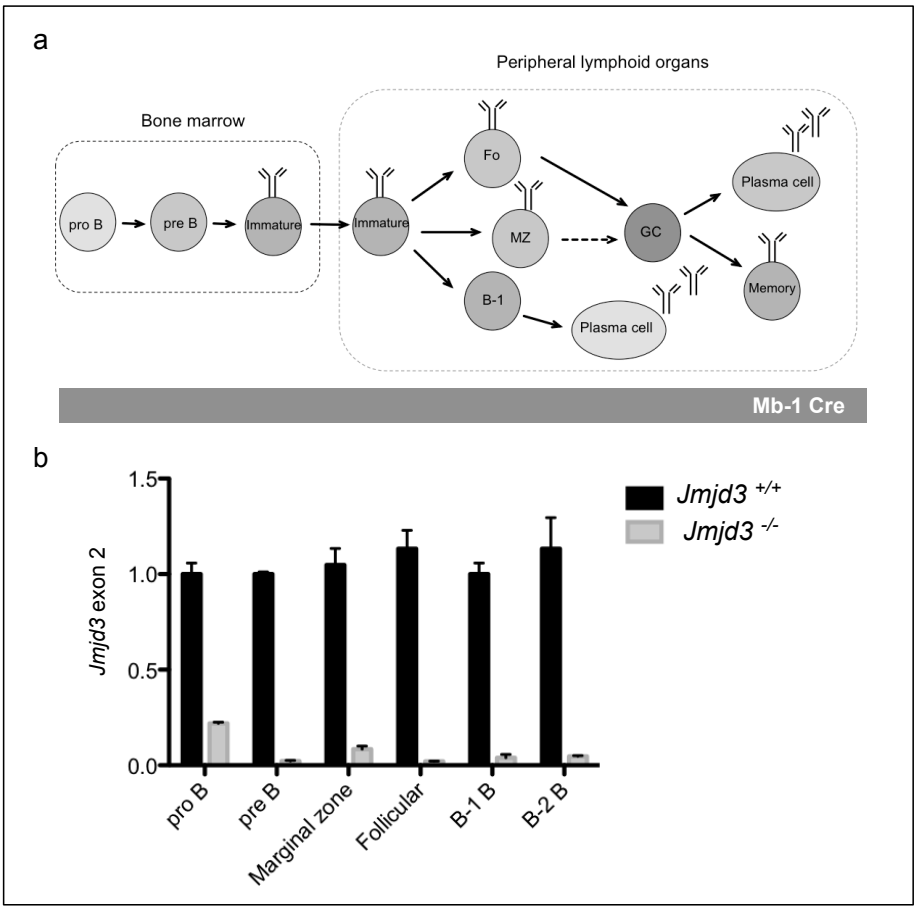

Figure 16. Selective inactivation of *Jmjd3* in B lineage cells. **a)** Schematic view of B cell development. Size of the bar below the scheme indicates expression levels of the Mb1-cre knock-in allele throughout B cell development. **b)** Genomic PCR quantification of residual exon 2 amplified in the indicated B cell subsets purified from Jmjd3 control (*Jmjd3*$^{+/+}$) and mutant (*Jmjd3*$^{-/-}$) mice. Residual exon 2 was determined in each sample after normalization for DNA input. Values are represented as relative to copies of exon 2 quantified in control proB cells. Mean values in three mutant and three control mice were plotted ± SD.

3.2.4. Jmjd3 expression fails to be induced in KO B cells upon activation *in vitro*

B cells express low basal levels of *Jmjd3* transcripts throughout differentiation. On the other hand, strong induction of JMJd3 transcripts is observed upon stimulation of B cells with a variety of antigens/ligands (see Figure 15). To verify the effects of Cre-mediated deletion at the Jmjd3 locus on Jmjd3 expression we isolated primary resting

B cells from the spleen of JMJd3$^{fl/fl}$; Mb1-cre mice and Mb1-cre controls and stimulated them *in vitro* with LPS. Using primers annealing to exons present within the loxP-flanked Jmjd3 gene segment, we performed qRT-PCR analyses on control and Jmjd3 mutant B cells. Whereas *Jmjd3* transcripts were strongly induced two hours after LPS stimulation of control B cells, we failed to detect Jmjd3 mRNA upregulation in cultures of Jmjd3 mutant B cells (Figure 17a). Similar results were obtained using primers annealing to exon16 and 17 (Figure 17b). We confirmed that B cells isolated from *Jmjd3$^{fl/fl}$;Mb1-cre* mice had undergone efficient Cre-mediated recombination at the JMJD3 locus, as over 80% loss of *Jmjd3* genomic DNA encompassing the floxed segment was observed (Figure 18).

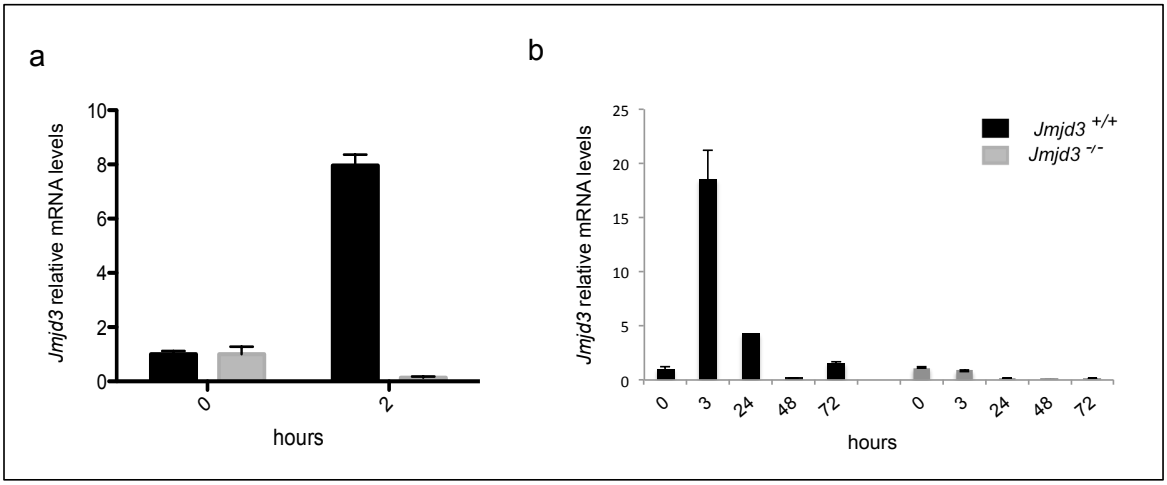

Figure 17. *Jmjd3$^{fl/fl}$;Mb1-cre* B cells fail to induce *Jmjd3* expression in response to LPS. Representative qRT-PCR analysis of *Jmjd3* transcripts in Jmjd3 control (*Jmjd3$^{+/+}$*) and conditional mutant (*Jmjd3$^{fl/fl}$;Mb1-cre; Jmjd3$^{-/-}$)* B cells at the indicated hours after LPS stimulation. *Jmjd3* mRNA levels were quantified using primer combinations annealing either to exons 2 and 3 encompassed within the loxP-flanked segment **(a)**, or to exons 16 and 17 **(b)**. Error bars represent the standard deviation across three technical replicates for a total of 2 control (Jmjd3$^{+/+}$) and 2 mutant (Jmjd3$^{-/-}$) B cell cultures.

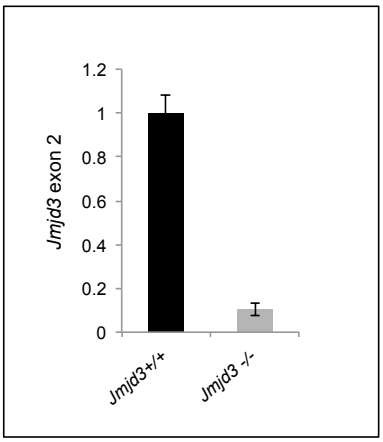

Figure 18. Efficient inactivation *Jmjd3* in LPS stimulated *Jmjd3* conditional mutant B cells. Residual *Jmjd3* exon 2 assessed by qPCR on genomic DNA extracted from control and Jmjd3 mutant B cell. Columns represent the mean values ± SD of triplicates.

Since the main Jmjd3 promoter sequence was included within the loxP flanked segment (De Santa et al., 2007; Lin et al., 2012), we anticipated the absence of downstream transcripts once Cre-mediated recombination had deleted the regulatory sequence. To confirm this scenario, control and *Jmjd3* mutant B cells were stimulated for 2 hr with LPS and subjected to qRT-PCR using a series of primer combinations annealing to Jmjd3 exons downstream of exon 4 (the last exon present within the loxP-flanked region). In accordance with our prediction, LPS stimulation of B cells from *Jmjd3*$^{fl/fl}$*;Mb1-cre* mice failed to up regulate transcripts containing exons mapping downstream of the floxed segment (Figure 19). These data suggest that *Jmjd3* expression in B cells is regulated by a promoter located within intron 1.

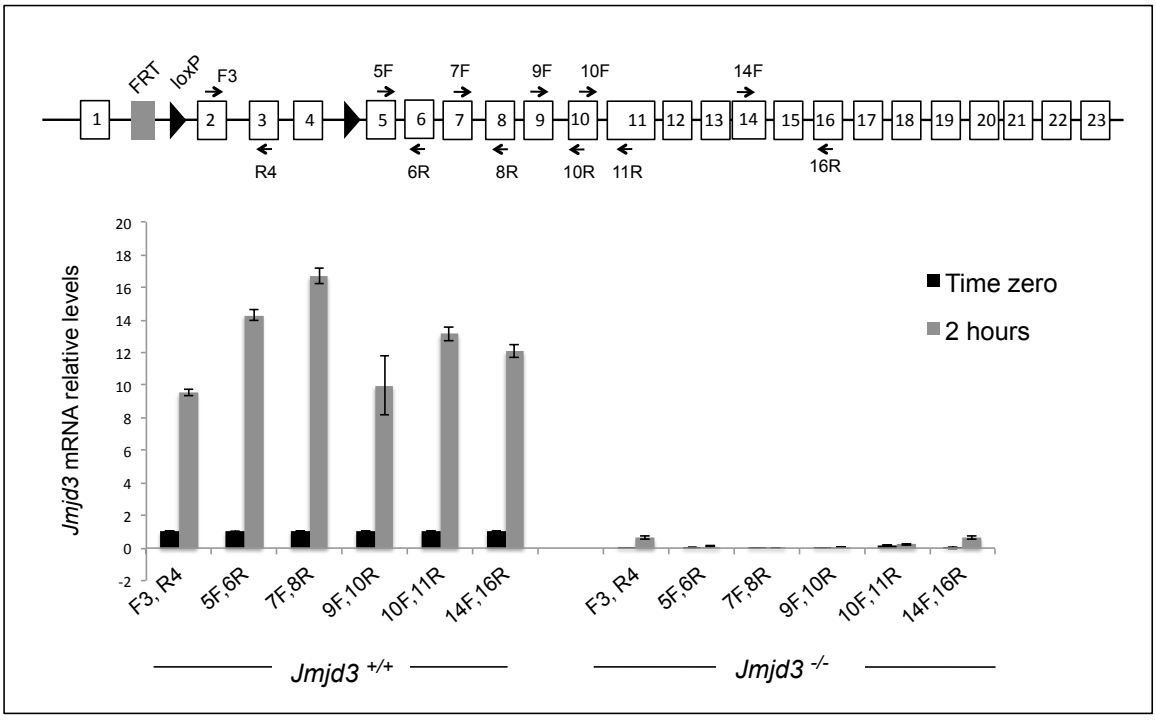

Figure 19. In B cells *Jmjd3* is transcribed from a single promoter mapping of exon 2. qRT-PCR analysis of specific segments of the *Jmjd3* transcript in *Jmjd3*$^{+/+}$ and *Jmjd3*$^{-/-}$ B cells before (black bars) and 2 hours after (grey bars) LPS activation. Arrows indicate primers used for the anlaysis. Combination of primers employed in individual qRT-PCR assays are indicated below each histogram bars. Bars indicate mean expression values ± SD of triplicates.

3.2.5. Global H3K27me3 levels were unaltered in *Jmjd3* mutant B cells

To assess whether the strong reduction in *Jmjd3* transcripts observed in primary *Jmjd3*$^{fl/fl}$; *Mb1-cre* B cells after LPS stimulation corresponded to a comparable loss in Jmjd3 protein levels we performed immunoblotting analyses. Total CD19^{+} B cells isolated from the spleen of *Jmjd3* mutant and control mice were purified and stimulated in vitro for 5 hours with LPS. Protein extracts from the stimulated cells was subjected to western blot analysis using a monoclonal anti-JMJD3 antibody. Quantification of the data revealed a reduction of over 80% of an ~200 KDa protein corresponding to full-length Jmjd3, in extracts of Jmjd3$^{fl/fl}$;Mb1-cre B cells (Figure 20).

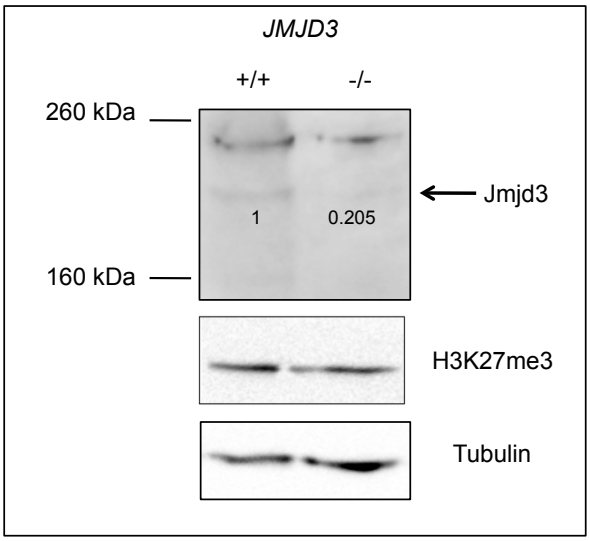

Figure 20. Western blot analysis for Jmjd3 and H3K27me3 in control andjmjd3 mutant B cells. Immunoblot analysis of Jmjd3 and H3k27me3 levels in lysates extracted from *Jmjd3* control (+/+) and mutant (-/-) $CD19^{+}$ B cells stimulated in vitro for 5 hours with LPS. The arrow indicates the predicted molecular weight size of Jmjd3 protein (210 kDA). Tubulin levels were assessed to control for protein input.

Given that Jmjd3 is one of two known H3K27me3-specific demethylases, we asked whether global levels of H3K27me3 differed between *Jmjd3* mutant and control B cells after 3 hr of LPS stimulation. Quantification of immunoblotting data revealed that H3K27me3 levels did not differ substantially between control and *Jmjd3* mutant B cells. These results are in accordance with previous studies where JMJD3 inactivation perturbed global H3K27me3 levels neither in macrophages nor microglia cells (De Santa, 2007 and 2009; Satoh et al., 2010; Przanowski et al., 2014)

3.3. *Jmjd3* and early B cell development

3.3.1. Reduced size of the Pre-B cell compartment upon *JMJD3* inactivation

To address the role of *Jmjd3* in B cell lymphopoiesis, we started analyzing early B cell development in the bone marrow of JMJD3$^{fl/fl;}$Mb1-cre compound mutants. Since JMJD3^{flox} mice were established from 129-derived ES cells, most of the analyses were performed with mice on a mixed genetic background (129/SV x C57BL/6). Flow cytometric analysis of BM cell suspensions displayed a mild (30%), yet significant, reduction in the absolute number of B220^{+} cells in *Jmjd3* $^{fl/fl}$; *Mb1Cre* (*Jmjd3* $^{-/-}$) mice when compared to *Jmjd3*$^{+/+}$; *Mb1Cre* (*Jmjd3* $^{+/+}$) control animals (Figure 21). Interestingly, a similar reduction was observed in B220^{+} BM cells of *Jmjd3*$^{fl/+}$; *Mb1Cre* (*Jmjd3* $^{+/-}$) mice, suggesting a requirement for two functional *Jmjd3* gene copies for the establishment of a normally sized BM B220^{+} B cell subset. To determine whether specific B cell subsets were affected by the inactivation of *Jmjd3,* we performed flow cytometric analysis on BM single cell suspensions.

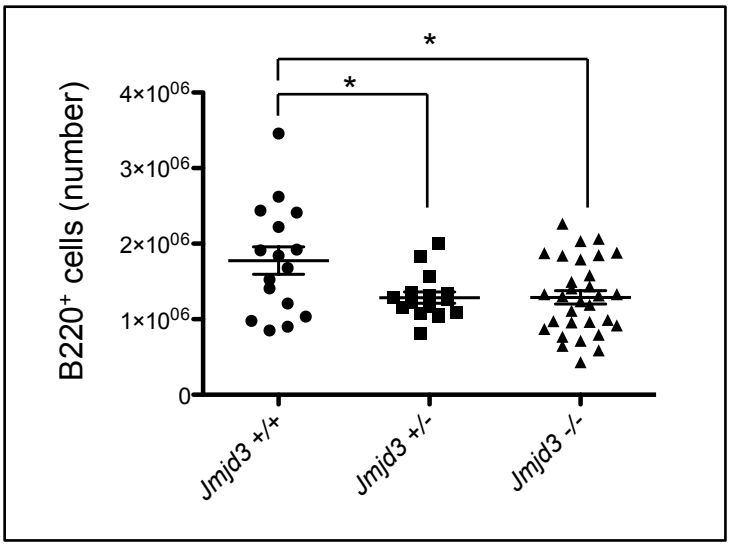

Figure 21. Absolute number of B220$^+$ B cells is reduced in the BM of *Jmjd3*$^{-/-}$ mutants. Absolute numbers of B220$^+$ gated cells assessed by flow cytometric analysis in *Jmjd3*$^{+/+}$ (*n=16*), *Jmjd3*$^{+/-}$ (*Jmjd3*$^{fl/+}$;*Mb1-cre*; *n=15*) and *Jmjd3*$^{-/-}$ (*Jmjd3*$^{fl/fl}$;*Mb1-cre*; *n=31*) mice. Each dot represents a mouse. Bars represent the mean value ± SEM (t-test; *,*p* value < 0.05).

Despite a substantial variability between mice of the same genotype (possibly due to the mixed genetic background), we found that both frequency and absolute number of B220$^+$ IgM$^-$ proB/preB cells was significantly reduced in *Jmjd3* $^{-/-}$ mutant mice in comparison to controls (Figure 21 and Figure 22). Using CD25 and CD43 as surface markers to distinguish respectively proB (CD43$^+$CD25$^-$) from preB (CD43$^-$CD25$^+$) cells, we observed, on average, a 40% reduction in the number and frequency of *Jmjd3*-mutant pre-B cells when compared to controls (Figure 23). This difference was statistically significant (p<0.05). Moreover, the frequency of *Jmjd3* mutant pro-B cells increased around 30% in comparison to controls (12.6% vs. 18.6%), while absolute numbers did not significantly differ between the two experimental groups (Figure 23). These results indicate that Jmjd3 controls the size of the pre-B cell pool. Interestingly, the reduction in pre-B cells was already seen in *Jmjd3*$^{+/-}$ haploinsufficient mice (*Jmjd3*$^{fl/+;}$*Mb1-cre*) pointing to a strict dependence of pre-B cells on two functional copies of *Jmjd3* (Figure 22 and Figure 23).

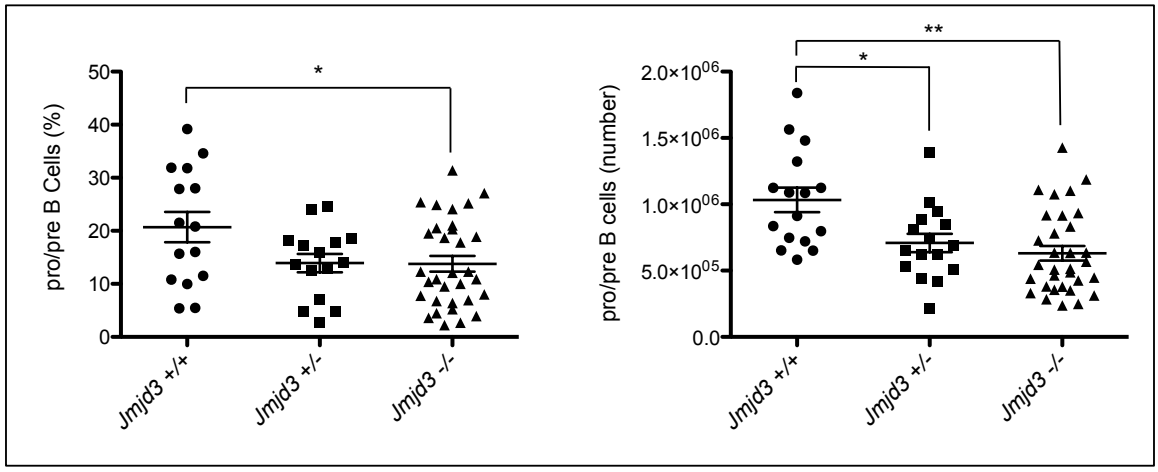

Figure 22. B cell progenitors are reduced upon *Jmjd3* inactivation. Frequency (left) and absolute number (right) of gated $IgM^{-}B220^{+}$ pro/pre B cells in $Jmjd3^{+/+}$ (*n=16*), $Jmjd3^{+/-}$ (*n=15*) and $Jmjd3^{-/-}$ (*n=31*) mice. Each dot represents a mouse. Bars represent the mean value ± SEM (t-test; * $p< 0.05$, ** $p< 0.01$).

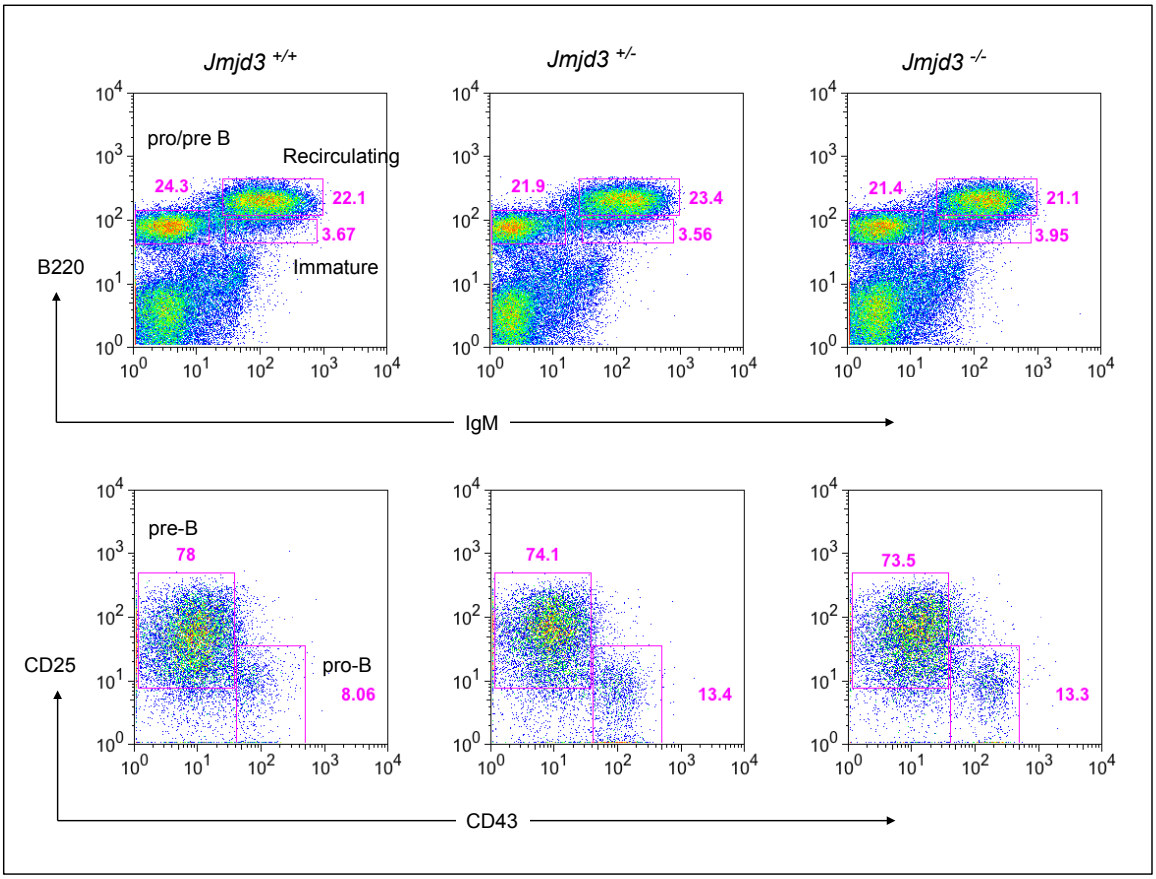

Figure 23. Increased frequency of pro-B cells upon *Jmjd3* inactivation. a) Representative flow cytometric analysis of BM cells from respectively *Jmjd3* control (*Jmjd3*$^{+/+}$), heterozygous (*Jmjd3*$^{+/-}$) and homozygous (*Jmjd3*$^{-/-}$) mutant mice. **b)** Representative FACS analysis of gated IgM^{-}B220^{+} progenitor B cells to identify respectively CD43^{+}CD25^{-} pro-B cells and CD43^{-}CD25^{+} pre-B cells in Jmjd3 control and mutant mice as indicated in a. Numbers within dot plot indicate frequencies of boxed cells. Plots are representative of five independent experiments.

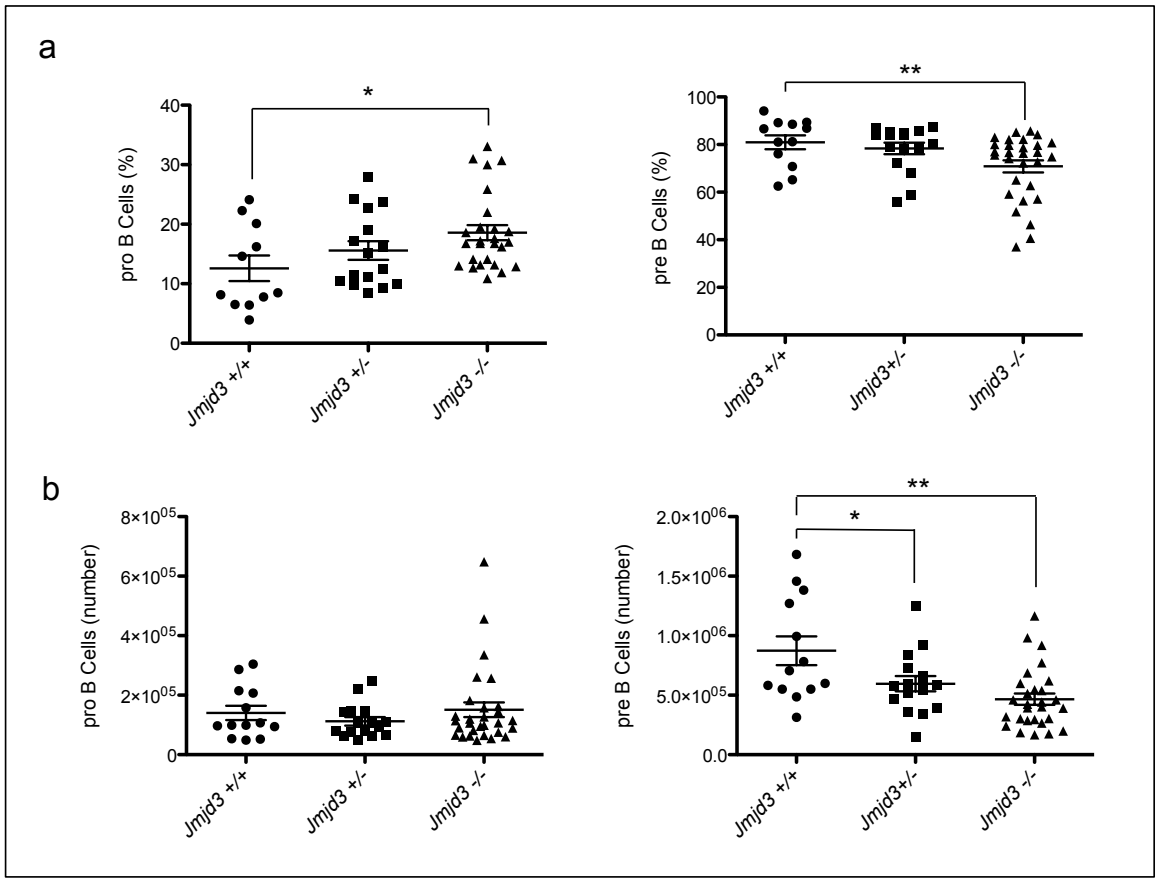

Figure 24. *Jmjd3* ablation causes a reduction of pre B cells. Frequency **(a)** and absolute number **(b)** of gated $B220^{+}IgM^{-}CD43^{-}CD25^{+}$ pre B cells in mice with the indicated genotype**.** Bars refer to mean values ± SEM. Each dot represents a mouse. (t-test, * $p< 0.05$; ** $p< 0.01$).

The reduced pre-B cell compartment seen in *Jmjd3* conditional mutant mice was associated to a contraction (40%) in the number of their $B220^{+}IgM^{lo}$ immature B cell derivatives (Figure 22 and Figure 25). Instead, both percentage and absolute number of $B220^{hi}IgM^{+}$ recirculating mature B cells were unaffected by *Jmjd3* inactivation (Figure 25).

To determine whether B cells in the BM of *Jmjd3* mutant mice had undergone Cre-mediated recombination, we sorted different B cell subsets and compared *Jmjd3* gene copy number to that of control (*Jmjd3*$^{+/+}$*;Mb1-cre*) B cells. Over 80% of *Jmjd3* alleles had undergone Cre-mediated recombination in both progenitor and immature *Jmjd3*$^{fl/fl}$*;Mb1-cre* B cells (Figure 26).

Taken together these results indicate that inactivation of *Jmjd3* in proB cells leads to a modest yet significant impairment in the size respectively of the pre-B and immature B cell compartments in the BM.

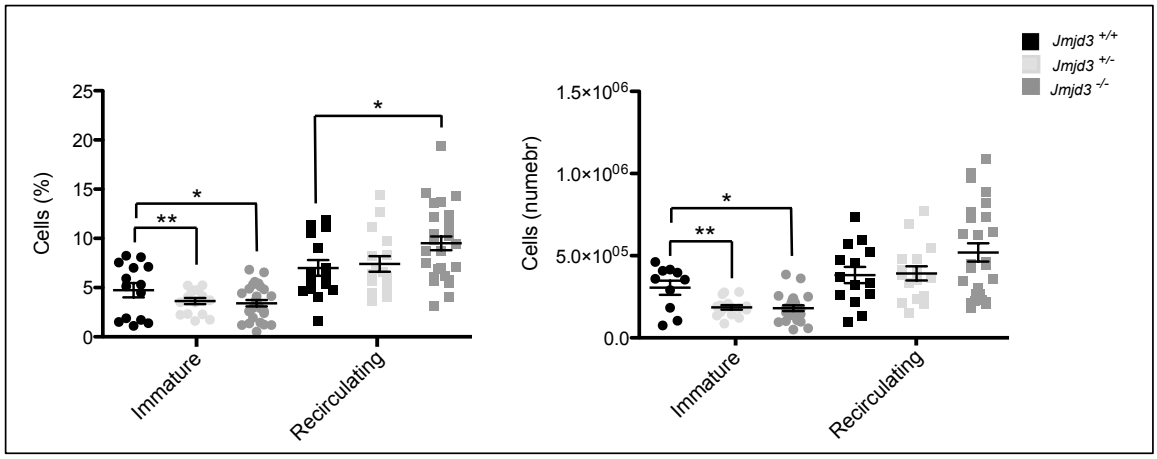

Figure 25. Analysis of BM IgM$^+$ B cell subsets after *Jmjd3* inactivation. Frequency (**a**) and absolute number (**b**) of gated B220^{lo}IgM$^+$ immature and B220$^+$IgM$^+$ recirculating B cells in the bone marrow of *Jmjd3* control , heterozygous and homozygous mutant mice. Each dot represents a mouse. Error bars indicate the mean values ± SEM.

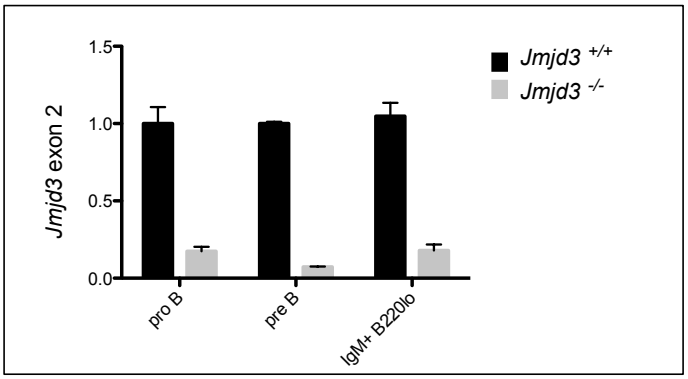

Figure 26. Efficiency of Cre-mediated inactivation of the *Jmjd3^{fl}* allele in B cell subsets. Genomic qPCR analysis to determine *Jmjd3* exon 2 copy number in the indicated B cell subsets purified from *Jmjd3* control (*Jmjd3+/+*) and mutant (*Jmjd3$^{-/-}$*) mice. Jmjd3 exon-2 mean values were plotted relative to those detected in control B cells belonging to the same subset ± SD of triplicates.

Moreover, phenotypic similarities between *Jmjd3* $^{-/-}$ and *Jmjd3* $^{+/-}$ mice indicate that haploinsufficiency of *Jmjd3* gene may be sufficient to interfere with early B cell development.

3.4. Jmjd3 and peripheral B cell development

3.4.1. Total number of mature B cells is unaffected by JMJD3 inactivation

To address the contribution of Jmjd3 in peripheral B cell development, a comprehensive immunophenotypic analysis was performed on single cell suspensions from secondary lymphoid organs of conditional *Jmjd3* mutant (*Jmjd3*$^{fl/fl}$*Mb1-cre)* and control (*Jmjd3*$^{+/+}$*; Mb1 Cre*) mice.

Jmjd3 inactivation had no substantial impact on the total number of B cells present in lymphoid organs including spleen, lymph nodes and intestinal Peyer's patches (Figure 27).

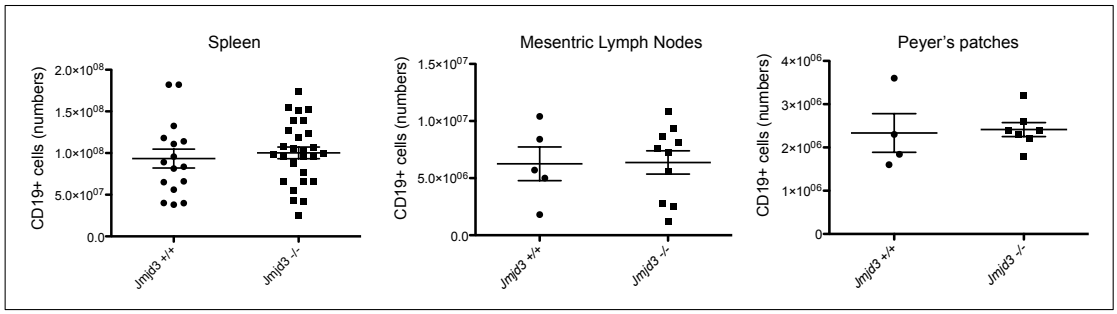

Figure 27. Number of CD19^{+} B cells is unchanged in secondary lymphoid organs of B-cell specific *Jmjd3* KO mice. Absolute number of gated CD19^{+} B cells in the indicated secondary lymphoid organs of *Jmjd3* control (*Jmjd3*$^{+/+}$) and conditional mutant (*Jmjd3*$^{-/-}$) mice were calculated based on flow cytometric analysis. Each dot corresponds to a mouse. Bars represent mean values ± SEM.

Considering the reduction in the immature B cell subset seen in the BM of *Jmjd3*-deficient mice, we next asked whether the corresponding transitional B cells in the spleen showed a similar contraction in size. Analysis of $B220^{+}AA4.1^{+}$ transitional B cells in the spleen of mutant mice displayed a normal-sized pool of transitional B cells (Figures 28,29). These results indicate that despite reduction in the number of daily produced B cells in the BM of the Jmjd3-deficient mice, comparable fraction of immature B cells in the spleen of mutant and control mice continue their development towards mature B cells.

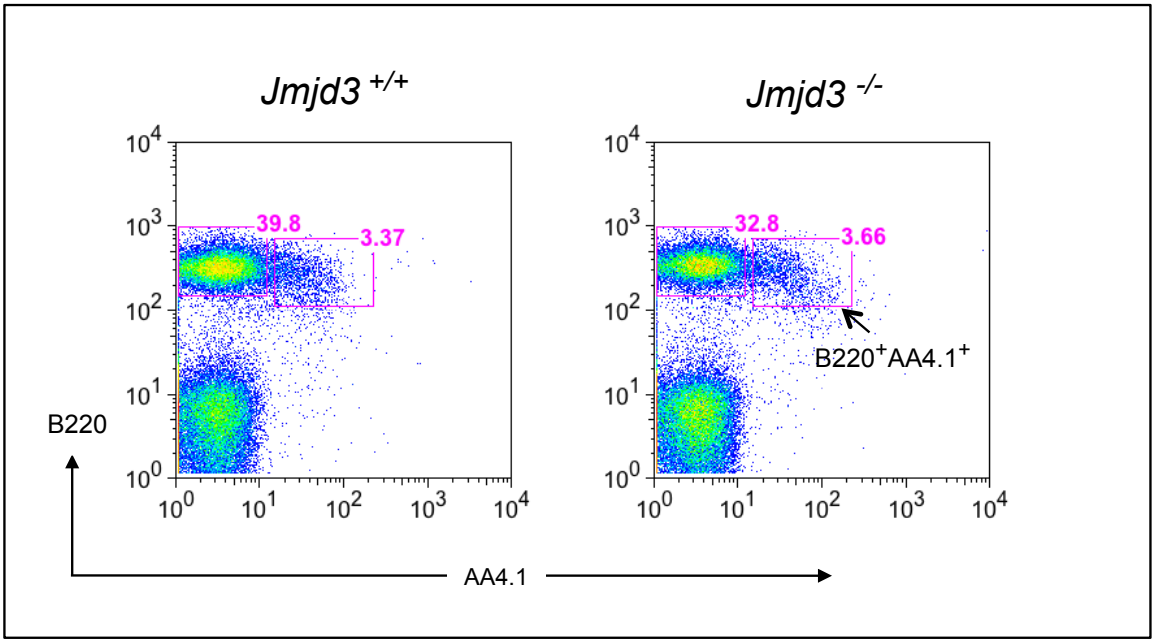

Figure 28. Immature B cells in the spleen of *Jmjd3*$^{-/-}$ mice. Representative flow cytometric analysis of splenocytes from *Jmjd3* control (*Jmjd3*+/+*)* and conditional mutant (*Jmjd3*$^{-/-}$) mice, assessed for respectively transitional ($B220^{lo}AA4.1^{+}$) and mature ($B220^{+}AA4.1^{-}$) B cells. Numbers indicate frequencies of boxed cells. Plots are representative of five independent experiments.

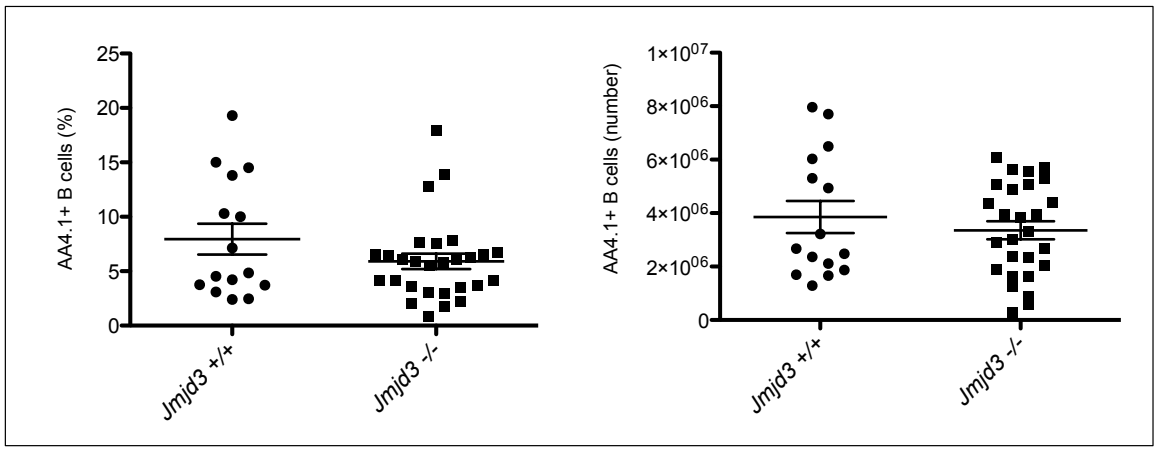

Figure 29. Quantification of transitional B cells in the spleen of *Jmjd3* mutant mice. Frequency (left) and absolute number (right) of $B220^{lo}AA4.1^{+}$ gated transitional B cells in *Jmjd3* control (*Jmjd3+/+)* and mutant (*Jmjd3-/-*) mice. Each dot represents one mouse. Error bars represent mean values ± SEM for 15 control and 28 mutant mice.

3.4.2. Jmjd3 controls the size of the MZ B cell pool

To determine whether Jmjd3 controlled B cell maturation, the absolute number respectively of Follicular (FO)/B-2, marginal zone (MZ) and B-1 B cell subsets in secondary lymphoid organs was determined and compared between *Mb1-cre* controls and *Jmjd3*$^{fl/fl}$*Mb1-cre* conditional mutant mice. In the spleen, FO B cells ($CD19^{+}$ $CD23^{+}CD21^{+}$) were similar in numbers between *Jmjd3* control and mutant animals (Figure 30). In contrast, both the number and frequency of MZ B cells ($CD19^{+}CD23^{lo}CD21^{hi}CD38^{hi}$) were significantly increased in *Jmjd3* mutant mice, being 1.5- to 1.8–fold higher than controls (Figure 30 and 31). The increase in the fraction of MZ B cells caused a corresponding decrease in the percentage of FO B cells in the spleen of *Jmjd3* mutant mice (Figure 30).

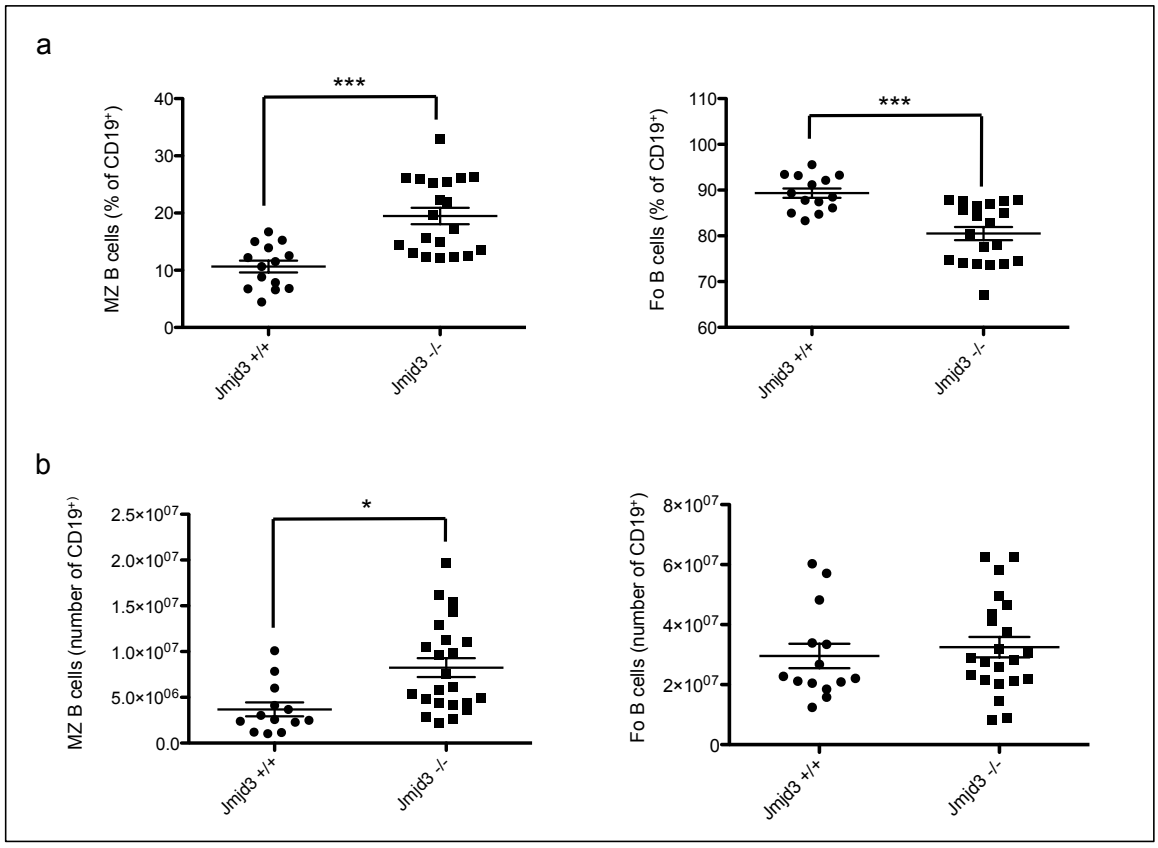

Figure 30. Quantification of mature B cell subsets in the spleen of *Jmjd3* mutant mice. Frequency (a) and absolute number (b) of the indicated mature B cell subsets in the spleen of *Jmjd3* control (*Jmjd3*$^{+/+}$) mutant (*Jmjd3*$^{-/-}$) mice as assessed by flow cytometric analysis. Numbers were obtained from the analysis respectively of 14 control and 20 *Jmjd3* conditional mutants. Bars represent the mean values ± SEM (t-test; * p <0.05, *** p < 0.001).

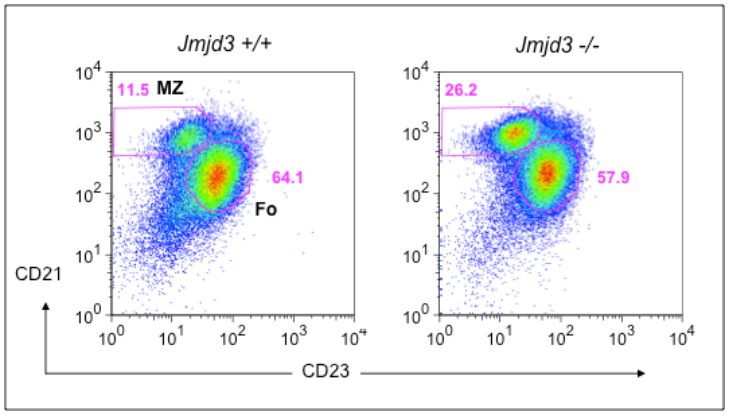

Figure 31. *Jmjd3* deficiency alters the proportion of mature B cell subsets in the spleen. Representative flow cytometric analysis of gated CD19^{+} splenic B cells in *Jmjd3* control (*Jmjd3*$^{+/+}$; n=10) and conditional mutants (*Jmjd3*$^{-/-}$; n=10^{-}). Numbers indicate frequencies respectively of MZ (CD21^{hi}CD23^{lo}) and Fo (CD21^{+}CD23^{+}) B cells.

The increased fraction of bona fide MZ B cells in Jmjd3 mutant mice was further assessed monitoring the expression pattern of the CD38 antigen (Vences-Catalan and Santos-Argumedo, 2011). As shown in Figure 27, the spleen of *Jmjd3* mutant mice showed a higher proportion of $CD19^{+}CD23^{lo}CD38^{hi}$ MZ B cells, hence confirming the results obtained with CD21 stainings (Figure 32). Finally, we performed immunofluorescence (IF) analysis of spleen sections of $Jmjd3^{-/-}$ and $Jmjd3^{+/+}$ mice to determine the size of the MZ area. Specifically we used antibodies against respectively B220 to detect B cells, and MOMA-1 to visualize metallophilic macrophages lining the marginal sinus (Kraal and Janse, 1986). Quantification of the data revealed a modest yet significant ($p<0.05$) increase in the area occupied by MZ B cells in Jmjd3 mutant mice (Figure 33 and Figure 34). All together these results indicate the *Jmjd3* inactivation leads to a selective expansion in the spleen of the MZ B cell compartment.

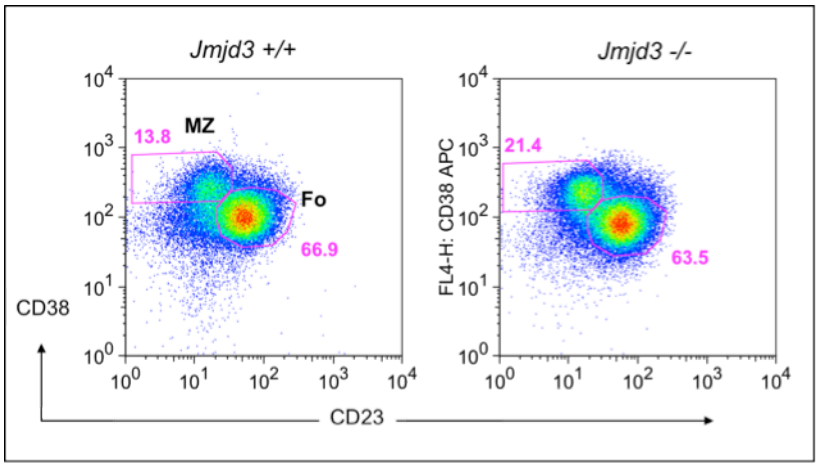

Figure 32. Fo and MZ B cells frequencies in *Jmjd3* mutants based on CD38 and CD23 surface markers. Representative flow cytometric analysis of $CD19^{+}$ gated B cells in the spleen of *Jmjd3* control ($Jmjd3^{+/+}$; n=10) and mutant ($Jmjd3^{-/-}$; n=10) mice stained for CD38 and CD23 expression. MZ B cells were defined as $CD23^{lo}CD38^{hi}$ cells, whereas Fo B cells are $CD23^{+}CD38^{+}$. Numbers indicate frequency of boxed cells. Plots are representative of five independent experiments.

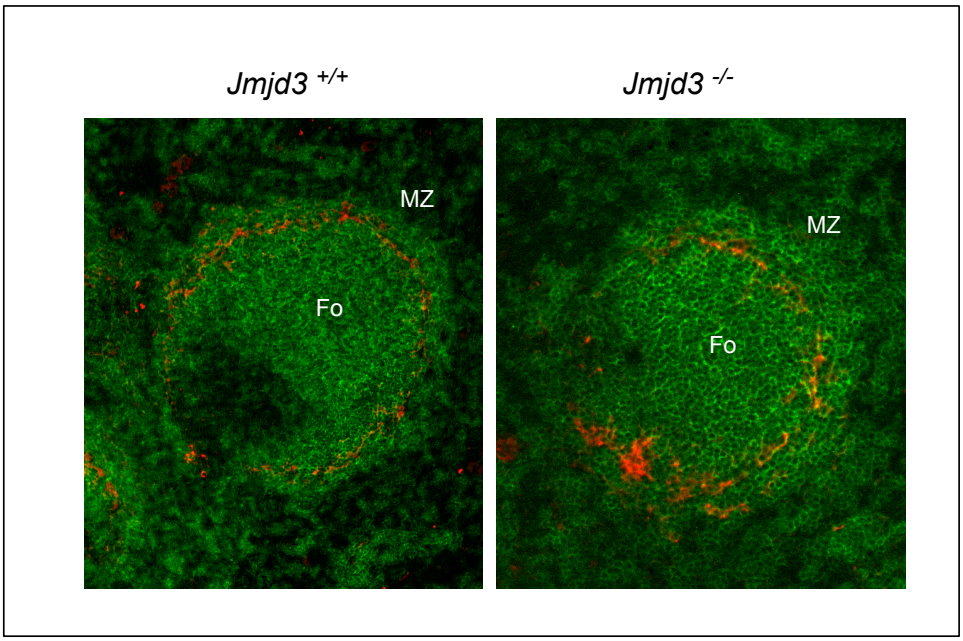

Figure 33. Accumulation of *Jmjd3*$^{-/-}$ B cells in MZ area of the spleen. Representative immunofluorescence analysis of splenic sections of *Jmjd3* control (*Jmjd3*$^{+/+}$) and mutant (*Jmjd3*$^{-/-}$) mmice stained for for B220 (green) and MOMA-1 (red). MZ B cells reside outside of the ring of MOMA-1^{+} macrophages delimiting the B cell follicle.

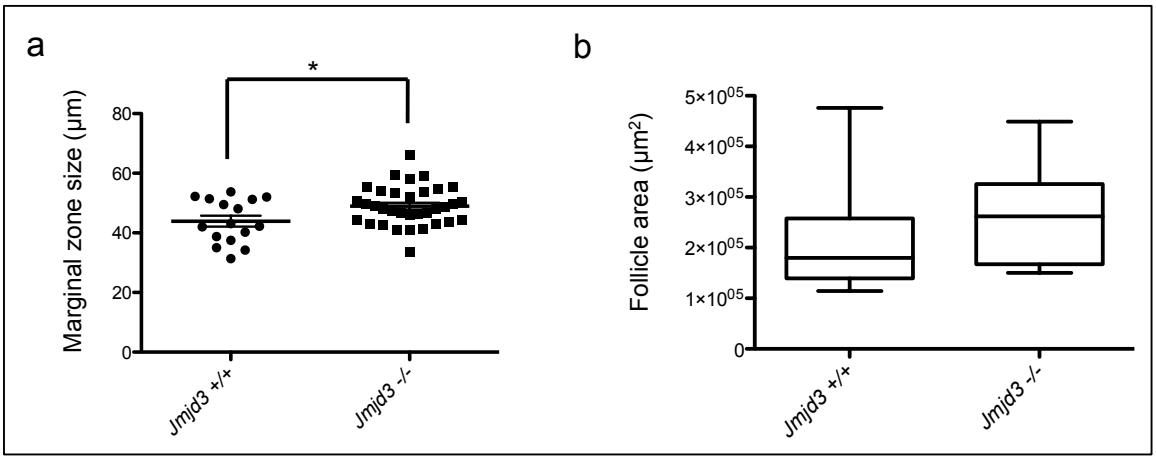

Figure 34. Quantification of the splenic marginal zone area in *Jmjd3* control and mutant animals. a) Quantification of the average thickness of the marginal zone in the spleen of *Jmjd3* control (*Jmjd3*$^{+/+}$) and mutant (*Jmjd3*$^{-/-}$) mice. Each dot represents the average thickness of an individual follicle. **b)** Average area of B-cell follicles in respectively three control and three *Jmjd3* mutant mice. 16 follicles for Jmjd3-proficient and 22 follicles of Jmjd3-deficient mice were analyzed respectively. Bars indicate mean values ± SEM.

3.4.3. Jmjd3 influences B-1a/B1-b B cell ratio

We next tested whether disruption of *Jmjd3* expression influenced development of B-1 B cells localized in body cavity serosa. On the basis of the CD5 marker, B-1 B cells are classified as B-1a ($CD5^+$) and B-1b ($CD5^-$) B cells, respectively. B-1a and B-1b B cells express higher levels of CD19 and lower levels of CD23 and B220 when compared to Fo/B2 B cells (Montecino-Rodriguez et al., 2012).

Flow cytometric analysis of peritoneal cavity lavages showed a comparable number of total $CD19^+$ B cells between *Jmjd3*$^{-/-}$(*Jmjd3*$^{fl/fl}$*;Mb1-cre*) and control (*Jmjd3*$^{+/+}$*;Mb1-cre*) mice (Figure 35). Among B cells, *Jmjd3* mutant mice showed a modest yet significant increase in the average number and frequency of $CD19^+B220^+$ B-2 B cells (Figure 31). Conversely, whereas the total number of $CD19^{hi}B220^{lo}$ B-1 B cells was comparable between control and *Jmjd3* KO mice, their distribution into B-1a and B1-b B cell subsets was altered in the mutant animals (figure 36 and 37). Specifically, we found that inactivation of *Jmjd3* caused a significant reduction in the subset of $CD5^+$ B-1a B cells (Figures 36 and 37). The contraction in $CD5^+$ B1-a B cells affected both the frequency (42.8% vs. 62% in controls) and absolute number (1.37 vs. 0.9×10^5 in controls) (Figure 36). The reduction of B1-a B cells was at the expense of $CD5^-CD19^{hi}$ B-1b cells that increased in numbers and frequency in *Jmjd3* mutant animals (Figure 36). These results point to a specific contribution of JMJD3 to B-1 B cell development.

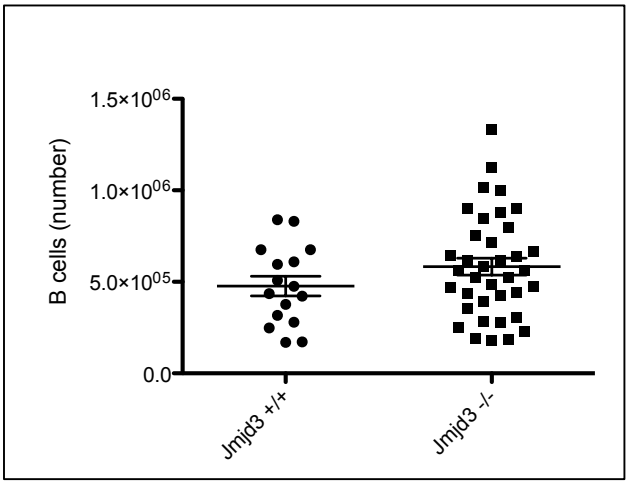

Figure 35. Absolute number of B cells in peritoneal cavity lavages of *Jmjd3* KO and wild-type mice. Flow cytometric determination of $CD19^+$ B cells in the peritoneum of *Jmjd3* control (*Jmjd3*$^{+/+}$) and conditional mutant (*Jmjd3*$^{-/-}$) mice. Each dot represents a mouse. Bars indicate mean values ± SEM.

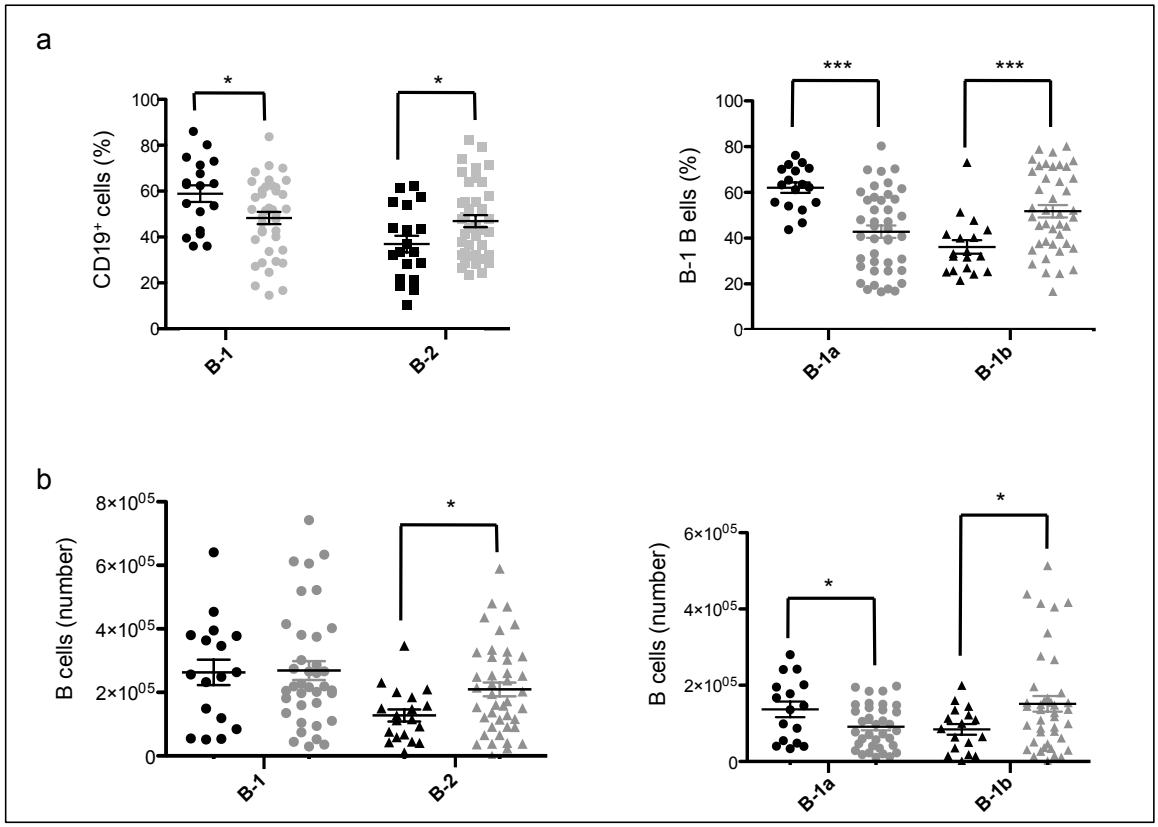

Figure 36. B cell subsets in peritoneal cavity lavages of *Jmjd3* control and mutant animals. Frequency (a) and absolute number of the indicated B cell population as determined by flow cytometric analysis in respectively 17 control (black) and 36 mutant (grey) animals. B-1 B cells were gated as $CD19^{hi}B220^{+}$, B1-a B cells were gated as $CD19^{hi}CD5^{+}$; B1-b B cells were $CD19^{hi}CD5^{-}$ (t-test; * p <0.05, *** p < 0.001).

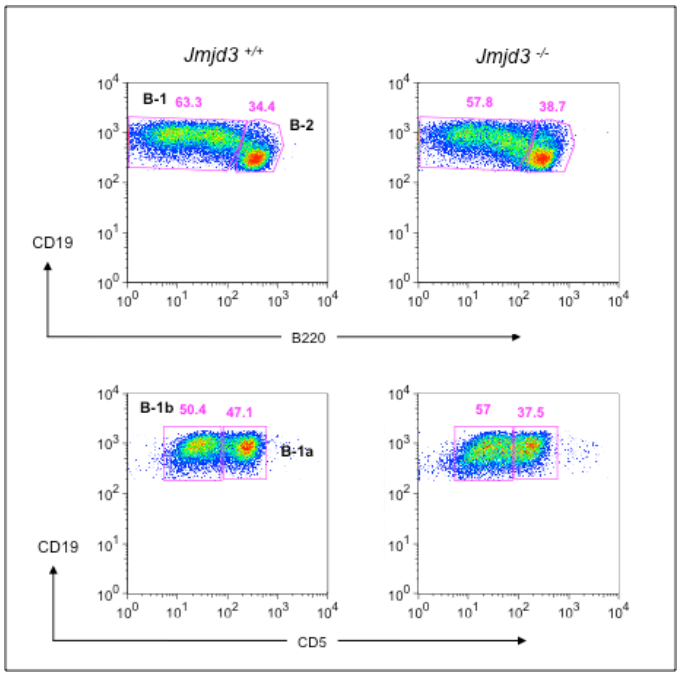

Figure 37. B-1a B cells are reduced in frequency in *Jmjd3* mutant mice. Representative flow cytometric analyses of respectively *Jmjd3* control and mutant peritoneal cavity lavages stained for the indicated surface markers. Identity of B cell subsets is indicated within each dot plot. Numbers indicate frequencies in boxed B cells among $CD19^{+}$ gated cells.

3.4.4. *JMJD3* inactivation is not counterselected upon B cell maturation

To confirm that B cell maturation is compatible with *Jmjd3* inactivation, we determined the status of the $Jmjd3^{fl}$ allele in mature B cells purified from the spleen and peritoneal cavity lavages of $Jmjd3^{fl/fl}$*;Mb1-cre* conditional mutant mice. We performed quantitative PCR on genomic DNA isolated respectively from B-2 and B-1 B cells to determine *Jmjd3* gene copy number. The analysis of qPCR data revealed that Fo, MZ and B-1 B cell compartments in $Jmjd3^{fl/fl}$*;Mb1-cre* mice were mainly composed of *Jmjd3* deficient B cells (Figure 38). All together, these results suggest that Jmjd3 has a selective, non-redundant, function in controlling the size of the MZ and B-1 B cell pools.

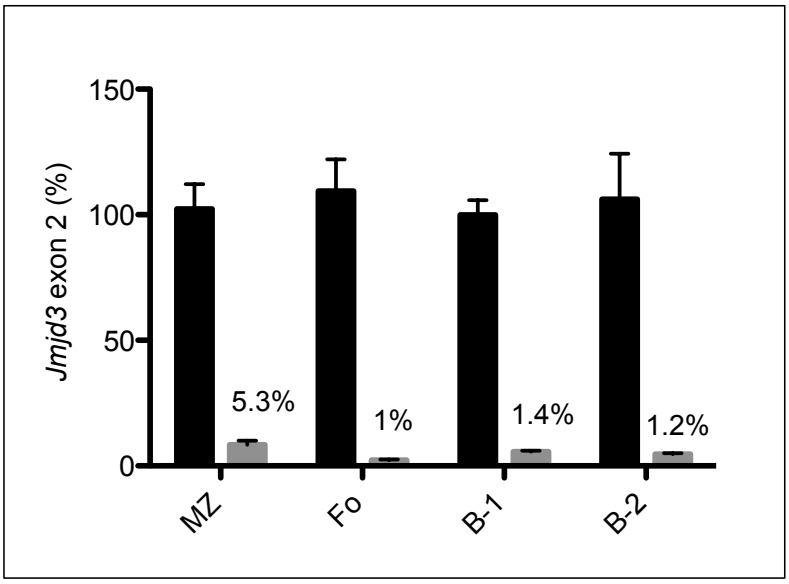

Figure 38. Efficiency of Cre-mediated recombination in *Jmjd3* conditional mutant mature B cells. Quantification by genomic PCR of exon 2 copy number in sorted B cell subsets isolated from Jmjd3 control (black bars) and conditional mutant (grey bars) mice. Values were normalized on the basis of DNA input and represented as relative to those measured in control B cells belonging to the same subset. Mean values were plotted ± SEM of triplicates.

3.5. Jmjd3 and B cell proliferation/turnover

The inactivation of Jmjd3 in B-lineage cells has revealed specific contributions of the demethylase during both early and late stages of B cell development. To investigate the possible mechanisms responsible for the changes in numbers and frequencies of B cells resulting from Jmjd3 inactivation we turned to in vivo Brdu labeling assays. The latter approach allows the in vivo investigation of the effects of specific insults (e.g. the induction of a genetic mutation) on population dynamics (Allman et al., 1993). In particular, we were interested to determine whether *Jmjd3* inactivation influenced the proliferation and turnover respectively of progenitor and mature B cells. To this aim we fed *Jmjd3* control and mutant mice with BrdU. Depending on the purpose of the experiment (proliferation vs. turnover), BrdU feeding times differed and hence will be described separately below.

3.5.1. *Jmjd3* inactivation reduces BrdU incorporation in progenitor B cells

Data described in section 3.3 have revealed that *Jmjd3* inactivation leads to a reduction in both the absolute number and percentage of BM preB cells. To test whether this effect was due to impaired/delayed proliferation of pre-B cells, we fed *Jmjd3* conditional and mutant mice with BrdU for seven days. FACS analysis of BM cells from *Jmjd3* control mice revealed 85% incorporation of the nucleotide analogue in gated IgM^-B220^+ pro/preB cells. Despite a certain degree of variability observed between mice, inactivation of *Jmjd3* led to fewer $BrdU^+$ IgM^-B220^+ pro/pre-B cells after 7 days of BrdU feeding (Figure 39). BrdU incorporation rates were instead comparable between mature IgM^+B220^{hi} BM B cells of *Jmjd3* control and mutant mice. These results suggest that *Jmjd3* controls the entry of preB cells into S-phase and hence progenitor B cell proliferation.

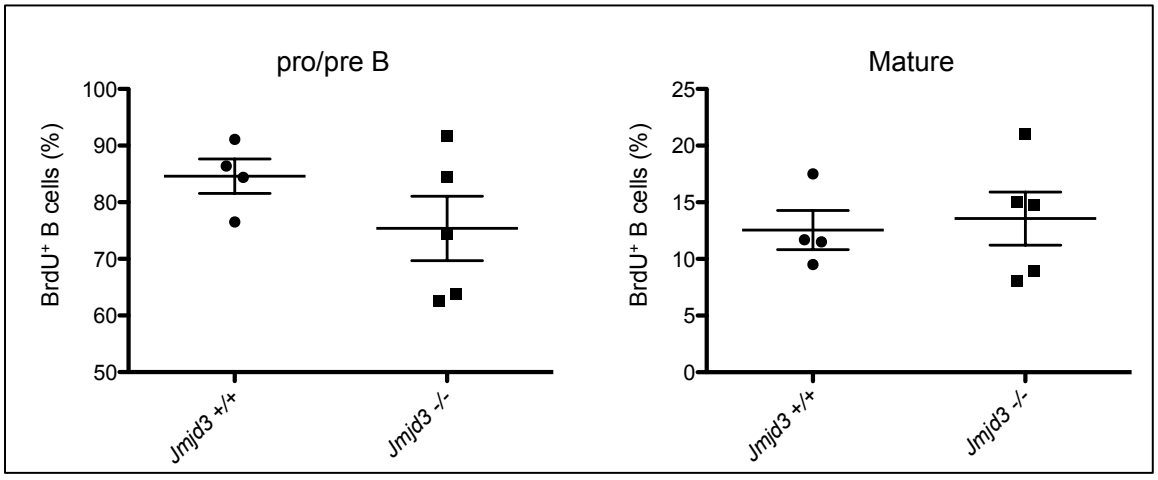

Figure 39. BrdU incorporation in Jmjd3 control and mutant B cells 7 days after in vivo labeling. Quantification by flow cytometric analysis of the percentage of $BrdU^+$ B cells among respectively B cell progenitors (IgM^-B220^+) and mature IgM^+B220^+ B cells present in the bone marrow of Jmjd3 control (*Jmjd3*$^{+/+}$) and mutant (*Jmjd3*$^{-/-}$) mice. Bars represent mean frequencies of BrdU+ B cells ± SEM in 5 control and 4 mutant mice.

To find further confirmation to this hypothesis, we fed Jmjd3 control and mutant mice with BrdU for only 16 hours and subjected BM cells to BrdU incorporation analysis by flow cytometry. The fraction of BrdU-labeled progenitor B cells was substantially lower in *Jmjd3* mutant animals in comparison to controls (Figure 39), hence supporting data obtained with 7 days of BrdU feeding. The delay in S-phase led to fewer BrdU labeled cells differentiating into $B220^{lo}IgM^{+}$ immature B cells in Jmjd3 conditional mutants (Figure 40).

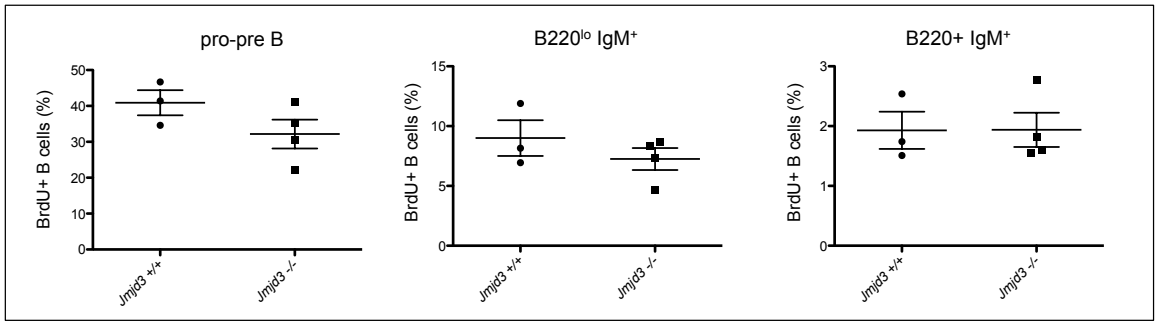

Figure 40. *Jmjd3* mutant B cell progenitors show reduced proliferation. Percentage of $BrdU^{+}$ B cells in the indicated subsets of BM B cells. Mice were treated with BrdU for 16 hours and analyzed immediately after by flow cytometry. Bars indicate mean frequencies ± SEM in 3 controls and 4 mutant mice.

3.5.2. *Jmjd3* influences peripheral B cell turnover

We have shown that *Jmjd3* inactivation alters the distribution of B cells into the three major peripheral B cell subsets. Jmjd3 may control the commitment of transitional B cells into specific mature B cell subsets such as the MZ or B-1B cell lineages. Alternatively, Jmjd3 may regulate the turnover of one or more peripheral B cell populations by regulating their life span. To study the turnover of B cells in peripheral lymphoid organs of *Jmjd3* mutant animals, we administrated BrdU for 7 days in the drinking water and analyzed BrdU incorporation in B cell subpopulations in the spleen and peritoneal cavity lavages. Short-lived $B220^{lo}AA4.1^{+}CD23^{+}$ splenic transitional T2 B cells that represent recent emigrants from the BM showed similar frequencies of

BrdU$^+$ cells between *Jmjd3* mutant and control mice. This result indicates that *Jmjd3* inactivation does not influence the output of B cells from the BM to peripheral lymphoid organs.

Despite a considerable variability in BrdU incorporation rates, JMJD3 mutant mice appeared to recruit fewer BrdU$^+$ B cells within the three major subsets of mature B cells (Figure 41). These results, pending confirmation by additional experiments, suggest a slower turnover of mature B cells lacking functional Jmdj3.

To test whether Jmjd3–deficient mature B cells acquired resistance to programmed cell death, we compared the fraction of apoptotic cells between control and mutant mice. For this purpose we determined the fraction of mature B cells expressing active/cleaved forms of caspases that were revealed through the binding to the Casp-GLOW reagent. Flow cytometric determination of CaspGLOW$^+$ cells revealed comparable fractions of apoptotic cells within the three major subsets of mature B cells of *Jmjd3* control and mutant mice (Table 11). Collectively, these results suggest that Jmjd3 does not regulate BM B cell efflux while in peripheral lymphoid organs it increases the turnover of mature B cells independent of the regulation of apoptosis.

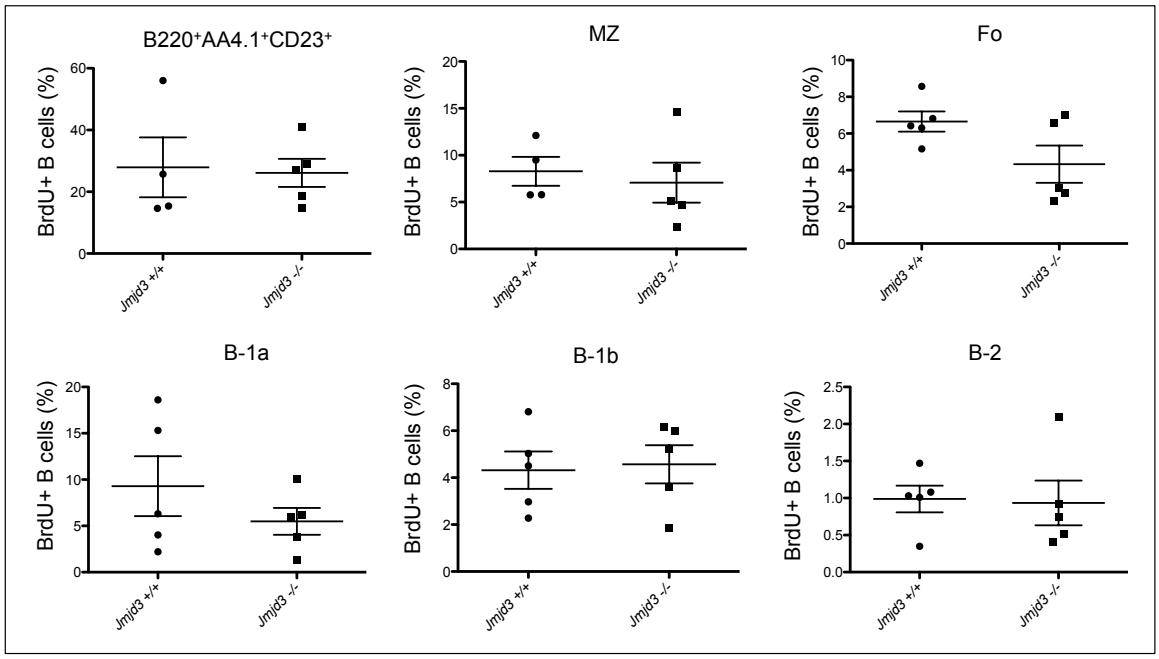

Figure 41. B-cell turnover within B cell subsets present in secondary lymphoid organs of *Jmjd3* control and mutant mice. Frequency of BrdU^{+} B cells within the indicated populations of B cells in Jmjd3 control (*Jmjd3*$^{+/+}$) and mutant (*Jmjd3*$^{-/-}$) animals, as assessed by flow cytometric analysis. Lower panels refer to B cell subsets present in peritoneal cavity lavages. Bars indicate mean frequencies ± SEM in 5 controls and 4 mutant mice.

Table 11. Frequency of apoptotic B cells in the spleen of *Jmjd3* control and mutant mice.

	Spleen			Peritoneal lavage		
Genotype	B220+AA4.1+ (%)	Marginal zone (%)	Follicular (%)	B-1a B (%)	B-1b B (%)	B-2 B (%)
Jmjd3 $^{+/+}$	3.33 ± 0.63	3.71 ± 0.175	1.81 ± 0.37	10.9 ± 1.6	6.75 ± 1.42	3.03 ± 1.4
Jmjd3 $^{-/-}$	3.34 ± 0.25	4.08 ± 0.4	2.62 ± 0.55	7.428 ± 0.41	4.022 ± 0.91	1.691 ± 0.294

Average frequency ± SEM of mature B cells expressing cleaved active forms of caspases as assessed by flow cytometry analysis using the Casp-GLOW reagent. Five mice for each genotype were analyzed.

3.6. Is Irf4 a critical target of Jmjd3 function in mature B cells?

A recent work has reported that inactivation of the transcription factor Irf4 in mature B cells leads to their accumulation in the marginal zone area as a result of the activation of the Notch2 pathway (Simonetti et al., 2013). Since Irf4 is a direct target of Jmjd3 in macrophages (Satoh et al., 2010), we asked whether Irf4 transcript levels were affected by Jmjd3 inactivation in MZ and Fo B cells. Expression of Irf4 was determined by qRT-PCR in Fo and MZ B cells of two independent *Jmjd3* mutant mice that showed a substantial increase in the fraction of MZ B cells. qRT-PCR analysis revealed 50% reduction in *Irf4* transcript levels in MZ and Fo B cells of mutant animals when compared to the demethylase-proficient counterparts (Figure 42). Interestingly, expression of Irf4 was not affected in a *Jmjd3* mutant animal in which we failed to observe a substantial increase in the MZ B cell subset. This result enforces the scenario whereby the increase in MZ B cells observed in Jmjd3 mutant animals is contributed, at least partly, by a downregulation of Irf4 expression, leading to a relocalization of mutant B cells to the MZ area and/or reprogramming of Fo B cells.

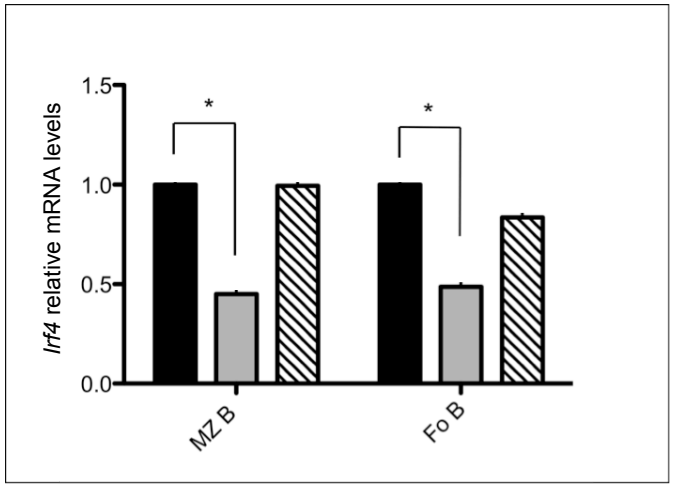

Figure 42. Irf4 expression is reduced in MZ and Fo B cells of Jmjd3 mutant mice. qRT-PCR determination of *Irf4* transcripts in sorted Jmjd3 control (black) and mutant (grey) MZ and Fo B cells. The analysis reveals also average *Irf4* transcript levels in a Jmjd3 conditional mutant (hatched bar) in which we failed to detect major changes in the proportion of Fo and MZ B cells. Columns represent the mean expression levels (t-test; *, $p < 0.05$).

3.7. Role of *Jmjd3* in B cell activation

3.7.1. Jmjd3 controls the proliferative response of B cells to TLR4 agonists

The strong, transient, upregulation of Jmjd3 measured in B cells stimulated with LPS, anti-RP105 and CD40 ligation pointed to a possible role for the demethylase in B cell activation (Figure 15). Therefore, we asked whether Jmjd3 influenced B cell proliferation in response to the above-indicated mitogenic stimulations. To this end we purified resting B cells from the spleen of *Jmjd3* control (*Mb1-cre*) and mutant (*Jmjd3*$^{fl/fl}$*;Mb1-cre*) animals and cultured them in vitro for 4 days in the presence of respectively LPS, LPS+IL-4, agonistic anti-CD180/RP-105 and anti-CD40+IL-4. The latter stimulations failed to induce *Jmjd3* expression in mutant B cells, confirming efficient Cre-mediated recombination of the *Jmjd3*^{fl} gene (Figure 43).

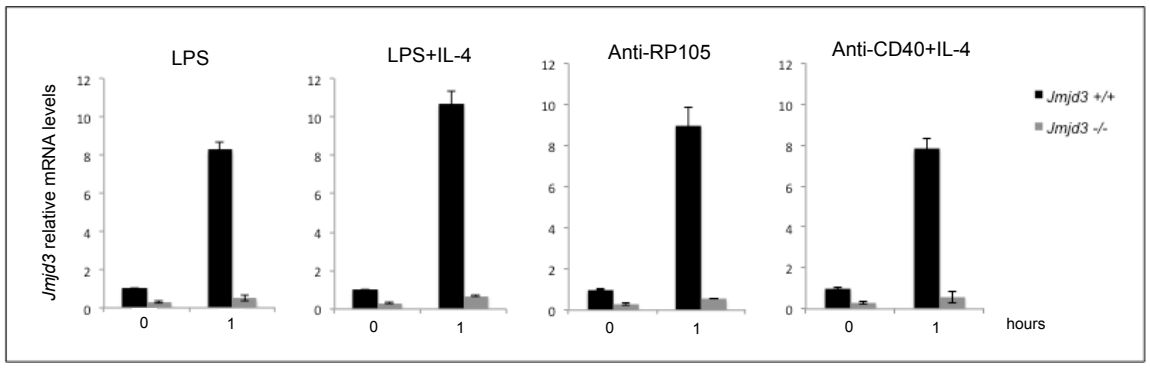

Figure 43. Failure to induce *Jmjd3* expression by activated Jmjd3 conditional mutant B cells. qRT-PCR determination of *Jmjd3* transcripts in *Jmjd3* control (*Jmjd3*$^{+/+}$) and mutant (*Jmjd3*$^{-/-}$) splenic B cells respectively before (0 hr) and 1 hr after activation with the indicated mitogenic stimuli. *Jmd3* transcripts were normalized to the housekeeping Rplp0 and represented as relative to the levels in resting B cells. Columns represent mean values of triplicates ± SD.

Growth curve analyses revealed a substantial delay and blunted response of *Jmjd3* mutant B cells to both LPS and anti-RP105 stimulation (Figure 43 a and b). *Jmjd3* mutant B cells showed two main types of responses to LPS stimulation. In most cases mutant B cells displayed a delayed growth that became apparent as early as 24 hr after stimulation stimulation (Figure 44b). Notably, the growth defect was restricted to the first 48hr, as doubling times became more comparable between mutant and control B cells after 2 days of stimulation. In few cases, defective growth of *Jmjd3* mutant B cells became apparent only at a later time point. (Figure 44b).

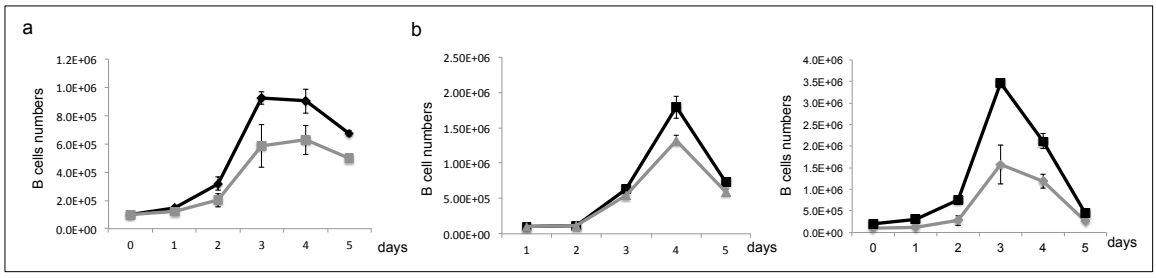

Figure 44. Jmjd3 mutant B cells show a delayed and blunted response to TLR4 agonists. a) Growth curves of *Jmjd3* control (black line) and mutant (grey line) B cells activated with anti-CD180/RP105, **b)** B cell counts in *Jmjd3* control (black line) and mutant (grey line) cultures at different days after LPS stimulation. In most cases mutant B cells revealed a delayed and blunted proliferative response to LPS (right growth curve). In few cases *Jmjd3* mutant B cells showed retarded growth detected only at a later time point (left). Graphs are representative of three independent experiments, each based on 2 control and Jmjd3 mutant B cell cultures.

We hypothesized that Jmjd3 mutant B cells that succeeded to proliferate in response to LPS stimulation could represent Cre escape variants and thus still expressed JMJd3. To test this, we quantified *Jmjd3* gene copy number in Jmjd3 mutant B cell cultures respectively 24 hr and 96 hr after LPS stimulation. Analysis of qPCR data revealed high efficiency Cre-mediated recombination at the Jmjd3^{fl} locus at both time points, excluding therefore counter selection of mutant B cells over the culture period (Figure 45).

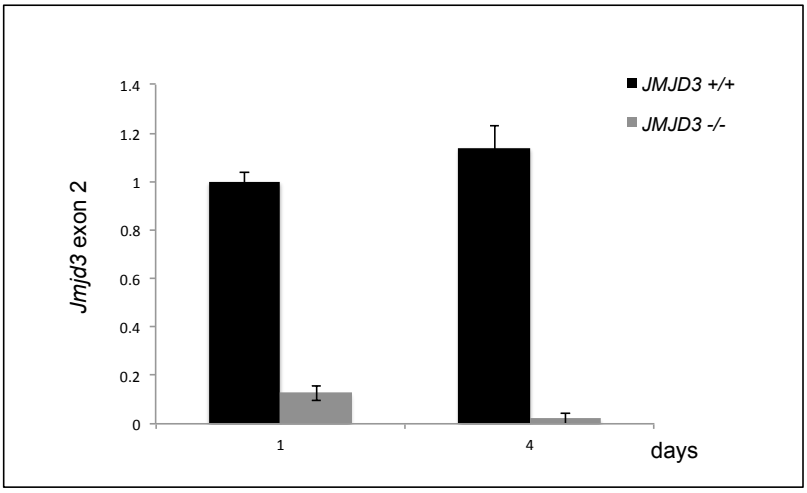

Figure 45. *Jmjd3* is efficiently inactivated in B cells *in vitro*. Quantification by genomic qPCR of *Jmjd3* exon 2 copy number in control (*Jmjd3*$^{+/+}$) and *Jmjd3* mutant (*Jmjd3*$^{-/-}$) B cells collected respectively at day-one and -four of LPS stimulation. Columns represent mean values of three mice ± SEM.

Notably, the combined stimulation of LPS and Interleukin-4 (IL-4) rescued partially the growth retardation of *Jmjd3*$^{-/-}$ cells.Along the same lines, stimulation of B cells through the CD40 receptor, in the presence of IL-4 was largely unaffected by the inactivation of Jmjd3 (Figure 46). All together these results indicate that Jmjd3 is selectively involved in activation of B cells by LPS and other TLR4 agonists, in the absence of Il-4 co-stimulation.

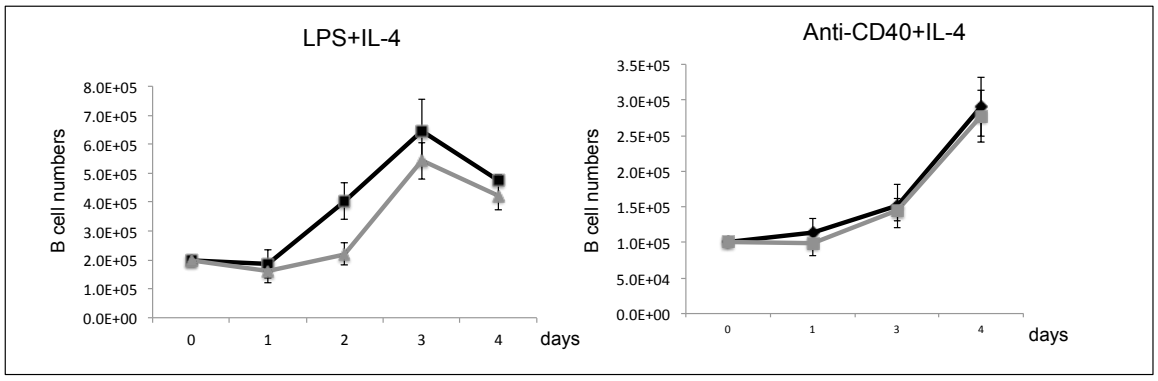

Figure 46. *Jmjd3*$^{-}$ mutant B cells respond fairly well to LPS+IL4 and CD40+IL4 stimulations. In vitro growth curves of *Jmjd3* control (black line) and mutant (grey) B cells after stimulation with the indicated mitogens. Graphs representative growth curves respectively of three control and three mutant mice.

3.7.2. Jmjd3 protects LPS-activated B cells from apoptosis

To characterize the mechanisms underlying the defective growth of *Jmjd3*$^{-/-}$ B cells, we measured cell viability after stimulation with LPS and LPS+IL-4 stimulation. Jmjd3 control and mutant B cells were collected at different time points after LPS +/- IL-4 stimulation and stained with propidium iodide (PI). Flow cytometric analysis of B cells stimulated with LPS+IL-4 revealed a comparable fraction of PI^{+} dead cells between *Jmjd3* mutant and control cultures. In contrast, when B cells were stimulated only with LPS, Jmjd3 inactivation reduced by 40% the fraction PI^{+} B cells after three days of stimulation (Figure 47). This difference became less apparent at later time points, when majority of B cells succumbed by nutrient exhaustion. To test whether *Jmjd3* protected B cells from programmed cell death, we stained mutant and control cultures (stimulated with LPS) with the caspGLOW reagent that reveals expression of active/cleaved forms of caspases. The results shown in Figure 42 indicate that Jmjd3 inhibition caused a significant reduction in the proportion of apoptotic B cells three days after LPS stimulation. Interestingly addition of IL-4 to the culture medium abolished the protective effect on apoptosis caused by Jmjd3 inactivation (Figure 48).

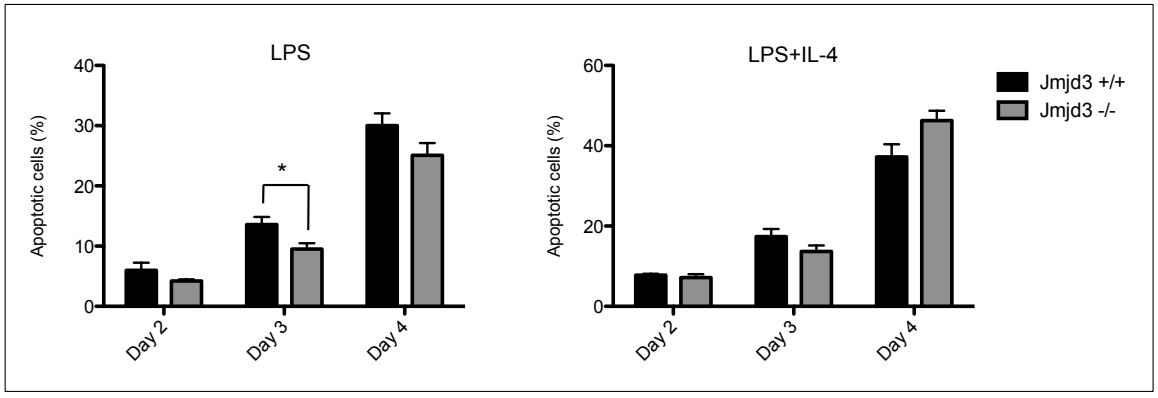

Figure 47. Increased viability of *Jmjd3* mutant B cells after LPS activation. Splenic B cells were collected at different days after LPS ± IL-4 stimulation and stained with propidium iodide (PI). Frequencies of PI^{+} dead cells were measured by flow cytometric analysis respectively in 4 controls and 6 mutants for each time point. Columns represent mean frequencies ± SEM. (*, p <0.05).

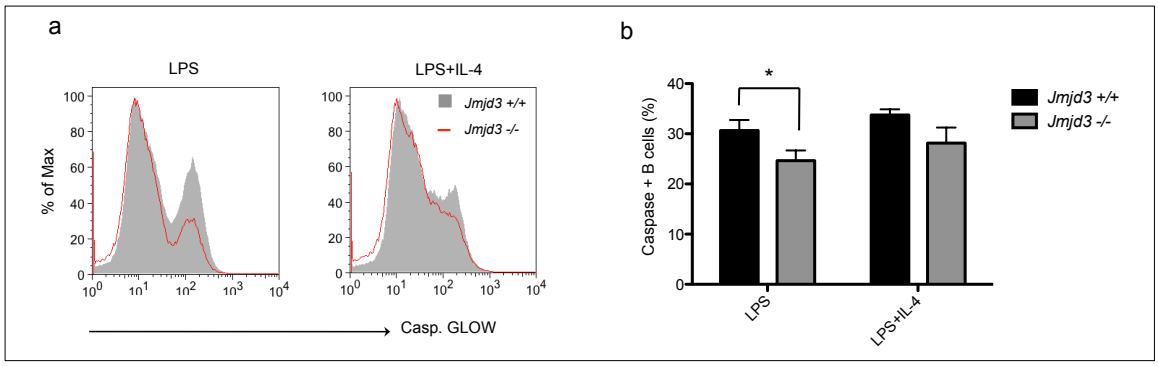

Figure 48. *Jmjd3* mutant B cells are resistant to apoptosis after LPS stimulation a) Representative histogram overlay of active caspase-positive B cells among *Jmjd3* control (gray filled line) and mutant (red thin line) B cells activated with either LPS (left) or LPS+IL-4 (right); **b)** Summary of data referred to the frequency of apoptotic (expressing active caspase(s)) B cells determined by flow cytometry in respectively 4 controls and 10 mutant animals. Columns represent mean frequencies ± SEM. (*, p <0.05).

The reduced susceptibility to undergo apoptosis is likely not accountable for the lower proliferative burst of Jmjd3 mutant B cells stimulated with LPS. Therefore, we asked whether loss of Jmjd3 impaired cycle progression. To address this, we performed cell cycle analysis on respectively LPS- and LPS+IL-4-activated B cells at different days of stimulation. Analysis of the data revealed comparable cell-cycle profiles between Jmjd3 control and mutant B cells 2 days after LPS stimulation. Instead, quite surprisingly, *Jmjd3* deficient B cells displayed a modest increase in the proportion of cells in S phase three days after stimulation (Figure 49). These results indicate that the delayed growth of Jmjd3 mutant B cells in response to LPS stimulation is not due to an arrest of the cells in a specific stage of the cell-cycle.

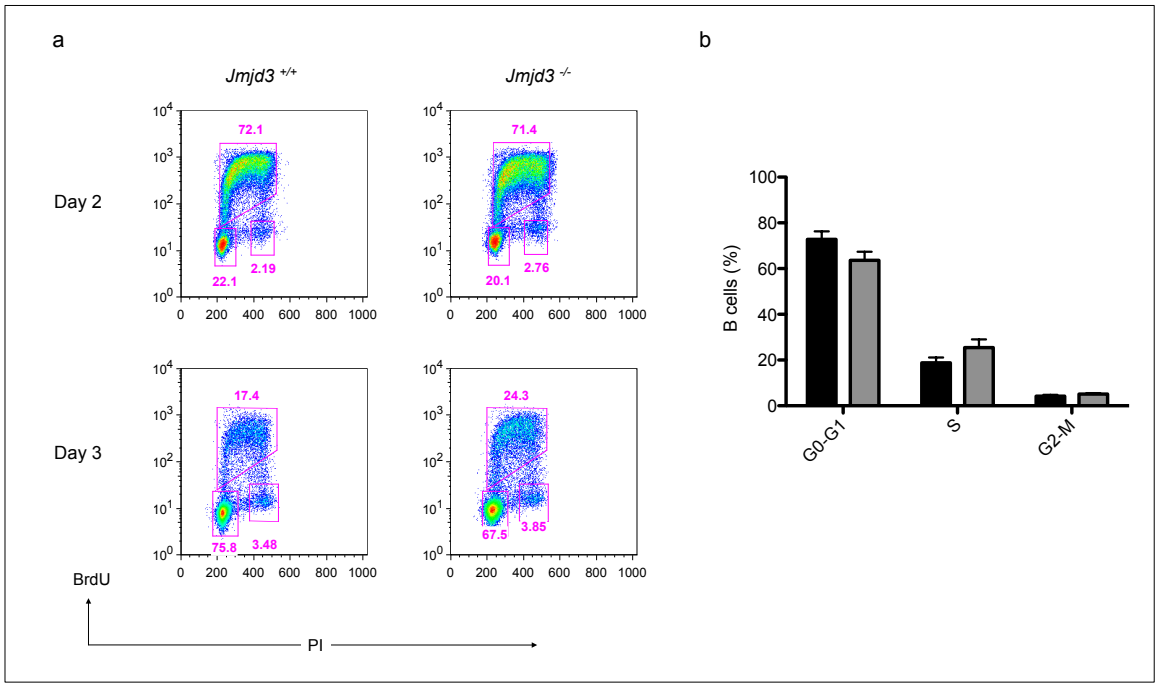

Figure 49. Cell cycle distribution analysis of *Jmjd3* control and mutant B cells upon LPS stimulation. a) Representative cell cycle analysis of Jmjd3 control and mutant mice at the indicated days after LPS stimulation. Numbers indicate the fraction of cells in the various boxed stages of the cell-cycle; **b)** Summary of cell cycle distribution data obtained respectively from 6 control (*Jmjd3*$^{+/+}$) and 12 *Jmjd3* mutant (*Jmjd3*$^{-/-}$) B cell cultures analyzed at day three of LPS stimulation. Columns represent mean values ± SD.

In accordance with growth curve data, cell-cycle distribution of Jmjd3 mutant B cells stimulated with LPS+IL-4 was comparable to that of controls (Figure 50). This result confirms that Jmjd3 plays a non-redundant function in B cell activation that is limited to selective forms of mitogenic stimulation.

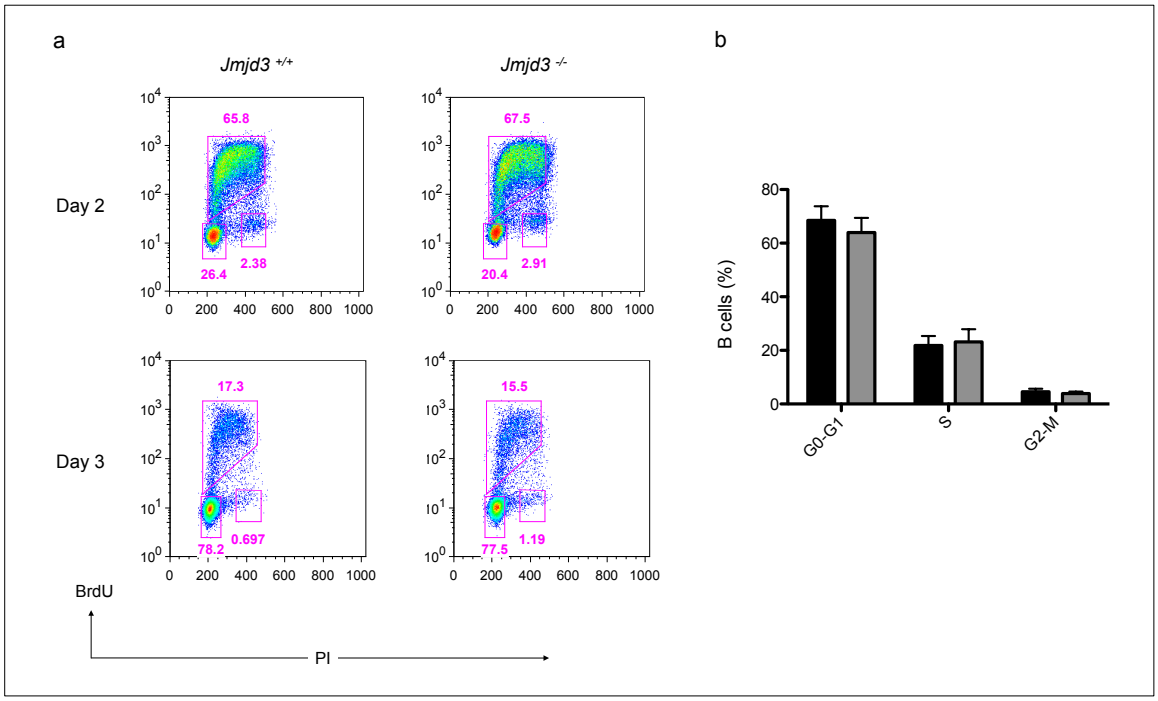

Figure 50. Normal cell cycle distribution in LPS+IL-4 stimulated *Jmjd3* mutant B cells. **a)** Representative cell-cycle distribution analysis of *Jmjd3* control (*Jmjd3*$^{+/+}$) and mutant (*Jmjd3*$^{-/-}$) B cells respectively at two and three days of LPS+IL-4 stimulation. **b)** Summary of cell cycle distribution analysis determined at day-3 of LPS stimulation respectively in 7 control and 12 *Jmjd3* mutant mice. Columns represent mean frequencies (± SD).

3.7.3. Jmjd3 controls expression of cell-cycle regulators

Satoh and colleagues (Satoh et al., 2010) have shown that *Jmjd3* controls cell cycle progression in bone marrow-derived macrophages through the regulation of the expression of cell-cycle genes including *c-Myc*, *c-Myb, Cyclin D1 (CCND1)* and *Cyclin D2 (CCND2)*. To determine whether the reduced proliferation of *Jmjd3*$^{-/-}$ B cells upon LPS activation was caused by impaired regulation of cell-cycle modulators, we quantified transcript levels of *c-Myc*, *Ccnd2* and *Ccnd3* in control and *Jmjd3* mutant B cell cultures activated with LPS. *c-Myc* expression was strongly induced 2 hours post LPS stimulation in control B cells. In contrast, *Jmjd3* mutant B cells failed to achieve comparable c-Myc mRNA levels at the same time point. The differences between control and mutant cultures in c-Myc transcripts persisted over the entire period of LPS stimulation. In a similar fashion *Ccnd2* and *Ccnd3* expression was significantly

blunted in *Jmjd3* mutant B cell cultures 24 hr after LPS activation. Importantly, whereas differences in *Ccnd2* transcript levels persisted between control and mutant B cells at later time points, *Ccnd3* mRNAs were affected by *Jmjd3* selectively at the 24hr time point of LPS stimulation (Figure 51). Given that Jmjd3 loss leads to growth retardation limited to the first 24-48 hr of LPS stimulation, it is possible that the major determinant for the delayed proliferative response is the transient failure of mutant B cells to activate *Ccnd3* expression.

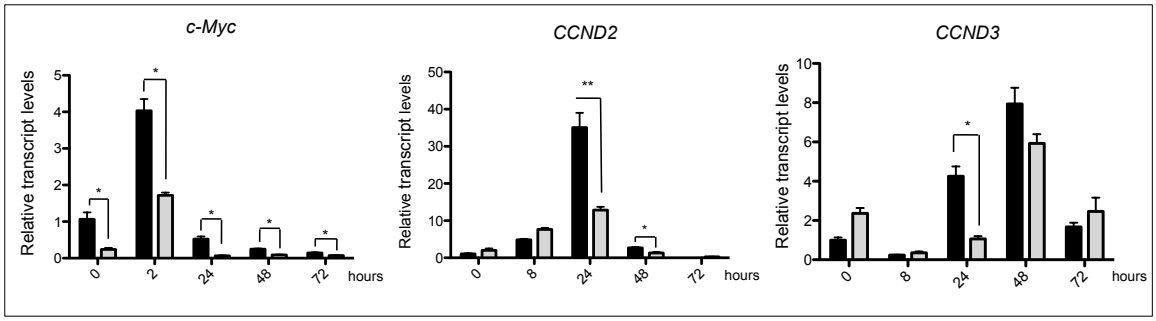

Figure 51. *Jmjd3* regulates expression of cell-cycle genes. Quantification by qRT-PCR of mRNA levels for the indicated cell cycle genes in *Jmjd3* control (black) and mutant (grey) B cell cultures at different time points (hr) after LPS stimulation. Transcript levels were normalized to the housekeeping gene *Rplp0* and represented as relative to mRNA levels of controls before LPS stimulation (0 hr). Columns represent mean transcript levels ± SEM (t-test; *,p <0.05; **, p <0.01).

In mouse embryonic fibroblasts *Jmjd3* activates expression of the *Cdkn2a* locus encoding for the tumor suppressors $p16^{INK4a}$ and $p19^{ARF}$ (Agger et al., 2009 and Barradas et al., 2009). To test whether a similar regulation occurred in B cells, we measured transcript levels for $p16^{INK4a}$ and $p19^{ARF}$ in *Jmjd3* control and mutant cultures after endotoxin treatment. In *Jmjd3* proficient B cells $p16^{INK4a}$ and $p19^{ARF}$ were strongly up-regulated 3 days after stimulation. In contrast, $p16^{INK4a}$ and, to a lesser extent, $p19^{ARF}$ were modestly induced in *Jmjd3* mutant B cells (Figure 52). The impaired activation of *Cdkn2a* expression in *Jmjd3* mutant cells, and in particular that of $p19^{ARF}$ could protect B cells from p53-mediated apoptosis (Ramiro et al., 2006).

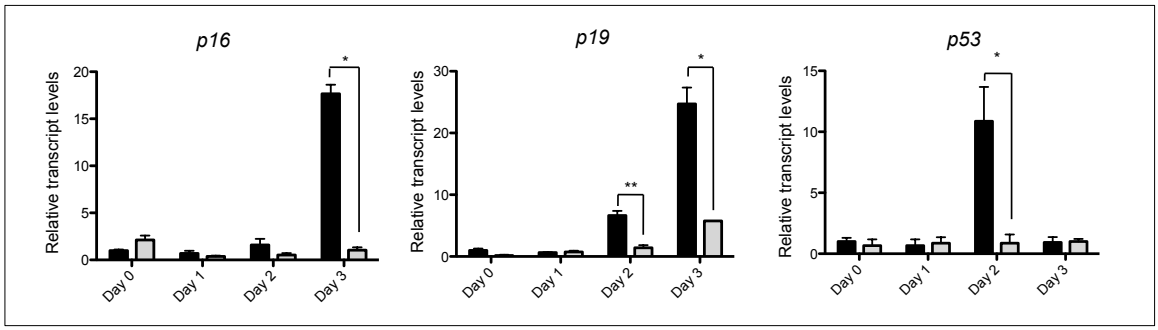

Figure 52. Tumor suppressors *p16*^{INK4a} , *p19*^{ARF} and *TP53* fail to be induced in *Jmjd3* mutant B cells after LPS stimulation. qRT-PCR analysis of Cdkn2a-encoded *p16*^{INK4a}, p19^{ARF} and of TP53 in control (black) and *Jmjd3* mutant (grey) B cells at the indicated days of in vitro LPS stimulation. Transcript levels were normalized to *Rplp0* and represented as relative to those in control B cells prior to stimulation (Day 0). Columns represent mean transcript levels of triplicates ± SEM (Wilcoxon test; *,*p* <0.05).

To further investigate a possible link between *Jmjd3* and p53, we measured *p53* transcript levels in control and mutant B cells activated with LPS. qRT-PCR analysis revealed that *Jmjd3* $^{-/-}$ B cells fail to induce p53 expression two days after LPS stimulation (Figure 52). This result suggests that Jmjd3 selectively induces the p53 expression in response to LPS stimulation.

These results identify two (apparently) opposing roles for Jmjd3 during B cell activation. Upon LPS stimulation, Jmjd3 activates the entry of B cell into cell cycle contributing to the upregulation of c-Myc and the cyclins D2 and D3. On the other hand Jmjd3 sensitizes B cells to senescence and/or p53-induced apoptosis through the regulation of *Cdkn2a and* possibly *Tp53* expression. The combination of these effects lead to a delayed proliferative response of B cells to LPS, while heightening their resistance to apoptotic signals.

3.7.4. *Jmjd3* limits plasma cell differentiation in response to LPS

Stimulation of B cells with LPS triggers plasma cell differentiation. Since Jmjd3 is potently induced during the early phases of LPS stimulation, we investigated whether inactivation of the histone demethylase could influence LPS-induced terminal differentiation. Primary B cells purified from the spleen of *Jmjd3* control (*Mb1-cre*) and conditional mutant (*Jmjd3$^{fl/fl}$;Mb1-cre*) mice were stimulated in vitro for four days with LPS +/- Il-4 and analyzed by flow cytometry. Staining with the plasma cell marker CD138/Syndecan-1 in combination with CD19 revealed a significant increase in the fraction of CD19^{lo}CD138^{+} pre-plasma cells (also called plasma blasts) in *Jmjd3* mutant cultures in comparison to controls (Figure 53). Interestingly, the higher proportion of PCs was seen in Jmjd3 mutant LPS cultures both at day-3 and day-4 of the stimulation, whereas the combined action of LPS and IL-4 led to a larger proportion of PCs in mutant cultures only at the later time point (day-4; Figure 53 and 54). These results are in accordance with our previous data, and suggest that stimulation through the IL-4 receptor rescues at least partly the alterations of Jmjd3 mutant B cells stimulated through TLR4.

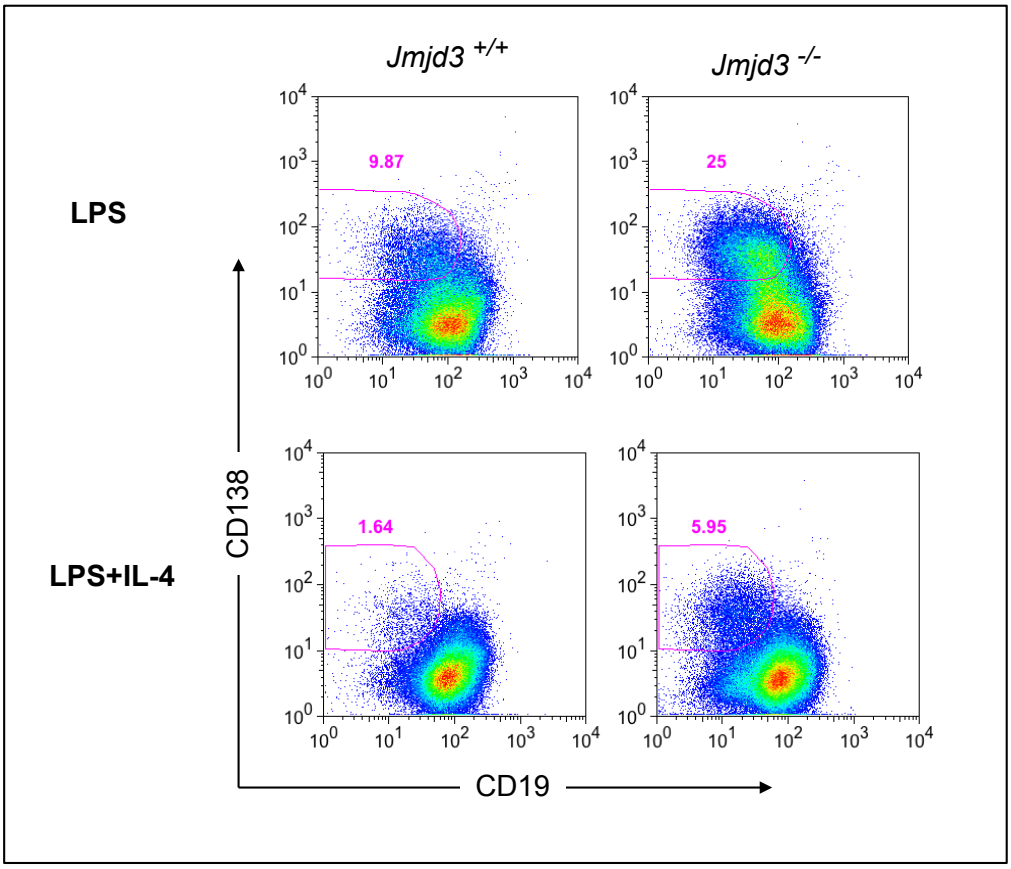

Figure 53. *In vitro* plasma cell differentiation of *Jmjd3* mutant B cells after LPS stimulation. Representative flow cytometric analysis of day-4 Jmjd3 control and mutant B cell cultures activated with either LPS (upper plots) or LPS+IL-4 (lower plots). Numbers indicate percentage of $CD19^{lo}CD138^{+}$ plasma blasts.

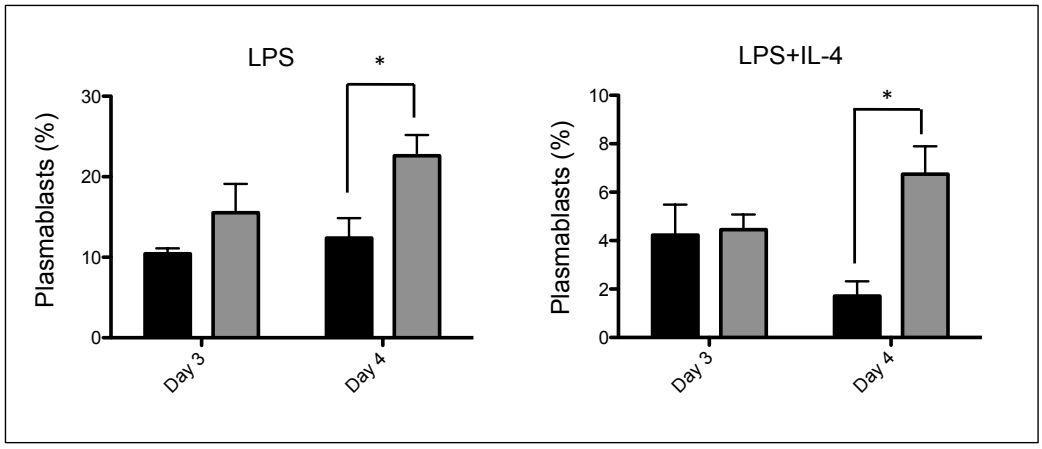

Figure 54. Frequency of plasmablasts generated *in vitro* after stimulation of *Jmjd3* control and mutant B cells. Summary of the data relative to the flow cytometric quantification of the percentage of $CD19^{lo}CD138^{+}$ plasmablasts detected respectively at day-3 and -4 of LPS +/- IL-4 stimulation in Jmjd3 control (black bars) and mutant (grey bars) animals. Mean frequencies were plotted ± SD. Data are representative of three independent experiments (t-test; *, $p< 0.05$).

In accordance with the increased fraction of Syndecan-1^{+} plasma cell precursors, the transcript levels for the transcription factor and PC determinant *Prdm1/Blimp1 (*which is essential for PC differentiation) were substantially increased in Jmjd3 mutant cultures simulated with LPS in comparison to controls (Figure 55). However, not all the genes associated with terminal differentiation were increased upon Jmjd3 inactivation; surprisingly, expression of Irf4 in mutant B cells was not induced at day two after LPS stimulation. This result was in contrast with previous studies describing that Irf4 is required for class switch recombination and plasma cell differentiation (Klein et al., 2006; Sciammas et al., 2006 ; Ochiai et al., 2013) (Figure 56).

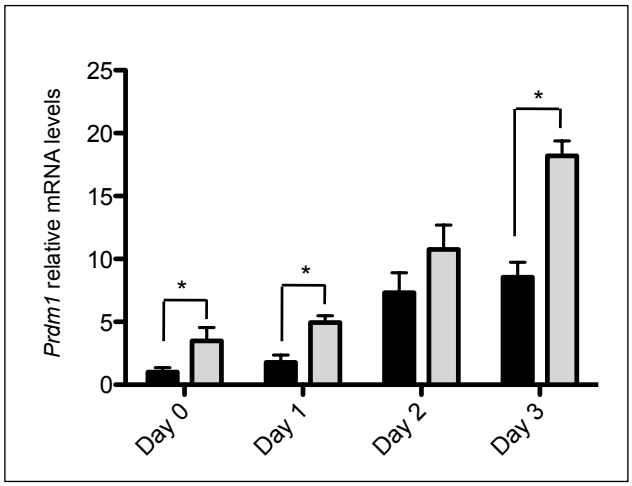

Figure 55. Higher *Prdm1* transcript levels in *Jmjd3* mutant B cell cultures after LPS stimulation. qRT-PCR determination of *Prdm1* transcripts in cultures respectively of *Jmjd3* control (black bars) and mutant (grey bars) B cells collected at the indicated time points. Data are representative of 2 independent experiments. Bars indicate mean frequencies of three mice ± SD (t-test; *, $p< 0.05$).

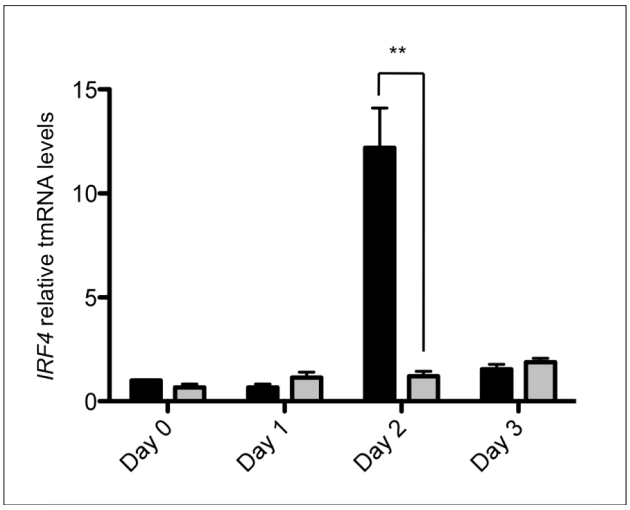

Figure 56. Irf4 is not upregulated in Jmjd3 mutant B cells upon LPS stimulation. Quantification by qRT-PCR of *Irf4* transcript levels in Jmjd3 control (Black bars) and mutant (grey bars) B cell cultures at the indicated time points after LPS stimulation. Bars represent mean values of three mice ± SD (*t*-test; **, $p< 0.01$)

3.7.5. *Jmjd3* and Ig isotype switching

To analyze the ability of *Jmjd3* $^{-/-}$ B cells to undergo Ig CSR, we activated B cells with either LPS or LPS+Il-4. The frequency of IgG3^{+} B cells was 2-fold reduced in *Jmjd3* $^{-/-}$ LPS culture when compared to controls, whereas LPS+IL-4 cultured mutant B cells displayed comparable frequencies of IgG1^{+} B cells to the controls (Figure 57 and Figure 58). Impaired switching of mutant B cells in response to LPS was in accordance with downregulation of Irf4 expression that is essential in CSR. Thus we conclude that *Jmjd3* inactivation facilitates the isotype switching *in vitro*.

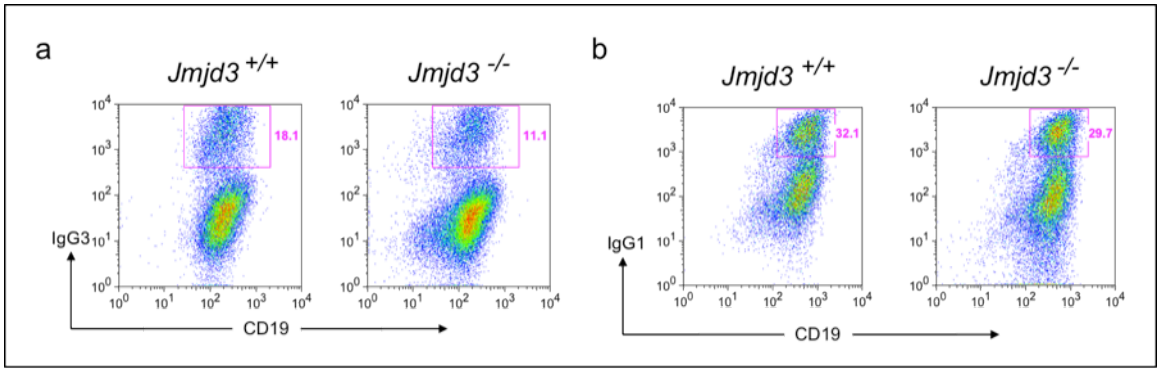

Figure 57. *In vitro* Ig class switch recombination analysis in Jmjd3 mutant B cells. Representative flow cytometric analysis of *Jmjd3* control (*Jmjd3*$^{+/+}$) and mutant (*Jmjd3*$^{-/-}$) B cells after four days of LPS **(a)** or LPS+IL-4 **(b)** stimulation, stained respectively for surface IgG3 and IgG1 expression. Numbers indicate percentage of boxed Ig class-switched B cells.

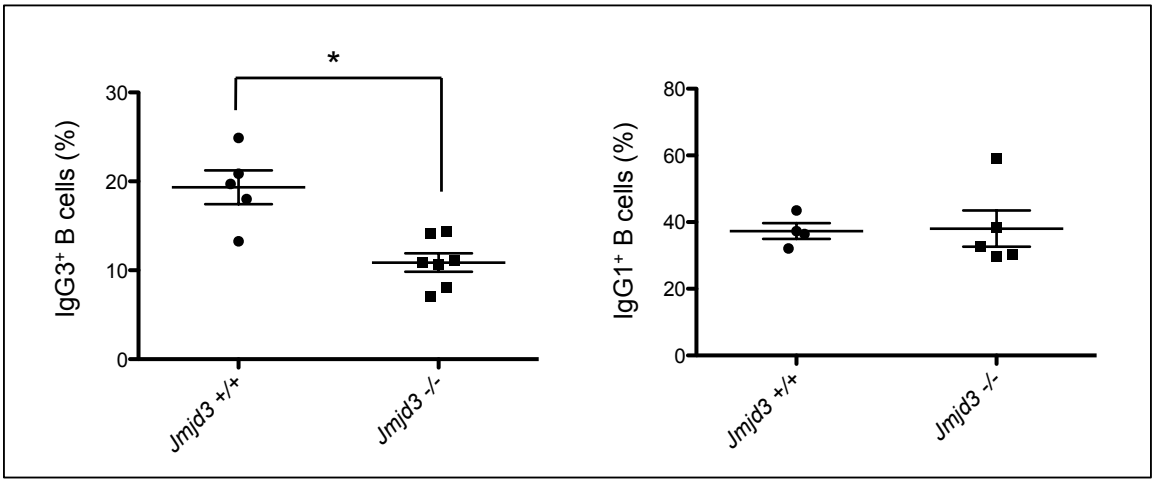

Figure 58. *Jmjd3* inactivation interferes with IgG3 class switch recombination after LPS stimulation. Percentage of IgG3$^+$ and IgG1$^+$ B cells generated in *Jmjd3* control (*Jmjd3*$^{+/+}$) and mutant (*Jmjd3*$^{-/-}$) cultures after four days of respectively LPS (left) or LPS+IL-4 (right) stimulation. Each dot represents one independent B cell culture. Bars indicate mean values ± SEM (t-test test; *, $p< 0.05$).

3.8 Humoral immunity in B-cell specific Jmjd3 mutant mice

3.8.1. *Jmjd3* inactivation does not affect serum Ig titers

The increased fraction of short-lived antibody-secreting PCs detected in Jmjd3 mutant B cell cultures in response to LPS stimulation, motivated us to measure serum immunoglobulin titers in Jmjd3 mutant mice. Enzyme Linked Immunosorbent assays (ELISA) showed that inactivation of Jmjd3 did not impair the ability of mutant animals to produce antibodies respectively of the IgG3, IgG1, IgG2c, IgA and IgM isotypes (Figure 59). These results point to a redundant role for Jmjd3 in the regulation of plasma cell homeostasis in vivo.

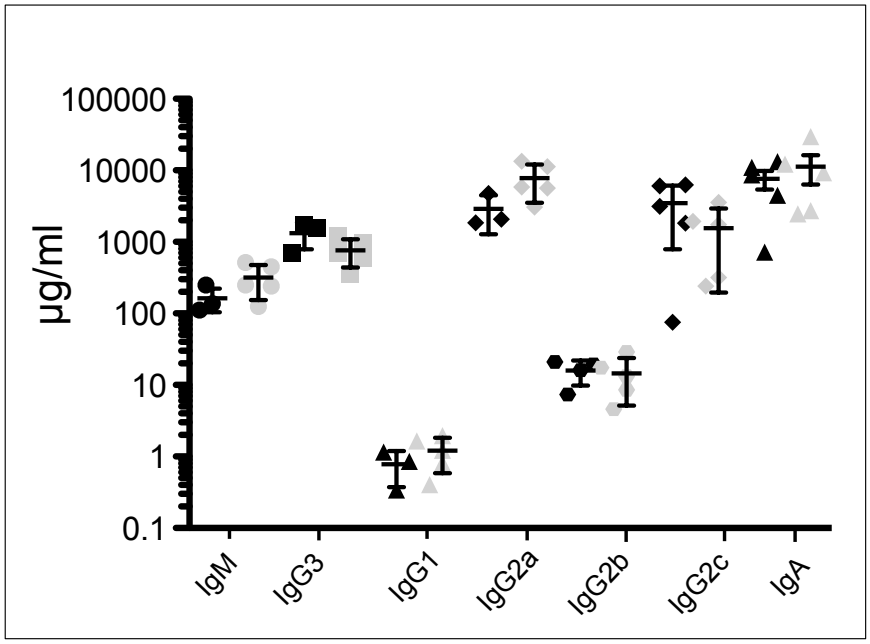

Figure 59. Ig serum titers in *Jmjd3* mutant mice. Quantification by ELISA of serum Ig titers in unimmunized *Jmjd3* control (black symbols; n=5) and mutant (grey symbols; n=5) mice. Each dot represents a mouse. Bars represent mean values ± SEM.

3.8.2. Jmjd3 and the recruitment of B cells into the germinal center reaction

The germinal center (GC) reaction plays a crucial role in humoral immune responses to T cell-dependent antigens by producing high-affinity antibody-secreting plasma cells and memory B cells (Klein and Dalla-Favera, 2008). To address whether B cells got recruited into the GC reaction in the absence of Jmjd3, we stained single cell suspensions from spleen, mesenteric lymph nodes (MLN) and Peyery's patches (PP) of control and mutant mice with antibodies against GC B cell markers. The frequency of $CD19^{+}CD95/Fas^{hi}CD38^{lo}$ GC B cells present in spleen and gut associated lymphoid tissues, which display chronic GCs, was comparable between controls and Jmjd3 mutant animals (Figure 60). Therefore we conclude that Jmjd3 does not control the entry and (presumably the persistence) of B cells into the GC reaction.

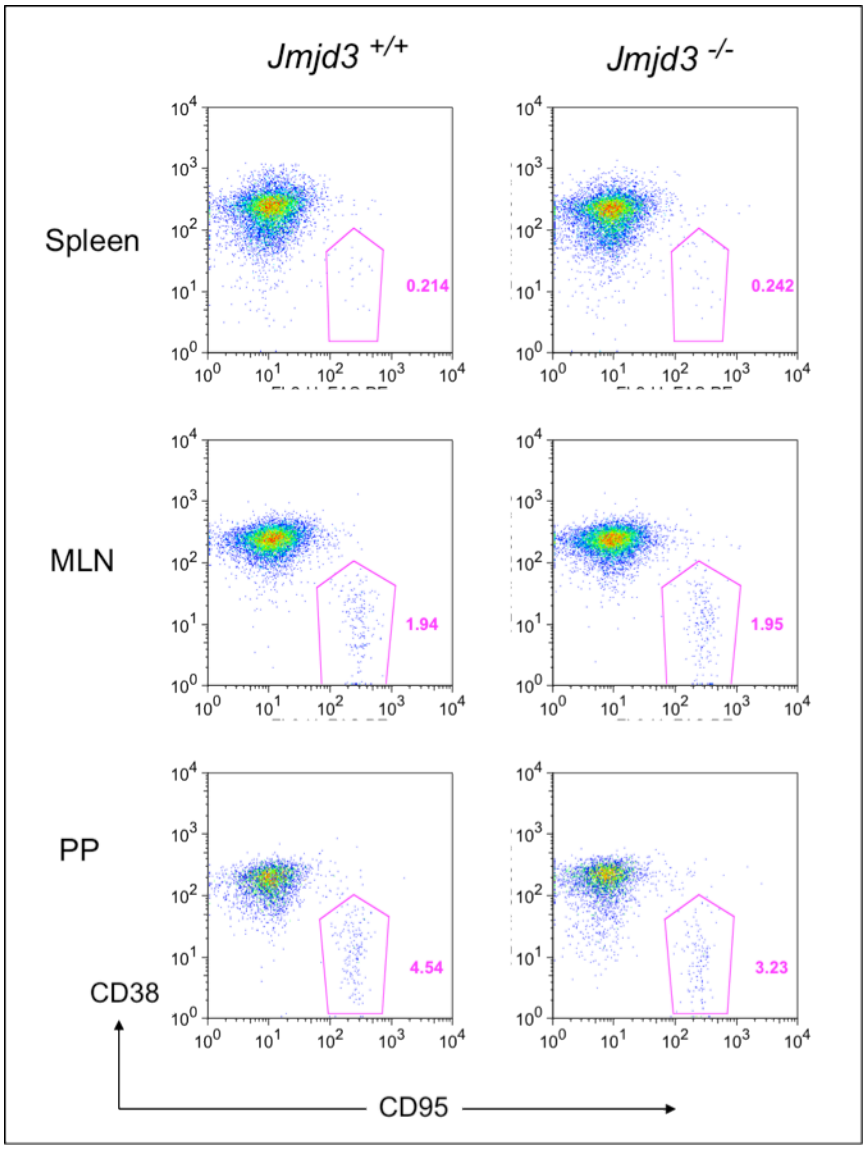

Figure 60. *Jmjd3* deficient B cells are able to form GCs. Flow cytometric analysis of $CD19^{+}CD38^{lo}CD95^{hi}$ GC B cells in spleen, mesenteric lymph nodes (MLN) and Peyer's Patches (PP) of *Jmjd3* control ($Jmjd3^{+/+}$) and mutant ($Jmjd3^{-/-}$) unimmunized mice. Numbers indicate percentage of GC B cells among gated $CD19^{+}$ cells.

Frequency and absolute numbers of GC B cells were comparable between *Jmjd3* $^{-/-}$ and control mice in the analyzed organs (Figure 61). We conclude that *Jmjd3* is dispensable for the formation and/or maintenance of germinal center B cells.

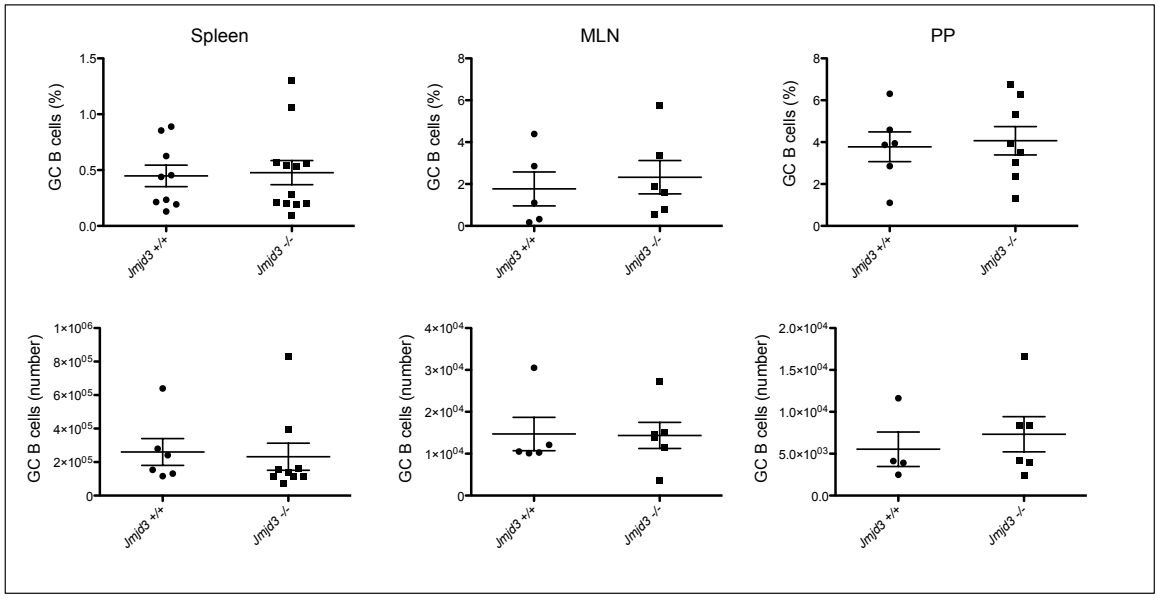

Figure 61. Frequency and absolute numbers of GC B cells in *Jmjd3* conditional mutant mice. Summary of data relative to frequencies (upper panel) and absolute numbers (lower panels) of GC B cells in the indicated lymphoid organs of *Jmjd3* control (*Jmjd3*$^{+/+}$) and mutant (*Jmjd3*$^{-/-}$) mice. Bars indicate mean frequencies ± SEM.

3.8.3. *Jmjd3* inactivation does not affect T-cell dependent antibody responses

We finally asked whether the recruitment of B cells into the GC in the absence of Jmjd3 could influence their ability to differentiate into antigen-specific antibody secreting cells. To this end, we immunized controls (Mb1-cre) and *Jmjd3*$^{-/-}$ (*Jmjd3*$^{fl/fl}$*;Mb1-cre*) mice with the T-cell dependent antigen NP_{27} coupled to chicken gamma globulin (NP-CGG). Blood serum was collected at different time points after the immunization and antigen-specific igG1 titers were quantified in the blood of control and mutant animals. Control and Jmjd3 mutant mice showed a comparable rise in NP-specific IgG1 serum levels in response to the immunization (Figure 62). These results exclude a major role in the generating of antibody-secreting plasma cells originating from the GC reaction.

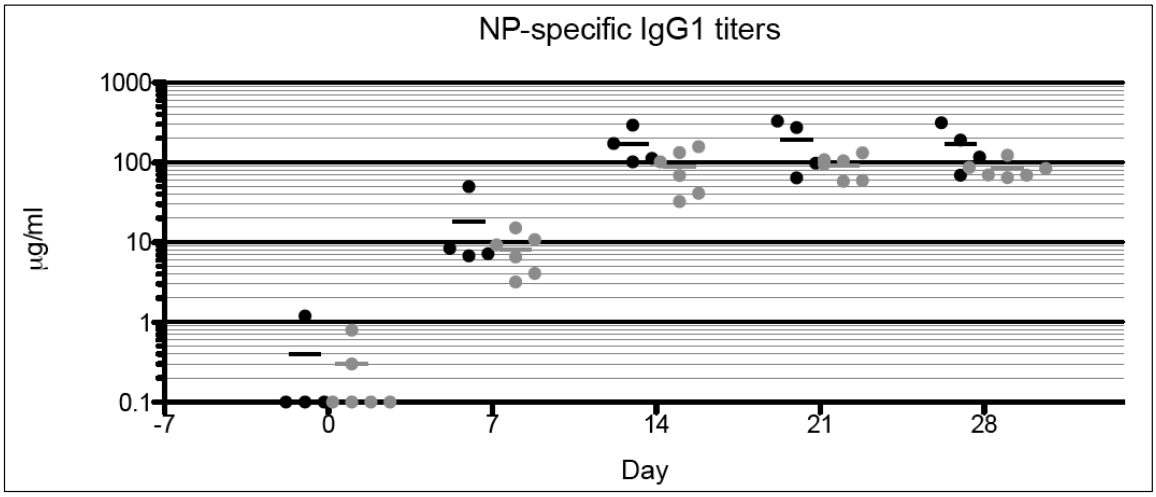

Figure 62. Antigen-specific IgG1 serum titers produced in *Jmjd3* mutant mice after immunization with the T-cell dependent antigen NP-CGG. Quantification by ELISA of NP-specific IgG1 titers in the serum of Jmjd3 control (black dots) and mutant (grey dots) mice at the indicated time points after NP-CGG immunization. Each dot represents a mouse. Bars indicate mean concentrations.

3.9. Effects of Jmjd3 inactivation on B cell development in mice on a pure C57BL/6J genetic background

The genetic background may influence the phenotypic outcome of a genetic mutation, especially if it affects an epigenetic determinant. Hence, the variable penetrance of phenotypes seen in Jmjd3 mutant mice could depend on the 129 x C57BL/6 mixed genetic background. To address this point we recently completed the backcross of Jmjd3^{fl} mice to obtain conditional mutants on a pure C57BL/6J genetic background. Preliminary analyses on the first mutant animals bred to the Mb1-cre strain will be described below.

3.9.1. *Jmjd3* is dispensable for early B cell development and MZ B cell differentiation in C57BL/6 mice

Flow cytometic analysis of BM cell suspensions revealed a fairly normal distribution of Jmjd3 mutant B cells between the fraction of progenitors ($B220^{lo}IgM^{-}$), immature ($B220^{lo}IgM^{+}$) and mature ($B220^{+}IgM^{+}$) recirculating B cells. Moreover, absolute number of the different B cell subset was comparable between control and mutant animals. (Figure 63). In a similar fashion, flow cytometric characterization of splenic B cell populations failed to show major alterations in the ratio between Fo and MZ B cells in response to Jmjd3 inactivation. Although preliminary, these data point to a substantial contribution of the 129SV genetic background to the B cell developmental defects observed in Jmjd3 mutant animals analyzed on the mixed genetic background.

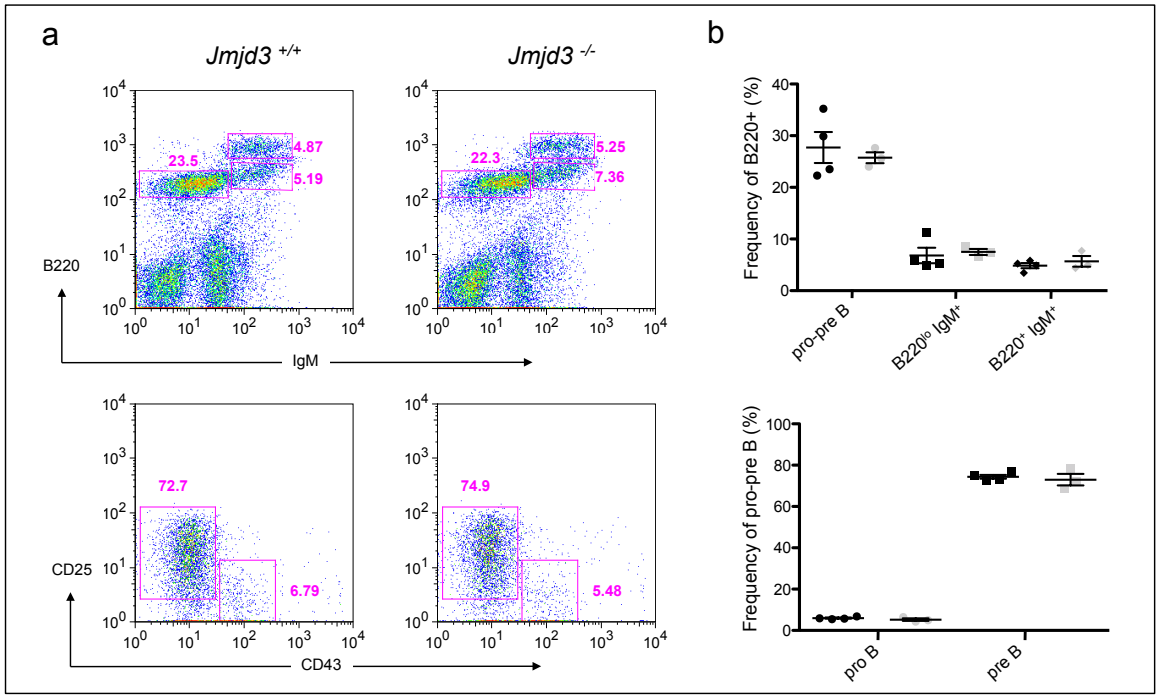

Figure 63. Analysis of early B cell development in *Jmjd3* mutant mice on the C57BL/6J pure genetic background. a) Representative flow cytometric analysis of *Jmjd3* control (*Jmjd3*$^{+/+}$) and mutant (*Jmjd3*$^{-/-}$) BM cells on the C57BL/6 background. Numbers indicate frequency of boxed populations. **b)** Frequency of pro-B and pre-B cells within gated IgM^{-} B220^{+} BM cells of representative cases of *Jmjd3* control (*Jmjd3*$^{+/+}$) and mutant (*Jmjd3*$^{-/-}$) animals on the C57BL/6J genetic background.

3.9.2. *Jmjd3* regulates B-1a B cell development in C57BL/6 mice

We next turned out attention to the analysis of B-1 B cell development in the absence of Jmjd3. For this purpose single cell suspensions from peritoneal cavity lavages were subjected to flow cytometric analysis. In analogy with what had been observed in mutant animals on the mixed genetic background, *Jmjd3* mutant C57BL/6J mice showed a lower frequency and absolute number of CD5^{+} B-1a B cells in comparison to controls (Figure 64, Figure 65).

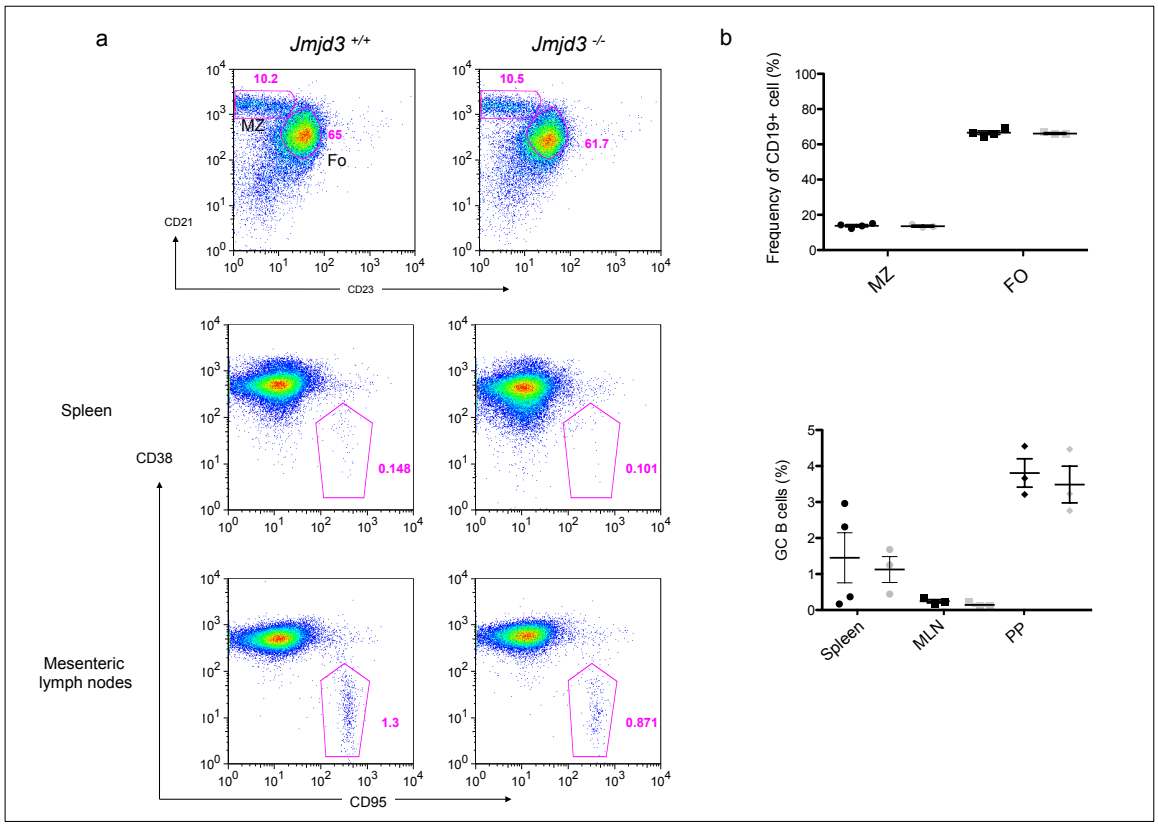

Figure 64. Peripheral B-cell development in *Jmjd3* deficient mice on the C57BL/6 genetic background. a) Representative flow cytometric analysis of gated $CD19^{+}$ splenic B cells in *Jmjd3* control ($Jmjd3^{+/+}$) and mutant ($Jmjd3^{-/-}$) animals. **b)** Summary of data related to frequencies of respectively Fo, MZ and GC B cells in *Jmjd3* control (black dots) and mutant (grey dots) animals.

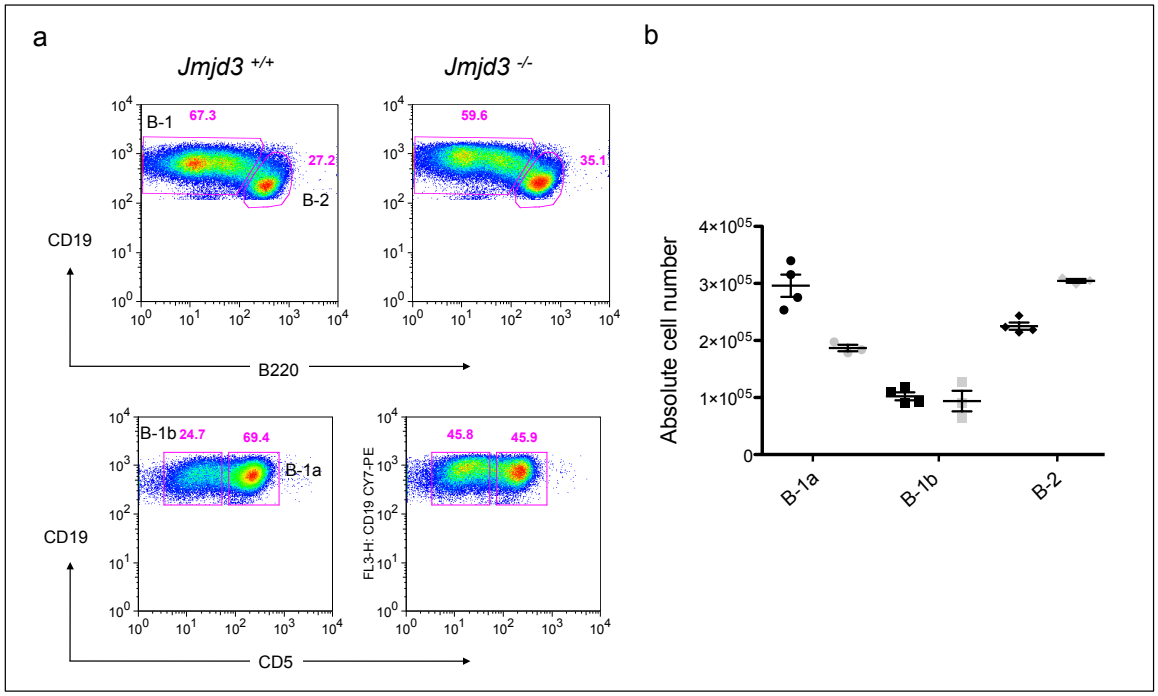

Figure 65. B-1 B cell development in *Jmjd3* mutant mice on the C57BL/6J genetic background. a) Representative flow cytometric analysis of gated $CD19^{+}$ B cells in peritoneal cavity lavages from *Jmjd3* control (*Jmjd3*$^{+/+}$) and mutant (*Jmjd3*$^{-/-}$) mice on the C57BL/6 genetic background; **(b)** Summary of the data on absolute numbers of the indicated B cell subsets in peritoneal cavity lavages of respectively four controls (black dots) and three mutant (grey dots) animals.

3.9.3. *Jmjd3* is required for LPS-driven C57BL/6J B cell activation

To determine whether Jmjd3 was critical for the response of C57BL/6 B cells to bacterial endotoxin, we stimulated control (Mb1-cre) and Jmjd3 mutant (Jmjd3fl/fl; Mb1-cre on pure C57BL/6J background) primary splenic B cells with LPS. Growth curve analysis confirmed the non-redundant role of *Jmjd3* in B cell responses to LPS in vitro. Indeed mutant B cell cultures showed a defective proliferative response that became evident as early as 24 hr after the initial stimulation (Figure 66).

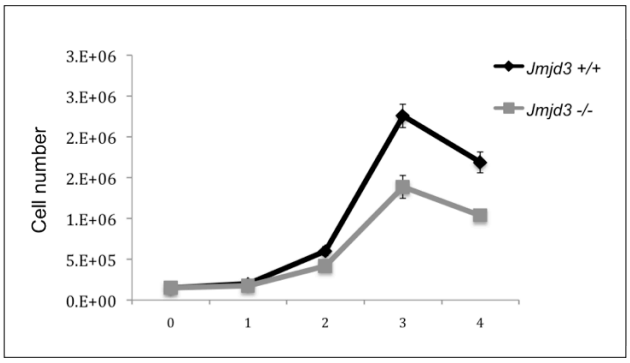

Figure 66. Growth defects of C57BL/6J *Jmjd3* mutant B cells after LPS stimulation. Representative growth curves of *Jmjd3* control (*Jmjd3*$^{+/+}$) and mutant (*Jmjd3*$^{-/-}$) B cells activated in vitro with LPS for the indicated days. Graph is representative of two control and two mutant mice. Bars indicate mean values of triplicates ± SEM.

To confirm that the *Jmjd3 floxed* segment had undergone Cre-mediated recombination. We performed quantitative genomic PCR on B cells three days after in vitro stimulation. As shown in Figure 67, B cells in mutant cultures were almost completely devoid of a functional jmjd3 allele. We conclude that Jmjd3 is required for optimal proliferation of B cells in response to the LPS.

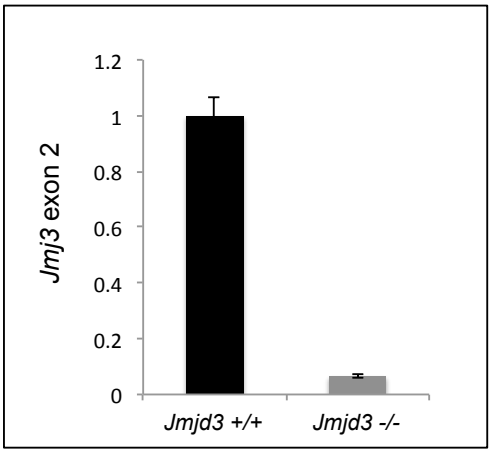

Figure 67. Efficiency of Cre-mediated recombination of the *Jmjd3*^{fl} allele in LPS-activated mutant B cells on the C57BL/6J genetic background. Quantification by genomic qPCR of *Jmjd3* exon2 copy number in *Jmjd3* control (*Jmjd3*$^{+/+}$) and mutant (*Jmjd3*$^{-/-}$) B cells collected 3 days after LPS stimulation. Values were normalized for DNA input and represented as relative to control B cells. Columns represent mean values of triplicates ± SEM.

4. Discussion

The work presented in this thesis has focused on the understanding of the in vivo role of the Histone H3 lysine demethylase Jmjd3 in B cell lymphopoiesis and activation. For this purpose, I generated mice carrying a conditional knock-out (KO) allele for the Jmjd3 gene. Using Cre/loxP recombination technology, inactivation of JMJD3 function was achieved throughout B cell development by means of the Mb1-cre knock-in strain. A comprehensive in vivo analysis of B cell-specific Jmjd3 KO mice has unraveled functional contributions of the histone demethylase at specific stages of B cell differentiation and for optimal response of B cells to innate immune stimuli.

Gene expression analysis on purified murine B cell subsets revealed that Jmjd3 is expressed moderately throughout B cell development at relatively constant levels. A transient potent up-regulation of JMJD3 gene expression is seen in B cells few hours after the exposure to different mitogens including LPS stimulation, CD40 ligation and B cell receptor cross-linking. These results led us to hypothesize a possible contribution of Jmjd3 to both B cell differentiation and activation to innate and adaptive stimuli. Indeed, the analysis of B-cell specific Jmjd3 mutant animals has revealed several abnormalities resulting from functional inactivation of the histone demethylase.

In early stages of B cell development, Jmjd3 controlled the size of the pre-B cell pool. This regulation was exerted, at least in part, by facilitating the entry into S-phase and hence acting mainly on the fraction of rapidly proliferating large pre-B cells. The loss of JMJD3 did not however fully prevent further differentiation of progenitor B cells, which progressed to the immature stage after successfully rearranging their immunoglobulin light chain genes. The recruitment of naïve/transitional B cells to the main three mature B cell subsets was affected by Jmjd3 inactivation. Specifically, I found a significant reduction in the number and percentage of B-1 B cells residing in the peritoneal cavity. Moreover, the subset of marginal zone B cells that resides in the spleen was enlarged in response to functional loss of JMJD3 activity. Instead, the major population of Follicular/B2 resting mature B cells was by and large comparable in numbers and frequencies between Jmjd3 control and mutant mice. Whereas, JMJD3 did not influence the efflux of immature/naive B cells from the bone marrow, in

vivo BrdU incorporation studies have suggested a slower turnover of mature B cells lacking Jmjd3.

In vitro activation studies have revealed an unexpected selectivity in the contribution of Jmjd3 to B cell proliferative responses. Indeed, whereas, Jmjd3 mRNA levels increased after stimulation of B cells through both innate (e.g. TLR4/RP105) and adaptive receptors (e.g. BCR and CD40), only LPS stimulation caused a major defect in the proliferation of Jmjd3 mutant B cells. Interestingly, the impaired proliferative response to endotoxin following Jmjd3 loss, affected primarily the first one/two cell divisions pointing to a possible role for the histone demethylase in the reprogramming of resting B cells into their proliferative counterpart.

The analysis of the data obtained through the analysis of Jmjd3 conditional mutant mice has provided me with the opportunity to interpret the results in the frame of the existing literature. I will discuss in the following paragraphs the major findings of this study in an attempt to reconcile the data within a scenario where Jmjd3 exerts a critical regulatory function in B cell differentiation and proliferation.

4.1. Jmjd3 and early B cell development

The inactivation of Jmjd3 in pro-B cells was achieved crossing $Jmjd3^{fl}$ mice to the Mb1-cre strain. The inactivation of Jmjd3 in pro B cells did not affect their number. Moreover, we could show that the vast majority of $B220^{+}CD43^{+}IgM^{-}$ proB cells had undergone Cre-mediated recombination, thus excluding a major counter selection of mutant cells. This result indicates that Jmjd3 is dispensable for the differentiation from pro-B to preB cells. The latter transition is dependent on the expression of a functional immunoglobulin heavy chain receptor that results from a productive VDJ recombination event. Previous work by Su et al has shown that the H3K27 thrimethylation activity of Ezh2 regulates in a critical fashion IgH VDJ recombination (Su et al., 2003). Specifically, it was hypothesized that H3K27me3 deposition at promoters of DH-proximal VH genes (leading to their silencing) is required to allow RAG proteins to employ distal VH elements in V-to DJ recombination reactions. The failure to observe major defects in the proB to preB cell transition in Jmjd3 mutant

mice excludes that removal of H3K27me3 from germline VH gene promoters is necessary to activate the VDJ recombination process. At the same time, we cannot exclude a possible functional redundancy between Jmjd3 and other histone H3K27 demthylases such as UTX in the regulation of VDJ recombination. Finally, it remains to be determined whether JMJD3 mutant mature B cells suffer from major skewing in the antibody heavy chain gene repertoire.

The loss of JMJD3 caused a contraction in the size of the pre-B cell compartment. This defect was mainly caused by a reduction in the number of proliferating pre-B cells, as confirmed by short in vivo BrdU pulse experiments. The failure of mutant pre-B cells to proliferate may result from the role of Jmjd3 in regulating pre-BCR effector functions. In particular, Jmjd3 may be required to induce the expression of G1-S-specific cyclins such as Cyclin D3 following pre-BCR signaling. Indeed, data from mature B cells show a failure of Jmjd3 mutants to induce Ccnd3 expression in response to LPS stimulation. Notably, Ccnd3 deficient mice show a selective defect in pre-B cell proliferation (Cooper et al., 2006). Pre-BCR signaling is enhanced by concomitant engagement of the Interleukin-7 (IL-7) receptor through its binding to IL-7 (Lu et al, 2003). Preliminary data obtained from bone marrow pro/pre B cell cultures indicated that Jmjd3 inactivation does not interfere with IL-7 driven pre-B cell proliferation (M. Rahmat and S. Casola, personal communication). It remains to be determined whether the positive regulation exerted by Jmjd3 on the expression of Interferon Regulatory Factor 4 (IRF4) transcription factor may also contribute to define the ultimate proliferative potential of progenitor B cells (Lu, 2008). Finally, previous reports indicated the property of Jmjd3 to induce the expression of the Cdkn2a tumor suppressor locus encoding respectively for the CDK inhibitor p16INK4a and the tumor suppressor p19ARF (Agger et al., 2009; Barradas et al., 2009; Sola et al., 2011; Zhao et al., 2013). Whether Jmjd3 controls Cdkn2a expression in pre B cells and whether this regulation sensitizes cells to apoptosis and/or counterbalances pro-proliferative signals represent the next questions to be addressed.

A better understanding of the contribution of Jmjd3 to pre-B cell proliferation will come from the comparison between the transcriptome profiles of Jmjd3-proficient and deficient large pre-B cells. These results will be intersected with genome wide distribution maps of H3K27me3 and H3K4me3 to be obtained from purified wild-type

pre-B cells, to ultimately define direct targets of JMJD3 function in proliferating pre-B cells.

In summary, by inducing concomitantly genes (e.g, Ccnd3, IRF4, Cdkn2a) with opposite roles in cell-cycle progression, Jmjd3 may exert a fine balance between pro-proliferative and pro-differentiation signals to ultimately control the size of the pre-B cell compartment.

4.2. Jmjd3 and peripheral B cell subset differentiation

Immature B cells expressing a functional, non-autoreactive, BCR exit the bone marrow and migrate to peripheral lymphoid organs. Here only a small fraction of these cells (less than 10%) will complete their differentiation to become ultimately either Follicular B2, marginal zone or B-1 B cells. Immunophenotypic analysis of single-cell suspensions from secondary lymphoid organs has unraveled selective contributions of Jmjd3 to peripheral B cell subset differentiation.

Upon Jmjd3 inactivation, the total number of $CD19^{+}$ B cells in the spleen remained unperturbed. Distribution of B cells among Fo and MZ B cell subsets revealed a preferential enrichment for Jmjd3 mutant B cells in the MZ B cell compartment. A recent study by Simonetti and co-workers (Simonetti et al., 2013) has assigned to Irf4 an important role in the regulation of the Fo versus MZ B cell lineage choice. Specifically, inducible loss of IRF4 in mature B cells caused a rapid repositioning of mutant Fo B cells to the MZ. This migration was driven by increased responsiveness of IRF-4-defective mature B cells to Notch-2. Importantly, Notch2 is essential for the development and persistence of MZ B cells (Saito et al., 2003). Since IRF4 was shown by us (present thesis) and others (Satoh et al., 2010) to be regulated by JMJD3, we hypothesize that the increased number of MZ B cells measured in Jmjd3 mutant mice may result from impaired IRF4 expression. We will attempt to address this question in the future by increasing IRF4 expression levels in Jmjd3 conditional mutant B cells via lentiviral complementation, using bone marrow transplantation approach.

B-cell receptor (BCR) signaling is required for the differentiation and survival of mature B cells (Kraus et al., 2004). Over the past years it has become increasingly evident that the strength of the BCR signal(s) contributes critically to peripheral B cell lineage commitment (Casola, 2007; Pillai and Cariappa, 2009) “Strong” BCR signals, possibly resulting from antigen recognition, facilitate B-1 B cell development whereas “weaker” signals facilitate MZ and/or Fo B cell development. We could show that upon Jmjd3 inactivation, B-1 B cell development was distorted. Specifically, in JMjd3 conditional mutants we observed a major and selective loss of $CD19^{hi}CD5^{+}$ B-1a B cells whereas, B-1b B cells ($CD19^{hi}CD5^{-}$) increased proportionally, leaving ultimately the total number of B-1 B cells largely unaffected.

Targeted disruption of genes encoding for effectors of BCR signaling often result in a substantial decrease or, in some cases, to complete absence of B-1a B cells (Berland and Wortis, 2002). BCR effectors important for B1-a B cell differentiation often regulate intracellular Ca2+ flux, which in turn activates the NFAT (Nuclear Factor of Activated T cells) family of transcription factors. Studies with gene-targeted mice have shown that NFATc1 is critical for development and/or survival of B-1a B cells (Berland and Wortis, 2003). MZ and B-1 cells are both recruited into T-cell independent antibody responses, (Cinamon et al., 2008; Martin and Kearney, 2002; Baumgarth, 2010). However, only B-1a B cells depend strictly on the function of NFATc1 for their development (Berland and Wortis, 2003). Interestingly, a study by Yasui and colleagues has recently described that NFATc1 expression is epigenetically regulated by Jmjd3 during murine osteoclast differentiation (Yasui et al., 2011). Hence, we suggest that Jmjd3 may control B-1a B cell development and/or maintenance through the regulation of NFATc1 expression. This prediction will be validated measuring Nfatc1 transcript levels in the remaining population of Jmjd3 mutant B-1a B cells. Should this experiment result uninformative (the remaining B-1a B cells in Jmjd3 mutants may have gone through a stringent selection process based on the expression of normal NFATc1 levels), we will consider the possibility to reconstitute lethally irradiated mice with B-cell specific Jmjd3 conditional mutant hematopoietic stem cells complemented with Nfatc1-expressing lentiviral vectors.

In vivo BrdU labeling experiments have also revealed a possible role for Jmjd3 in mature B cell homeostasis. Indeed, recruitment of immature B cells into the three

major mature B cell subsets was reduced in response to B-cell specific Jmd3 inactivation. Since, the frequency of immature B cells that gets recruited into the mature B cell compartments is strictly dependent on the turnover of the latter population, we conclude from this that Jmjd3 plays a role in the regulation of mature B cell lifespan. This control is not exerted through a control of B cell survival as we failed to observe major changes in the fraction of apoptotic cells in the various mature B cell subsets following Jmjd3 inactivation.

The stepwise transition of B cells through subsequent stages of development is driven by the continuous rewiring of the transcriptional program sustaining B cell function and identity. Factors such as Jmjd3 acting on the H3K27me3/H3K4me3 epigenetic axis may exert essential functions at very defined stages of differentiation where the fine balance in expression levels of a limited set of transcription factors defines the fate of the developing B cells. Hence identifying Jmjd3 target genes in mature B cells will provide precious insights into the molecular mechanisms through which Jmjd3 may support peripheral B cell development.

4.3. Jmjd3 and B cell activation and terminal differentiation

4.3.1. Jmjd3 gets rapidly induced upon B cell activation

Stimulation of B cells through both adaptive (BCR and CD40) and innate immune receptors (TLRs) triggers important molecular responses that range from a transient phase of clonal expansion to differentiation into terminally differentiated antibody-secreting plasma cells. B cell activation through these receptors is also accompanied to genetic rearrangements occurring at the IgH locus whereby the Cμ constant region is replaced by that of other isotypes including Cγ3, Cγ1, Cε and Cα.

We have shown that Jmjd3 expression is substantially increased in response to in vitro stimulation of resting primary B cells through respectively BCR, CD40 and TLR4 receptors. The induction of Jmjd3 was transient and reached its peak on average 2-to-3 hr after the initial stimulation. After reaching its highest levels, Jmjd3 was rapidly down-regulated reaching basal low levels comparable to those of resting mature B cells. Previous work has shown that members of the NF-κB transcription factor family

are responsible for Jmjd3 induction in macrophages in response to LPS stimulation (De Santa et al., 2007 and 2009). Given that BCR, CD40 and TLRs activate the NF-κB pathway in response to cognate ligand interaction, we propose that B cells, as macrophage, employ the NF-κB signaling pathway to rapidly induce Jmjd3 expression.

In vitro activation of Jmjd3 mutant B cells revealed a surprising behavior of the cells. Specifically, stimulation of mutant B cells through BCR or CD40 receptors triggered a robust proliferative burst that was comparable to that observed in control cultures. In sharp contrast, stimulation with LPS induced a selective impairment in the proliferative response of Jmjd3 mutant cells. Similar results were observed when we mimicked LPS stimulation using an agonistic antibody against RP-105 (Miyake et al., 1995). The analysis of growth curves of B cells stimulated with LPS showed a peculiar behavior of Jmjd3 mutant cultures. Upon LPS stimulation, the lack of Jmjd3 delayed substantially the first cell division. Instead growth of mutant cells proceeded in a fairly comparable fashion to that of control B cells starting from the third day of stimulation. Hence the lack of Jmjd3 seems to impair/delay/interfere with the activation of a transcriptional program that ensures robust continuous proliferation of B cells for 3 to 4 days following the initial stimulation with endotoxin. Interestingly, the defect seen in LPS cultures of Jmjd3 mutant B cells was alleviated when interleukin-4 (IL-4) was added to the culture medium. Given that IL-4 stimulation leads to the activation of the JAK/STAT pathway, we infer that the latter may compensate for JMJD3 loss to promote cell proliferation in response to LPS stimulation. Recent work in microglia cells has revealed that the JAK/STAT pathway can potentiate NF-κB dependent induction of Jmjd3 expression in response to LPS stimulation (Przanowski et al., 2014). These data point to a convergence of the JAK/STAT and NF-κB pathways on Jmjd3 to execute downstream transcriptional programs including the induction of pro-inflammatory genes. Notably, constitutive activation alone of the JAK/STAT pathway was sufficient to induce a subset such pro-inflammatory genes whereas this was not achieved after Jmjd3 overexpression. Hence, we can envision a scenario whereby activation of the JAK/STAT pathway may overcome the requirement for Jmjd3 to induce one or more genes necessary to trigger B cell proliferation in response to LPS stimulation. The identification of such genes will represent a major focus of our future studies.

To understand the mechanisms responsible for the delayed proliferative response of Jmjd3 mutant B cells after LPS stimulation, we performed cell-cycle distribution analysis. However, these studies failed to reveal specific defects (e.g. blocks at defined stages of the cell-cycle) in mutant B cells. Hence, from this we hypothesize that transient induction of Jmjd3 is necessary in resting B cells for optimal activation of different set of genes that permit respectively the entry and the progression through the various stages of the first cell cycle following LPS stimulation. In accordance with previous reports (Satoh et al., 2010), we could show that Jmjd3 regulated optimal expression in B cells of the G1/S cyclins Ccnd2 and Cnnd3. In particular, loss of Jmjd3 blunted Ccnd2 induction and delayed Ccnd3 upregulation. The latter result may help explain the delayed progression through the first cell-cycle displayed by Jmjd3 mutant B cells following LPS activation.

While this thesis was finalized, we obtained the first analyses of RNA sequencing data from Jmjd3 control and mutant B cells, isolated respectively before and 24 hr after LPS stimulation. Among the differentially expressed genes that were down regulated in Jmjd3 mutant B cells we found a strong enrichment for gene ontology categories associated to multiple cell cycle checkpoints and to mitosis (M. Rahmat, F. Zanardi and S. Casola, data not shown). Notably, such transcriptomic changes were already observed in Jmjd3 mutant B cells prior to stimulation. These results are consistent with a scenario whereby B cells require Jmjd3 to express optimal, basal, levels of mRNAs encoding for cell-cycle genes that become crucial to initiate the first cell division once they get stimulated with LPS. Why Jmjd3 requirement is restricted to LPS stimulated B cells represents a major focus of our future studies.

Previous work has proposed a role for Jmjd3 in the induction of the Cdkn2a tumor suppressor locus (Agger et al., 2009; Barradas et al., 2009; Sola et al., 2011). This regulation was recently shown to provide a barrier to somatic cell reprogramming (Zhao et al., 2013). In accordance with these data, we found lower transcript levels for both $p16^{INK4a}$ and $p19^{ARF}$ tumor suppressors in Jmjd3 mutant B cells activated via TLR4. The failure to up regulate $p19^{ARF}$ may confer resistance to p53–dependent apoptosis following LPS stimulation. Indeed, we could show that by day-3 of LPS activation, there was a lower fraction of apoptotic cells within Jmjd3 mutant cultures when compared to controls. The property of Jmjd3 to induce Cdkn2a expression in

activated B cells may represent a fail-safe mechanism to limit the chance of acquiring chromosomal translocations as bystander effects of Ig isotype switching catalyzed by Activation Induced Cytidine deaminase (AID). Taken together these results position Jmjd3 within a regulatory network that guarantees on one hand optimal B cell proliferation in response to LPS stimulation, and, on the other, sensitizes cells to p53-dependent apoptosis through a direct regulation of Cdkn2a expression.

From the first bioinformatics analyses of RNA sequencing data, 2628 genes resulted differentially expressed in a significant manner between resting wild-type and Jmjd3 mutant B cells. These genes were almost equally distributed among down- (56%) and up- (44%) regulated genes in Jmjd3 mutants. Gene ontology analysis revealed that genes downregulated in Jmjd3 mutant B cells were significantly enriched for categories related to the cell-cycle and DNA replication. Up-regulated genes were instead enriched for gene categories involved in immune response to stimuli.

Interestingly (and quite unexpectedly) the comparison of transcriptomes between Jmjd3 mutant and control B cells analyzed at 24 hr after LPS stimulation revealed a smaller number (595) of differentially expressed genes. The majority (82%) of the latter genes resulted up-regulated in mutant B cells.

We next assessed whether genes differentially expressed in Jmjd3 mutant B cells were marked respectively by H3K27me3 and/or H3K4me3 in their wild type counterparts. For this analysis we took advantage of H3K4me3 and H3K27me3 genome-wide distribution maps that our lab has recently generated for different B cell subsets including follicular and marginal zone B cells (C. Carrisi and S. Casola, unpublished data). We intersected lists of differentially expressed genes with targets respectively of H3K27me3-only, H3K4me3-only and both histone marks in Fo and MZ B cells. Preliminary results indicate that over 70% of differentially expressed genes in resting Jmjd3 mutant B cells (1873 out of 2628) were marked by H3K4me3-only in their corresponding wild-type cells. These results are in accordance with previous data obtained in macrophages showing the preferential recruitment of Jmjd3 to target genes marked by high levels of H3K4me3 (De Santa et al., 2009). These preliminary data will be validated determining the H3K4me3 status of differentially expressed genes in Jmjd3 mutant B cells.

4.3.2. Jmjd3 and terminal B cell differentiation

Stimulation of B cells with LPS triggers terminal differentiation of B cells. This process is strictly dependent on the up regulation of Irf4, Prdm1, Xbp-1 transcription factors (Klein et al., 2006, Sciammas et al., 2006). Given that *Blimp1* and *Irf4* genes are marked by H3K27me3 and are tightly regulated by Ezh2 to prevent premature plasma cell differentiation, we hypothesized that inactivation of Jmdj3 demethylase activity could prevent terminal differentiation. Moreover, we scored lower Irf4 transcript levels in Jmjd3 mutant B cell cultures after LPS activation. However, flow cytometric analysis indicated that the frequency of $CD19^{lo}Cd138^{hi}$ plasma blasts (PBs) was not reduced in *Jmjd3* mutant B cell cultures. Actually, we found a higher proportion of PBs in day-4 cultures of LPS-activated mutant B cells. We interpret the latter result with a delayed activation and improved survival of mutant B cells, which hence may lead to the detection of a higher fraction of PBs at day-4 of LPS stimulation. In summary, inactivation of Jmjd3 does not prevent onset of terminal differentiation. Measurement of Ig serum titers in unimmunized mice revealed comparable levels of all isotypes in controls and Jmjd3 mutant animals. Although we have yet to determine *Jmjd3* gene status in ex vivo isolated PCs, these results suggest a minor contribution of Jmjd3 to plasma cell homeostasis.

4.3.3. Jmjd3 and Immunoglobulin class-switch recombination

Stimulation of B cells with LPS leads to a potent induction of AID expression and consequently to IgG3 isotype switching. Hence, we asked whether Jmjd3 inactivation had an influence on the generation of IgG3 class-switched B cells. Indeed, flow cytometric analyses revealed a lower proportion of $IgG3^+$ B cells in Jmjd3 mutant cultures. The reduction in Ig-switched Jmjd3 mutant B cells is likely not due to impaired AID expression as we observed comparable frequencies of $IgG1^+$ B cells in mutant and control cultures after stimulation with LPS+IL-4. Since Ig class switch recombination correlates with number of cell divisions (Deenick et al., 1999) and given that *Jmjd3* mutant B cells showed a defective proliferative response to LPS (but not LPS + IL-4), we conclude that the reduced fraction of $IgG3^+$ B cells in *Jmjd3* mutant cultures is primarily caused by impaired proliferation.

4.4. Jmjd3 and the germinal center reaction

Our laboratory has recently assigned a critical role to Ezh2 methyltransferase activity in the regulation of the germinal center reaction (Caganova et al., 2013). Hence we asked whether inactivation of the H3k27me3 demethylase activity of Jmjd3 could impact on the formation and maintenance of germinal center responses. To this end, we performed flow cytometric analyses in gut associated lymphoid tissues (mesentheric lymph nodes and Peyer's patches) that show chronic germinal centers as a result of continuous microbial stimulation. Analyses revealed a comparable fraction of GC B cells between control and *Jmjd3* mutant animals. We extended these analyses performing immunizations with the T-cell dependent antigen NP-CGG. The measurement of antigen-specific IgG1 titers at different time points after immunization excluded a major contribution of Jmjd3 to GC responses. This result will be ultimately confirmed analyzing the fraction of GC B cells in the spleen of mutant and control animals at different time points after immunization. Moreover, since serum high-affinity antigen-specific IgG1 antibody levels were comparable between control and Jmjd3 mutant animals in recall responses, we conclude that Jmjd3 is not essential for memory B cell generation.

In conclusion, analysis of Jmjd3 conditional knockout mice has revealed essential contributions of the histone demethylase to B cell subset differentiation and to B cell activation in response to innate immune stimuli such as microbial LPS.

5. References

Adamietz P, Rudolph A (1984) ADP-ribosylation of nuclear proteins *in vivo*. Identification of histone H2B as a major acceptor for mono- and poly(ADP-ribose) in dimethyl sulfate-treated heptoma AH 7974 cells. J Biol Chem. 259:6841-6846.

Agger K, Cloos PA, Christensen J, Pasini D, Rose S, Rappsilber J, Issaeva I, Saclini AE, Helin C (2007) UTX and Jmjd3 are histone H3K27 demethylases involved in Hox gene regulation and development. Nature 449:731-734.

Agger K, Cloos PA, Rudkjaer L, Williams K, Anderson G, Christensen J, Hellin K (2009) The H3K27me3 demethylase JMJD3 contributes to the activation of the INK4A-ARF locus in response to oncogene- and stress-induced senescence. Genes Dev. 23(10):1171-6.

Akamine R, Yamamoto T, Watanabe M, Yamazaki N, Kataoka M, Ishikawa M, Ooie T, Baba Y, Shinohara Y (2007) Usefulness of the 5' region of the cDNA encoding acidic ribosomal phosphoprotein P0 conserved among rats, mice, and humans as a standard probe for gene expression analysis in different tissues and animal species. J Biochem Biophys Methods 70:481-486.

Allman, D. M., Ferguson, S. E., Lentz, V. M., and Cancro, M. P. (1993). Peripheral B cell maturation. II. Heat-stable antigen(hi) splenic B cells are an immature developmental intermediate in the production of long-lived marrow-derived B cells. J Immunol 151, 4431-4444.

Allman D, Lindsiey RC, DeMuth W, Rudd K, Shinton SA, Hardy RR (2001) Resolution of three nonproliferative immature splenic B cell subsets reveals multiple selection points during peripheral B cell maturation. J Immunol. 167(12):6834-40.

Anderton JA, Bose S, Vockerodt M, Vrzalikova K, Wei W, Kuo M, Helin K, Christensen J, Rowe M, Murray PG, Woodman CB (2011) The H3K27me3 demethylase ,KDM6B, is induced by Epstein-Barr virus and over-expressed in Hodgkin's lymphma. Oncogene 30(17):2037-43.

Annunziato AT, Eason MB, Perry CA (1995) Relationship between methylation and acetylation of arginine-rich histones in cycling and arrested HeLa cells. Biochemistry 34:2916-2924.

Barradas M, Anderton E, Acosta JC, Li S, Banito A and Gil J (2009). Histone demethylase JMJD3 contributes to epigenetic control of INK4A/ARF by oncogenic RAS. Genes Dev. 23(10)1177-82.

Barski A, Cuddapah S, Cui K, Schones DE, Wang Z, Wei G, Chepelev I, Zhao K (2007) High-resolution profiling of histone methylation in the human genome. Cell. 129(4):823-37.

Basso K, Dalla-Favera R (2010) Bcl6: master regulator of the germinal center reaction and key oncogene in B cell lymphomagenesis. Adv Immunol 105:193-210.

Baumgarth N (2010) The double life of a B-1 cells: self-reactivity selects for protective effector functions. Nat Rev Immunol. 11(1):34-46.

Beguelin W, Popovic R, Teater M, Jiang Y, Elemento O and Melnick AM (2013) EZH2 is required for germinal center formation and somatic EZH2 mutations promote lymphoid transformation. Cancer Cell 23(5):677-92.

Berland R, Wortis HH (2002) Origins and functions of B-1 cells with notes on the role of CD5. Annu Rev Immunol. 20:253-300.

Berland R, Wortis HH (2003) Normal B-1a cell development requires B-cell intrinsic NFATz1 activity. Proc Natl Acad Sci USA 100(23):13459-64.

Bernstein BE, Mikkelsen TS, Xie X, Kamal M, Huebert DJ (2006) A bivalent chromatin structure marks key developmental genes in embryonic stem cells. Cell 125:315-326.

Bhaumik SR, Smith E, Shilatifard A (2007) Covalant modifications of histones during development and diseases pathogenesis. Nat Struct Mol Biol. 14:1008-1016.

Blackledge N, Farcas AM, Kondo T, Koseki H and Klose RJ (2014) Varient PRC1 complex-dependent H2A ubiquitination drives PRC2 recruitment and polycomb domain formation. Cell 157(6):1445-1459.

Borun TW, Pearson D, Paik WK (1972) Studies of histone methyltion during the HeLa S-3 cell cycle. J Biochem. 247:4288-4298.

Bracken AP, Kleine-Kohlbrecher D, Dietrich N, Pasini D, Gargiulo G, Beekman C, Theilgaard-Monch K, Minucci S, Porse BT, Marine JC (2007) The polycomb group proteins bind throughout the INK4A-ARF locus and are disaccociated in senescent cells. Genes Dev. 21:525-530.

Burgold T, Spreafico F, De Santa F, Tatoro MG, Prosperini E, Natoli G, Testa G (2008) The histone lysine 27-specific demethylase Jmjd3 is required for neural commitment. PLoS ONE 3(8):e3034.

Burgold T, Voituron N, Caganova M, Tripathi PP, Menuet C, Tusi BK, Spreafico F, Bevengut M, Gestreau C, Buontempo S, Simeone A, Kruidenier L, Natoli G, Casola S, Hilaire G, Testa G (2012)

The H3K27 demethylase JMJD3 is required for maintenance of the embryonic respiratory neural network, neonatal breathing, and survival. Cell Rep. 2(5):1244-58.

Byvoet P, Shepherd GR, Hardin JM, Noland BJ (1972) The distribution and turnover of labled methyl groups in histone fractions of cultured mammalian cells. Arch Biochem Biophys. 148:558-567.

Caganova M, Carrisi C, Varano G, Mainoldi M, Zanardi F, Germain PL, George L, Alberghini F, Talukder AK, Ponzoni M, Testa G, Nojima T, Doglioni C, Kitamura D, Toeliner KM, Casola S (2013) Germinal center dysregulation by histone methyltransferase EZH2 promotes lymphomagenesis. J Clin Invest. 123(12):5009-22.

Calame K, Lin KT, Tunyaplin C (2003) Regulatory mechanisms that determine the development and function of plasma cell. Ann Rev Immunol 21:205-230.

Calfon M, Zeng H, Urano F, Till JH, Hubbard SR, Harding HP, Clark SG, Ron D (2002) IRE1 couples endoplasmic reticulum lead to secretory capacity by processing the XBP-1 mRNA. Nature 415(6867):92-6.

Cambier JC, Gauld SB, Marrell KT, Vilen BJ (2007) B-cell anergy:from transgenic models to naturally occurring anergic B cells? Nat Re Immunol. 7(8):633-43.

Canovas S, Cibelli JB, Ross PJ (2012) Jumonji domain-containing protein 3 regulates histone 3 lysine 27 methylation during bovine preimplantation development. Proc Natl Acad Sci U S A 109(7):2400-5.

Cao Q, Wang X, Zhao M, Yang R, Mlik R, Chinnaiyan AM et al. (2014) The central role of EEd in the orchestration of polycomb group complexes. Nat Commun. 5:3127.

Casola, S., Otipoby, K. L., Alimzhanov, M., Humme, S., Uyttersprot, N., Kutok, J. L., Carroll, M. C. et al. (2004) B-cell receptor signal strength determines B-cell fate. Nat. Immunol. 5: 317–327.
Casola S (2007) Control of peripheral B cell development. Curr Opin Immunol 19(2):143-9.

Cattoretti G, Pasqualucci L, Ballon G, Tam W, Nandula SV, Shen Q, Mo T, Murty VV, Dalla-Favera R (2005) Deregulated BCL6 expression recapitulate the pathogenesis of human diffuse large B cell lymphomas in mice. Cancer Cell 7:445-55.
Cenci S, Sitia R (2007) Managing and exploiting stress in the antibody factory. FEBS Lett. 581(19):3652-7.

Cenci S (2012) The proteasome in terminal plasma cell differentiation. Semin Hematol. 49(3):215-22.

Choi MS, Brines RD, Holman MJ, Klaus GG (1994) Induction of NF-AT in normal B lymphocytes by anti-immunoglobulin or CD40 ligand in conjuction with IL-4. Immunity 1:1179-187.

Chuikov S, Kurash JK, Wilson JR, Xiao B, Justin N (2004) Regulation of p53 activity through lysine methylation. Nature 432:823-827.

Cinamon G, Zachariah MA, Lam OM, Foss FW, Cyster JG (2008). Follicular shuttling of marginal zone B cells facilitates antigen transport. Nature immunology 9:54-62.
Cloos PA, Christensen J, Agger K, Maiolica A, Rappsilber J (2006) The putative oncogene GASC1 demethylates tri- and dimethylated lysine 9 on histone H3. Nature 442:307-11.

Cobaleda C, Schebesta A, Delogu A, Busslinger M (2007a) Pax5: the guardian of B cell identity and function. Nat immunol 8(5):463-70.

Cobaleda C, Jochum W, Busslinger M (2007b) Conversion of mature B cells into T cells by differentiation to uncommitted progenitors. Nature 449(7161):473-7.

Cooper AB, Sawai CM, SicinskaE, Powers SE, Sicinski P, Clark MR, Aifntis I (2006) A unique function for cyclin D3 in early B cell development . Nat immunol. 7(5):489-97.

Cooper, Dienstbier M, Hassan R, Schermelleh L, Heger A and Brockdorff N (2014) Targeting polycomb to pericentric heterochromatin in embryonic stem cells reveals a role for H2AK119ub1 in PRC2 recruitment. Cell Rep. 7(5):1456-70.

Crabtree GR, Olson EN (2002) NFAT signaling: choreographing the social lives of cells. Cell 109 Suppl:S67-S79.

Crowley JE, Scholz JL, Quinn WJ, Stadanlick JE, Treml, JF, Treml LS, Hao Y, Geonka R, O'neill PJ, Mattthews AH, st al. (2008) Homeostatic control of B lymphocyte subsets, Immunol Res 42(1-3):75-83.

Czermin B, Melfi R, McCabe D, Seitz V, Imholf A, Pirrotta V (2002) Drosophila enhancer of zeste/ESC complexes have a histone H3 methyltransferase activity that marks chromosomal polycomb sites. Cell 111:185-196.

Davie JR, Murphy LC (1990) Level of ubiquitinated histone H2B in chromatin is coupled to ongoing transcription. Biochemistry 29:4752-4757.

Deenick EK, Hasbold J, Hodgkin PD (1999) Switching to IgG3, IgG2b and IgA is division linked and independent, revealing a stochastic framework for describing differentiation. J Immunol. 163(9):4707-14.

De Santa F, Totaro MG, Prosperini E, Notarbartolo S, Testa G, Natoli G (2007) The histone H3 lysine-27 demethylase Jmjd3 links inflammation to inhibition of polycomb-mediated gene silencing. Cell 130(6):1083-94.

Dorshkind K, Montecino-Rodriguez E (2007) Fetal B-cell lymphopoiesis and the emergence of B-1 cell potential. Nat Rev Immunol. 7:213-219.

Edry E, Melamed D (2004) Receptor editing in positive and negative selection of B lymphopoiesis. J Immunol. 173(7):4265-71.

Ene CI, Edwards L, Raddick G, Baysan M, Fine H et al. (2012) Histone demethylase Jumonji D3 (JMJD3) as a tumor suppressor by regulating p53 protein nuclear stabilization. PLoS ONE 7(12):e51407.

Estaras C, Fueyo R, Akizu N, Beltran S, Martinez-Balbas MA (2013) RNA polymerase II progression through H3K27me3-enriched gene bodies requires JMJD3 histone demethylase. Mol Biol Cell 24(3):351-60.

Fodor BD, Kubicek S, Yonezawa M, O'Sullivan RJ, Sengupta R (2006) Jmjd2b antagonizes H3K9 trimethylation at pericentric heterochromatin in mammalian cells. Genes Dev. 20:1557-62.

Furqan M, Mukhi N, Lee B, Liu D (2013) Dysregulation of JAK-STAT pathway in hematological malignancies and JAK inhibitors for clinical application. Biomark Res. 1(1):5.

Fuxa M, Skok J, Souabni A, Salvagiotto G, Roldan E, Busslinger M (2004) Pax5 induces V-to-DJ rearrangements and locus contraction of the immunoglobulin heavy-chain gene. Genes Dev. 18(4):411-22.

Fuxa M, Busslinger M (2007) Reporter gee insertions reveal a strictly B lymphoid-specific expression pattern of Pax5 in support of its B cell identity function. J Immunol. 178(5):3031-7.

Gieni RS, Hendzel MJ (2009). Polycomb group protein gene silencing, non-coding RNA, stem cells and cancer. Biochem Cell Biol 87:711-746.

Grunstein M (1997) Histone acetylation in chromatin structure and transcription. Nature 389:349-352.

Gupta S, Jiang M, Anthony A, Pernis AB (1999) Lineage-specific modulation of interleukin 4 signaling by interferon regulatory factor 4. J Exp Med. 190(12):1837-48.
Gururajan M, Haga CL, Das S, Leu AM, Hodson D, Josson S, Turner M, Cooper M (2010) MicroRNA 125b inhibition of B cell differentiation in germinal centers. Int Immunol. 22(7):583-92.

Hardy R, Hayakawa K (2001) B cell development pathways. Annu. Rev.Immunol. 19:595-621.
Hardy RR (2006) B-1 B cell development. J Immunol. 177(5):2749-54.

Herzenberg LA (2000) B-1 cells: the lineage question revisited. Immunol Rev. 175:9-22.
Hobeika E, Thiemann S, Storch B, Jumaa H, Nielsen PJ, Pelanda R, Reth M (2006) Testing gene function early in the B cell lineage in mb1-cre mice. Proc Natl Acad Sci USA. 103(37): 13789-13794.

Hoim K, Melek M, Gellert M (1998) DNA transposition by the RAG1 and RAG2 proteins: a possible source of oncogenic translocations. Cell 94(4):463-70.

Huang J, Sengupta R, Espejo AB, Lee MG, Dorsey JA (2007) P53 is regulated by the lysine demethylase LSD1. Nature 449:105-108.

Hymes J, Fleischhauer K, Wolf B (1995) Biotinylation of histones by human biotinidase: assessment of biotinyl-transferase activity in sera from normal individuals and children with biotinidase deficiency. Biochem Mol Med. 56:76-83.

Ishii M, Wen H, Corsa CA, Liu T, Coelho AL, Allen RM, Carson WF 4th, Cavassani KS, Lukacs NW, Hogaboam CM, Dou Y, Kunkel SL (2009) Epigenetic regulation of the alternatively activated macrophage phenotype. Blood 114(15):3244-54.

Ivashkiv LB (2103) Epigenetic regulation of macrophage polarization and function. Trends Immunol. 34(5):216-23.

Jaenisch R, Bird A (2003) Epigenetic regulation of gene expression: how the genome integrate intrinsic and environmental signals. Nat Genet. 33:245-54.

Jenuwein T, Allis CD (2001)Translating the histone code. Science 293:1074-1080.
Jones RS, Gelbart WM (1993) The *Drosophila* Polycomb-group gene Engancer of zeste contains a region with sequence similarity to trithorax. Mol Cell Biol. 13:6357-6366.

Jost PJ, Ruland J (2006) Aberrant NF-κB signaling in lymphoma: mechanisms, consequences and therapeutic implications. Blood 109(7):2700-7.

Kalb R, Latwiel S, Baymaz HL, Jansen PW, Muller CW, Vermeulen M, Muller J (2014) Histone H2A monoubiquitination promotes histone methylation in polycomb repression. Nat Struct Mol Biol. 21(6):569-71.

Kallies A, Hasbold J, Fairfax K, Pridans C, Emsile D, McKenizie BS, Lew AM, Corcoran LM, Hodgkin PD, Tarlinton DM (2007) Initiation of plasma cell differentiation in independent of the transcription factor Blimp-1. Immunity 26:555-566.

Kartikasari AE, Zhou JX; Kanji MS, Chan DN, Lowry WE, Bhushan A (2013) The histone demethylase Jmjd3 sequentially associates with the transcription factors Tbx3 and Eomes to drive endoderm differentiation. EMBO J. 32:1393-1408.

Kerenyi MA, Shao Z, Hsu YJ, Guo G, Luc S, O'Brein K, Fujiwara Y, Peng C, Nguyen M, Orkin SH (2013) Histone demethylase Lsd1 represses hematopoietic stem and progenitor cell signature during blood cell maturation. 2:e00633.

Khan WN (2009) B cell receptor and BAFF receptor signaling regulation of B cell homeostasis. J Immunol. 183:3561-3567.

Kirmizis A, Bartley SM, Kuzmichev A, Margueron R, Reinberg D, Green R, Farnham PJ (2004) Silencing of human polycomb target genes is associated with methylation of histone H3 Lys 27. Genes Dev. 18:1592-1605.

Klein U, Casola S,Cattoretti G, Shen Q, Lia M, Ludwig T, Rajewsky K, Della-Favera R (2006) Transcription factor IRF4 controls plasma cell differentiation and class-switch recombination. Nat Immunol 7(7):773-82.

Klein U, Dalla-Favera R (2008) Germinal centers: role in B-cell physiology and malignancy. Nat Rev Immunol. 8(1):22-33.

Kooistra SM, Helin K (2012) Molecular mechanisms and potential functions of histone demethylases. Nat Rev Cell Biol. 13(5):297-311.

Kopan R, Ilagan MX (2009) The canonical Notch signaling pathway:unfolding the activation mechanism. Cell 137(2):216-33.

Kotake Y, Cao R, Viatour P, Sage J, Zhang Y, Xiong Y (2007) “pRB” family proteins are required for H3K27 trimethylation and polycomb repression complexes binding to and silencing p16INK4alpha tumor suppressor gene. Genes Dev. 21(1):49-54.

Kraal G, Janse M (1986) Marginal metallophilic cells of the mouse spleen identified by a monoclonal antibody. Immunology 58:665-669.

Kraus M, Alimzhanov MB, Rajewsky N, Rajewsky K (2004) Survival of resting mature B lymphocytes depends on BCR signalin via the Igalpha/beta heterodimer. Cell 117(6):787-800.

Kurado K, Han H, Tani S, Tanigaki K, Tun T, Furukawa T, Taniguchi Y, Kurooka H, Hamada Y, Toyokuni S, Honjo T (2003) Regulation of marginal zone B cell development by MINT, a suppressor of Noth/RBP-J signaling pathway. Immunity 18(2):301-12.

Kwon H, Thierry-Mieg J, Kim HP, Oh J, Tunyaplin C, Carotta S, Donovan CE, Goldman ML, Tailor P (2009) Analysis of interleukin-21-induced prdm1 gene regulation reveals functional cooperation of STAT3 and IRF4 transcription factors. Immunity 31:941-952.

Laborda J (1991) 36B4 cDNA used as an estradiol-independent mRNA control is the cDNA human acidic ribosomal phosphoprotein P0. Necleic Acids Res. 19(14):3998.

Lachner M, O’Sullivan RJ, Jenuwein T (2003) An epigenetic road map for histone lysine methylation. J. Cell Sci. 116:2117-2124.

Lallemand Y, Luria V, Haffner-Krausz R, Lonai P (1998) Maternally expressed PGK-Cre transgene as a tool for early and uniform activation of the Cre site-specific recombinase. Transgenic Res. 7(2):105-12.

Lan F, Bayliss PE, Rinn JL, Whetstine JR, Wang JK (2007) A histone H3 lysine 27 demethylase regulates animal posterior development. Nature 449(7163):689-94.
Lee HY, Choi K, Oh H, Park YK, Park H (2014) HIF-1-dependent induction of Jumonji domain-containing protein (JMJD)3 under hypoxic conditions. Mol Cell 37(1):43-50.

Leibich HM, Gesele E, Wirth C, Woll J, Jobst K, Lakatos A (1993) Non-enzymatic glycation of histones. Biol Mass Spectrom 22:121-123.

Li CL, Johnson GR (1995) Murine hematopoietic stem and progenitor cells: I. Enrichment and biologic characterization. Blood 85:1472-1479.

Lin TY, Cheng YC, Yang CC, Lai PL, Shieh SY (2012) Loss of the candidate tumor suppressor BTG3 triggers acute cellular senescence via the ERK-JMJD3-p16(INK4a) signaling axis. Oncogene 31(27):3287-97.

Liu J, Mercher T, Scholl C, Brumme K, Gilliland DG, Zhu N (2012) A functional role for the histone demethylase UTX in normal and malignant hematopoietic cells. Exp Hematol. 40(6):487-98.

Liu X, Wu H, Loring J, Hormuzdi S, Disteche CM (1997) Trisomy eight in ES cells is a common potential problem in gene targeting and interference with germline transmission. Dev Dyn 209:85-91.

Longo L, Bygrave A, Grosveld FG, Pandolfi PP (1997) The chromosoml make-up of mouse embryonic stem cells is predictive of somatic and germ cell chimerism. Transgenic Res 6:321-328.

Lu R, Median KL, Lancki DW, Singh H (2003) IRF-4,8 orchestrates the pre-B-to-B transition in lymphocyte development. Genes Dev. 17(14):1703-8.
Lu R (2008) Interferon regulatory factor 4 and 8 in B cell development. Trends Immunol. 29(10):487-92.
Luger K (2003) Structure and dynamic behavior of nucleosomes. Curr Opin Genet Dev. 13:127-135.
Mackay F, Browning J (2002) BAFF: a fundamental survival factor for B cells. Nat Rev Immunol. 2(7):465-75.

Margueron R, Li G, Sarma K, Blais A, Zavadil J, Woodcock CL, Dyniacht BD, Reinberg D (2008) Ezh1 and Ezh2 maintain repressive chromatin through different mechanisms. Mol Cell 32(4):503-18.

Martensson IL, Ceredig R (2000) Role of the surrogate light chain and the pre-B cell receptor in mouse B-cell development. Immunology 101(4):435-441.

Martin F, Kearney JF (2002) Marginal-zone B cells. Nat rev Immunol.2:323-335.
Lopes-Carvalho T, Kearney JF (2004). Development and selection of marginal zone B cells. Immunol Rev. 197:192-205.

Martin F, Kearney JF (2002) Marginal zone B cells. Nat Rev Immunol. 2:323-335.

Matsuzawa A, Tseng PH, Vallabhapurapu S, Luo JL, Zhang W, Wang H, Vignali DA, Gallagher E, Karin M (2008) Essential cytoplasmic translocation of a cytokine receptor-assembled signaling complex. Science 321(5889):663-668.

McBlane JF, Van Gent DC, Ramsden DA, Romeo C, Cuomo CA, Geller M, O ettinger MA (1995) Cleavage at the V(D)J recombination signal requires only RAG1 and RAG2 proteins and occursin two steps. Cell 83:387-395.

McCabe MT, Graves AP, Ganji G, Diaz E, Schwartz B and Creasy CL (2012) Mutation of A677 in histone methyltransferase EZH2 in human B-cell lymphoma promotes hypertrimethylation of histone H3 on lysine 27 (H3K27). Proc Natl Acad Sci USA 109(8):2989-94.

Mikkelsen TS, Ku M, Jaffe DB, Issac B, Lieberman E (2007) genome-wide maps of chromatin state in pluripotent and lineage- committed cells. Nature 448:553-560.

Miller SA, Mohn SE, Weinmann AS (2010) Jmjd3 and UTX play a demethylase-independent role in chromatin remodeling to regulate T-box family member-dependent gene expression. Mol Cell 40: 594-605.

Mitchell TJ, John S (2005) Signal transducer and activator of transcription (STAT) signaling and T-cell lymphoma. Immunology 114(3):301-12.

Mittrucker HW, Matsuyama T, Grossman A, Kundig TM, Potter J, Shahinian A, Wakeham A, Patterson B, Ohashi PS, Mak TW (1997) Requirement for the transcription factor LSIRF/IRF4 for mature B and T lymphocyte fnction. Science 275(5299):540-3.

Miyake K, Yamashita Y, Ogata M, Sudo T, Kimoto M (1995) RP105, a novel B cell surface molecule implicated in B cell activation, is a member of the leucine-rich repeat protein family. J Immunol. 154:3333-3340.

Montecino-Rodriguez E, Dorshkind Keneth (2012) B-1 B cell development in the fetus and adult. Immunity 36(1):13-21.

Morin RD, Johnson NA, Severson TM, Mungall AJ, An J, Goya R and Marra MA (2010) Somatic mutation of EZH2 (Y641) in follicular and Diffuse large B cell lymphomas of germinal center origin. Nat Genet. 42(2):181-185.

Muller MR, Rao A (2010) NFAT, immunity and cancer: a transcription factor comes of age. Nat Rev Immunol 10(9):645-656.

Muramatsu M, Kinoshita K, Fagarasan S, Yamada S, Shinkai Y, Honjo T (2000) Class switch recombination and hypermutation require activation-induced cytidine demainase (AID), a potential RNA editing enzyme. Cell 102(5):553-63.

Klein U, Tu Y, Stolovitzky GA, Keller JL, Hadda JJ, Miljkovic V, Cattoretti G, Califano A, Dalla-Favera R (2003) Transcription analysis of the B cell germinal center reaction. Proc Natl Acad Sci U S A 100(5):2639-44.

Nathan D, Sterner DE, Berger SL (2003) Histone modifications: now summoning sumoylation. Proc Natl Acad Sci USA 100:13118-13120.

Nemazee D (2006) Receptor editing in lymphocyte development and central tolerance. Nat Rev Immunol. 6:728-740.

Nera KP, Kohonen P, Narvi E, Peippo A, Terho P, Koskela K, Buerstedde JM, Lassila O (2006) Loss of Pax5 promotes plasma cell differentiation. Immunity 24(3):283-93.

Nowak SJ, Corces VG (2004) Phosphorylation of histone H3: a balancing act between chromosome condensation and transcriptional activation. Trends Genet. 20:214-220.

Nutt SL, Heavy B, Rolink AG, Busslinger M (1999) Cimmitment to the B-lymphoi lineage depends on the transcription factor Pax5. Nature 41:556-562.
Ochiai K, Maienschein-Cline M, Simonetti G, Chen J, Klein U, Dinner AR, Singh H, Sciammas R (2013) Transcription of germinal center B and plasma cell fates by dynamical control of IRF4. Immunity 38(5):918-29.

Oeckinghaus A, Ghosh S (2009) The NF-κB family of transcription factors and its regulation. Cold Spring Harb Perspect Biol 1(4):a000034.

Ohtani K, Zhao C, Dobreva G, Manavski Y, Reiger MA, Zeiher AM, Dimmeler S (2013) Jmjd3 controls mesodermal and cardiovascular differentiation of embryonic stem cells. Circ. Res. 113(7):856-62.

Pasqualucci L, Khiabanian H, Fangazio M, Vasishtha M, Messina M et al. (2013) Genetics of follicular lymphoma transformation. Cell Rep. 6(1):130-40.

Patke A, Mecklenbrauker I, Erdjument-Bromage H, Tempst P, Tarakovsky A (2006) BAFF controls B cell metabolic fitness through a PKC beta- and Akt-dependent mechanism. J Exp Med. 203(11):2551-62.

Peperzak V, Vikstrom I, Walker J, Glaser SP, LePage M, Coquery CM, Erikson LD, Fairfax K, Mackay F, Strasser A, Nutt SL, Tarlinton DM (2013) Mcl-1 is essential for the survival of plasma cells. Nat Immunol. 14(3): 290-7.

Pereira F, Barbachano A, Silva J, Bonilla F, Campbell MJ, Munza A, Larriba MJ (2011) KDM6B/JMJD3 hisone demethylase is induced by vitamin D and modulates its effects in colon cancer cells. Hum Mol Genet. 20(23):4655-65.

Pillai S, Caiappa A, Moran ST (2004) Positive selection and lineage commitment during peripheral B-lymphocyte development. Immunol Rev. 197:206-18.

Pillai S, Cariappa A (2009) The follicular versus marginal zone B lymphocyte cell fate decision. Nat Rev Immunol. 9(11):767-77.

Przanowski P, Dabrowski M, Ellert-Mikiaszewska A, Kloss M, Mieczkowski, Kaza B, Ronowisz A, Hu F, Piotrowski A, Kattenmann H, Komorowski J, Kaminska B (2014) The signl transducers Stat1 and Stat3 and their novel target Jmjd3 rive the expression of inflammatory genes in microglia. J Mol Med (Berl) 92(3):239-54.

Radtke F, Wilson A, Mancini SJ, MacDonald HR (2004a) Notch regulation of lymphocyte development and function. Nat Immunol. 5(3):247-53.

Radtke F, Wilson A, MacDonald HR (2004b) Notch signaling in T- and B-cell development. Curr Opin Immunol. 16(2):174-9.

Rajewsky, K. (1996). Clonal selection and learning in the antibody system. Nature 381, 751-758.

Rao A, Luo C, Hogan PG (1997) Transcription factors of the NFAT family: regulation and function. 15:707-747.

Reimold AM, Iwakoshi NN, Manis J, Vallabhajosyula P. Szomolanyi-Tsuda E, Grasvallese EM, Friend D, Grusby MJ, Alt F, Glimcher LH (2001) Plasma cell differentiation requires the transcription factor XBP-1. Nature 412(6844):300-7.

Revilla IDR, Bilic I, Vilagos B, Tagoh H, Ebert A, Tamir IM, Smeenk L, Trupke J, Sommer A, Jaritz M et al. (2012) The B-cell identity factor Pax5 regulates distinct transcriptional programmes in early and late B lymphopoiesis. EMBO J. 31(14):3130-46.

Rodriguez C, Buchholz F, Galloway J, Sequerra R, Kasper J, Ayala R, Stewart AF, Dymecki SM (2000) High-deficiency delete mice show that FLPe is an alternative to Cre-loxP. Nat Genet. 25(2):139-40.

Saito T, Chiba S, Ichikawa M, Kunisato A, Asai T et al. (2003) Notch2 is preferentially expressed in mature B cells and indispnsable for marginal zone B lineage development. Immunity 18(5):675-85.

Santenard A, Zeigler-Birling C, Koch M, Tora L, Bannister AJ, Torres-Padilla ME (2010) Heterochromatin formation in the mouse embryo requires critical residues of the histone variant H3.3. Nat cell Biol 12:853-62.

Satoh T, Takeuchi O, Vandenbon A, Yasuda K, Tanaka Y, Kumagai Y, Miyake T, Matsushita K, Okazaki T, Saitoh T, Honma K, Matsuyama T, Yui K, Tsujimura T, Stanley DM, Nakanishi K, Nakai K, Akira S (2010) The Jmjd3-Irf4 axis regulates M2 macrophage polarization and host responses against helminth infection.

Sauvageau M, Sauvageau G (2010) Polycomb group proteins:Multi-faced regulators of somatic stem cells and cancer. Cell Stem cell 7:299-313.

Scott ML (2001) An essential role for BAFF in the normal development of B cells through a BCMA-independent pathway. Science 293(5537):2111-4.

Scheeren FA, Naspetti M, Diehl S, Schotte R, Nagasawa M, Winjnands E, Gimeno R, Vyth-Dreese FA, Blom B, Spits H (2005) STAT5 regulates the self-renewal capacity and differentiation of human memory B cells and conrols Bcl-6 expression. Nat Immunol. 6(3):303-13.

Schiemann B, Gommerman JL, Vora K, Cachero TG, Shulga-Morskaya S, Dobles M,

Frew E, Scott ML (2001) An essential role for BAFF in the normal development of B cells

through a BCMA-independent pathway. Science 293(5537):2111-4.

Schneider P, Tschopp J (2003) BAFF and the regulation of B cell survival. Immunol Lett. 88(1):57-62.

Scholz JL, Crowley JE, Tomayko MM, Steinel N, O'Neill PJ, Quinn WJ, Geonka R, Miller JP, Cho YH, Long V, et al, (2008) BLys inhibition eliminates primary B cells but leaves natural and acquired humoral immunity intact.Proc Natl Acad Sci U S A 105(40):15517-22.

Schuettengruber B, Cavalli G (2009) Recruitment of polycomb group complexes and their role in the dynamic regulation of cell fate choice. Development 136:3531-3542.

Schweighoffer E, Vanes L, Nys J, Cantrell D, McCleary S, Smithers N, Tybulewicz VL (2013) The BAFF receptor transduces survival signals by co-opting the B cell receptor signaling pathway. Immunity 38(3):475-88.

Sciammas R, Davis MM (2004) Modular nature of Blimp-1 in the regulation of gene expression during B cell maturation. J Immunol. 172(9):5427-40.

Sciammas R, Shaffer AL, Schatz JH, Zhao H, Staudt LM, Singh H (2006) Graded expression of interferon regulatory factor-4 coordinates isotype switching with plasma cell differentiation. Immunity 25(2):225-36.

Seenundun S, Rapalli S, Liu QC, Aziz A, Palii C, Hong S, Blais A, rand M, Ge K, Dilworth FJ (2010) UTX mediates demethylation of H3K27me3 at muscle-specific genes during miogenesis. EMBO J. 29: 1401-1411.

Serrano M, Hannon GJ, Beach D (1993) A new regulatory motif in cell-cycle control causing specific inhibition of cyclin D/CDK4. Nature 366 (6456):704-7.

Shaffer AL, Shapire-Shelef M, Iwakoshi NN, Lee AH, Qian SB, Zhao H, Yu X, Yang L, Tan BK, Rosenwald A (2004) XBP1, downstream of Blimp-1, expands the secretory apparatus and other organelles, and increase protein synthesis in plasma cell differentiation. Immunity 21:81-93.

Shaffer AL, Emre NC, Romesser PB, Staudt LM (2009) IRF4:Immunity.Malignancy! Therapy? Clin Cancer Res. 15(9):2954-61.

Shapiro-Shelef M, Lin KI, McHeyzer-Williams LJ, Liao J, McHeyzer-Williams MG, Calame K (2003) Blimp-1 is required for the formation of immunoglobulin secreting plasma cells and plasma memory B cells. Immunity 19:607-620.

Sherr CJ (2001) The INK4a/ARF network in tumor suppression. Nat Rev Mol Biol. 2(10):731-7.

Shen Y, Guo X, Wang Y, Qiu W, Chang Y, Zhang A, Duan X (2012) Expression and significance of histone H3K27 demethylases in renal cell carcinoma. BMC Cancer. 12:470.

Shi Y, Lan F, Matson C, Mulligan P, Whestine JR, Cole PA, Casero RA (2004) Histone demethylation mediated by the nuclear amine oxidase homolog LSD1. Cell 119:941-953.

Shi X, Kachirskaia I, Yamaguchi H, West LE, Wen H (2007) Modulation of p53 function by SET8-mediated methylation at lysine 382. Mol Cell 27:636-646.

Simon JA, Kingston RE (2009) Mechanisms of polycob gene silencing: knowns and unknowns. Nat rev Mol Cell Biol 10:697-708.

Simonetti G, Carrette A, Silva K, Wang H, J. Shlomchik M and Klein U (2013) IRF4 controls the positioning of mature B cells in the lymphoid microenvironment by regulating NOTCH2 expression and activity. J Exp Med. 210(13):2887-902.

Sneeringer CJ, Scott MP, Kuntz KW, Knutson SK, Pollock RM, Richon VM, Copeland RA (2010) Coordinated activities of wild-type plus mutant EZH2 drive tumor-associated hypertrimethylation of lysine 27 on histone H3 (H3K27) in human B-cell lymphomas. Proc Natl Acad Sci U S A. 107(49):20980-5.

Sola S, Zavier JM, Santos DM, Aranha MM, Morgado AL, Jepsen K, Rodriguez CM (2011) P53 interactyion with JMJD3 results in its nuclear distyribution during mouse neural stem cell differentiation. PLoS ONE 6(3):e18421.

Souabni A, Cobaleda C, Schebesta M, Busslinger M (2002) Pax5 promotes B lymphopoiesis and blocks T cell development by repressing Notch1. Immunity 17(6):781-93.

Sparmann A, van Lohuizen M (2006) Polycomb silencers control cell fate, development and cancer. Nat Rev Cancer 6:846-856.

Stall A, Adams S, Herzenberg L, Kantor A (1992) Characteristics and development of the murine B-1b (Ly-1B) cell population. Ann NY Acad. Sci 651:33-43.

Stassen MJ, Bailey D, Nelson S, Chinwalla V, Harte PJ (1995) The *Drosophila* trithorax proteins contain a novel varient of the conserved motif found in other chromosomal proteins. Mech Dev. 52:209-223.

Su IH, Basavaraj A, Krutchinsky AN, Hobert O, Ullrich A, Chait BT, Tarakovsky A (2003) Ezh2 controls B cell development through histone H3 methylation and IgH rearrangement. Nat Immunol. 4(2):124-31.

Svotelis A, Bianco S, Madore J, Huppe G, Nordell-Markovits A, Mes-Masson AM, Gevry N (2011) EMBO J. 30(19):3947-61.

Tanigaki K, Han H, Yamamoto N, Tashiro K, Ikegawa M, Kuroda K, Suzuki A, Nakano T, Honjo T (2002) Notch-RBP-J signaling is involved in cell fate determination of marginal zone B cells. Nat Immunol 3(5):443-50.

Tang Y, Li T, Yang J, Liu H, Xhang XJ, Le W (2014) Jmjd3 is essential for the epigenetic modulation of microglia phenotypes in the immune pathogenesis of Parkinson‘s diseases. Cell Death Differ. 21(3):369-80.

Testa G, Schaft J, van der Hoeven F, Glaser S, Anastassiadis K, (2004) A reliable LacZ expression reporter cassette for multipurpose, knockout-first alleles. Genesis 38:151-158.
Thieme S, Gyarfas T, Richter C, Ozhan G, Fu J, Alexopoulou D, Mudres MH, Michalk I and Brenner S (2013) The histone demethylase UTX regulates stem cell migration and hematopoiesis. Blood 121(3):2462-73.

Tschiersch B, Hofmann A, Krauss V, Dorn R, Korge G, Reuter G (1994) The protein encoded by the *Drosophila* position-effect variegation suppressor gene Su(var)3-9 combines domains of antagonistic regulators of homeotic gene complexes. EMBO L. 13:3822-3831.
Tsukada Y, Fang J, Erdjumnet-Bromage H, Warren ME, Borchers CH (2006) Histone demethylation by a family of JmjC domain-containing proteins. Nature 439:811-16.

Van der Meulen J, Speleman F, Van Vlierberghe P (2014) The H3K27me3 demethylase UTX in normal development and disease. Epigenetics 9(5):658-68.

van Gent DC, McBlane JF, Ramsden DA, Sadofsky MJ, Hesse JE, Gellert M (1995) Initiation of V(D)J recombination in a cell-free system. Cell 81:925-934.

Van Haaften G, Dalgliesh GL, Davies H, Chen L, Bignell G, Greenman C, Edkins S, Hardy C et al. (2009) Somatic mutations of the histone H3K27 demethylase gene UTX in human cancer. Nat. Genet. 41:521-523.

Vences-Catalan F, Santos-Argumedo L (2011) CD38 through the life of a murine B lymphocyte. IUBMB Life 63(10):840-6.

Verweij CL., Guidos C, Crabtree GR (1990) Cell type specificity and activation requirments for NFAT-1 (nuclear factor of activated T cells) transcriptional activity determined by a new method using transgenic mice to assay transcriptional activity of an individual nuclear factor. J boil Chem. 265(26): 15788-95.

Waddington CH (1942) The epigenotype. Endeavour 1:18-20.
Walkley CR, Orkin SH (2006) Rb is dispensible for self'renowal and multilineage differentiation of adult hematopoietic stem cells. Proc Natl Acad Sci U S A 103(24):9057-62.

Wang Ns, McHeyzer-Williams LJ, Okitsu SL, Burris TP, Reiner SL, McHeyzer-Williams MG (2012) Divergent transcriptional programming of class-specific B cell memory by T-bet and RORα. Nat Immunol. 13(6):604-11.

Welner RS, Pelayo R, Kincade PW (2008) Evolving views on the genealogy of B cells. Nat Rev. Immunol. 8(2):95-106.

Whetstine JR, Nottke A, Lan F, Huarte M, Smolikov S (2006) Reversal of histone lysine trimethylation by the JMJD2 family of histone demethylases. Cell 125:467-81.

Williams K, Christensen J, Rappsilber J, Nielsen AL, Johnsen JV, Hellin K (2014) The histone lysine demethylase JMJD3/KDM6B is recruited to p53 bound promoters and enhancer elements in a p53 dependent manner. PLoS One, 9(5):e96545.

Wondrak GT, Cervantes-Laurean D, Jacobson EL, Jacobson MK (2000) Histone carbonylation *in vivo* and *in vitro*. Biochem J. 351:769-777.

Woodland RT, Schmidt MR, Thompson CB (2006) BLyS and B cell homeostasis. Semin immunol. 18: 318-326.

Yoshida T, Mei H, Dorner T, Hiepe F, Radbruch A, Fillaatreau S, Hoyber BF (2010) Memory B and memory plasma cells. Immunol Rev. 237(11):117-39.

Yasui T, Hirose J, Tsutsumi S, Nakamura K, Aburatani H, Tanaka S (2011) Epigenetic regulation of osteoclast differentiation: possible involvement of Jmjd3 in the histone demethylation of Nfatc1. J Bone Miner Res. 26(11):2665-71.

Zhang Y, Reinberg D (2001) Transcriptional regulation by histone methylation: interplay between different covalent modifications of the core histone tails. Genes Dev. 15:2343-2360.

Zhao W, Li Q, Ayers S, Gu Y, Shi Z, Zhu Q, Chen Y, Wang HY, Wang RF (2013) Jmjd3 inhibits reprogramming by upregulating expression of INK4a/ARF and targeting PHF20 for ubiquitination. Cell 152(5):1037-50.

Acknowledgement

I would like to express my gratitude to the people whom without their help this work would have been hard to achieve, if not impossible.

First and most of all, I am sincerely grateful to my thesis supervisor, *Dr. Stefano Casola* for his invaluable guidance, encouragement and support during the course of PhD. *Stefano*, thanks for all the things you taught me in research and life. It was my honor to have you as mentor during my PhD life.

I wish to thank the past and present members of our group for their friendship and supprot: *Federica Mainoldi, Federica Zanardi, Marieta Caganova, Gabriele Varano, Federica Alberghini, Giulia Fragola, Chiara carrisi, Rashmi Kumar and Valentina petrocelli*. It was a pleasure working with you.

Furthermore, I would like to extend my gratitude to our collaborators *Dr. Giuseppe Testa, Thomas Burgold* and *Betsabeh Khoramian Tusi* in European Institute of Oncology (IEO) for sharing *Jmjd3* targeting vector and fruitful discussions.

I am grateful to my external co-supervisor *Dr. Thomas Milne* and my internal co-supervisor *Dr. Marina Mapelli* for scientific discussions, my examiners *Professor Doron Melamed* and *Dr. Diego Pasini* for evaluation of my thesis and helpful comments.

I would like to thank all IFOM-IEO facility staff, in particular *Elisa Allievi* from Transgenic facility for her essential role in generation of chimeric animals.

I wish to thank *Betsabeh* and *Leila* for their support and encouragement. No matter the distance, I am sure our friendship will last forever.

And I am grateful to my lovely family for endless support. Thank you dad, mom, *Mehdi, Meysam, Homa, Mansooreh* and our little angel *Nika*. Hearing your voices, even thinking of you makes me strong to face life challenges. Thank you.